NSWCDD/TR-93/339

ELECTROMAGNETIC REVERBERATION CHARACTERISTICS OF A LARGE TRANSPORT AIRCRAFT

BY MICHAEL O. HATFIELD
SHIP DEFENSE SYSTEMS DEPARTMENT

GUSTAV J. FREYER
UNIVERSAL SYSTEMS INCORPORATED

D. MARK JOHNSON CHARLES L. FARTHING
COMPUTER SCIENCES CORPORATION

JULY 1994

NAVAL SURFACE WARFARE CENTER
DAHLGREN DIVISION
Dahlgren, Virginia 22448-5100

NSWCDD/TR-93/339

ELECTROMAGNETIC REVERBERATION CHARACTERISTICS OF A LARGE TRANSPORT AIRCRAFT

BY MICHAEL O. HATFIELD
SHIP DEFENSE SYSTEMS DEPARTMENT

GUSTAV J. FREYER
UNIVERSAL SYSTEMS INCORPORATED

D. MARK JOHNSON CHARLES L. FARTHING
COMPUTER SCIENCES CORPORATION

JULY 1994

NAVAL SURFACE WARFARE CENTER
DAHLGREN DIVISION
Dahlgren, Virginia 22448-5100

FOREWORD

The electromagnetic measurements discussed in this report were obtained by the Systems Electromagnetic Effects Branch (F52), Electromagnetic Effects Division of the Naval Surface Warfare Center, Dahlgren Division. The work was funded by the Langley Research Center of the National Aeronautics and Space Administration through the Lawrence Livermore National Laboratory (LLNL).

The test was conducted in a decommissioned Boeing 707-720B aircraft at the Aerospace Maintenance and Regeneration Center, Davis Monthan Air Force Base, Tucson, Arizona. The aircraft was excited from 100 MHz to 18 GHz by horn and wire antennas in several locations within the avionics bay and cockpit. The received power was measured by horn and wire antennas also placed in several locations in the avionics bay and cockpit.

The authors wish to acknowledge R. Zacharias and C. Avalle of the Nuclear Energy Systems Division of LLNL for their participation in statistical data collection during the first half of the field test period.

This report has been reviewed by William Lenzi, Head, Systems Electromagnetic Effects Branch and Leonard Fontenot, Head, Electromagnetic Effects Division.

Approved by:

THOMAS C. PENDERGRAFT, Head
Ship Defense Systems Department

ABSTRACT

A demonstration test to investigate the reverberation characteristics of the avionics bay and cockpit of a typical commercial aircraft was conducted on a decommissioned Boeing 707-720B aircraft. The aircraft, located at the Aerospace Maintenance and Regeneration Center, Davis Monthan Air Force Base, Arizona, had a significant fraction of its electronics equipment remaining in the avionics bay and cockpit and the passenger compartment was essentially intact. A simulated avionics box was placed in an equipment rack and a trace on an internal circuit board was monitored. The simulated avionics box was also tested in the Naval Surface Warfare Center, Dahlgren Division (NSWCDD) mode stirred chamber (MSC).

The avionics bay and cockpit were internally excited from 100 MHz to 18 GHz using a pair of horn and wire antennas placed in several locations. Aluminum foil tuners, each 2 x 2 ft, were located in the avionics bay and the cockpit. The internal electromagnetic environment was measured by a horn and a wire antenna placed successively in several locations in the avionics bay and cockpit. Limited measurements of the local ambient environment, both external to the aircraft and within the aircraft, were obtained for the FM band (88 to 108 MHz) and the VHF/UHF bands (100 MHz to 1 GHz).

Cavity losses were characterized by comparing the received power to the input power. The cavity loss for the avionics bay was about 15 dB greater than the loss in the NSWCDD MSC. The loss for the cockpit was about 12 dB greater than the NSWCDD MSC.

The observed stirring ratios (ratio of maximum received signal to minimum received signal at a particular frequency as the tuner rotates) were generally less than 10 dB up to about 800 MHz. Above 800 MHz, a substantial number of data points exceeded 20 dB, the commonly accepted empirical criterion for adequate mode stirring in a MSC. The responses of the simulated avionics box in the avionics bay and in the MSC showed good agreement.

The limited data obtained implies the possibility that the shielding effectiveness for the avionics bay and cockpit may be as low as 0 dB over a portion of the frequency range 88 MHz to 1 GHz.

CONTENTS

CONTENTS (CONTINUED)

ILLUSTRATIONS

ILLUSTRATIONS (CONTINUED)

ILLUSTRATIONS (CONTINUED)

ILLUSTRATIONS (CONTINUED)

TABLES

1.0 INTRODUCTION

1.1 BACKGROUND

There is significant current interest in the response of aircraft avionics systems to high-intensity radiated fields (HIRF). This interest arises from the convergence of three trends.

- The ambient electromagnetic environment (EME) is increasing in density and intensity.
- Electronic systems are replacing mechanical systems that perform flight-critical/essential functions.
- The use of composite materials may reduce the shielding effectiveness (SE) provided by the aircraft structure.

The Federal Aviation Administration (FAA), along with its European counterpart, the Joint Aviation Authorities is proposing revised aircraft electromagnetic (EM) airworthiness certification standards. The new standards will apply to normal, utility, aerobatic, and commuter airplanes (Part 23 of the Federal Aviation Regulations); transport airplanes (Part 25); normal rotorcraft (Part 27); and, transport rotorcraft (Part 29). Particularly at frequencies above 400 MHz, the proposed certification levels are substantially higher than previous levels. Table 1-1 shows the proposed certification levels as of December 1993. (Note that all tables and figures in this report can be found at the end of each chapter.)

A current issue for both the FAA and industry is how to perform credible certification tests for the aircraft and for the avionics systems within reasonable costs and schedules. Mode stirred chambers (MSC) have been suggested as a cost-effective means to demonstrate avionics susceptibility level compliance with the HIRF standards above 100 MHz. (Readers unfamiliar with the concept of a mode-stirred or reverberation chamber should review Reference 1). Figures 1-1 and 1-2 show proposed routes to certification as documented in the December 1992 draft *Advisory Circular*. The items marked with an asterisk indicate potential applications of MSCs for critical systems. A single asterisk indicates mode-stirring techniques are permitted for radiated susceptibility testing above 100 MHz. A double asterisk indicates where mode-stirring techniques have potential applications. To accept this test technique, there must be a demonstrated relationship between the EM test environment in a MSC and the aircraft cavity EME that results from external illumination of the aircraft.

---

[1]Crawford, M. L. and Koepke, G. H., *Design, Evaluation and Use of a Reverberation Chamber for Performing Electromagnetic Susceptibility/Vulnerability Measurements*, NBS TN 1092, 1986.

A typical compliance test sequence would include

- Low-level plane wave illumination of the aircraft
- Measurement of the EME within the aircraft during the illumination (e.g., coupling measurements)
- Testing the avionics in a MSC at levels determined by extrapolation from the aircraft illumination level and the internal environment to the HIRF specification

Several technical issues must be resolved before this compliance test sequence can be used with confidence. One of the issues is the ability to characterize the internal EME during external illumination.

When EM energy is introduced into an aircraft cavity it is expected that field intensity maxima and minima will be distributed throughout the cavity as a result of the superposition of the cavity modes. The field intensity distribution will be dependent on the EM frequency, the details of the cavity configuration, and the excitation mechanism. Due to this expected frequency and configuration-dependent mode structure, some in the technical community suggest it will be difficult, if not operationally impossible, to characterize the internal environment resulting from external illumination in the frequency range above 100 MHz. However, if a cavity has an adequate mode density and a sufficiently high-quality factor, Q, or equivalently a low loss factor, it may be possible to bound the bay response under reverberation or mode-stirred conditions. Thus key issues in the compliance test sequence are whether an aircraft cavity will behave like a reverberation chamber/MSC when it is excited by EM energy in the frequency range of interest and whether the responses of avionics systems will be the same in both environments.

Several positions on the response of an aircraft cavity to EM excitation can be found in the technical community. One suggestion is that the absorption within the aircraft is so great that it would behave more like an anechoic chamber than a MSC. A second position is that while a cavity may not behave like an anechoic chamber, the internal losses would be sufficient to prevent effective use of the mode structure.

The second issue to be resolved is whether a system response in a MSC test is representative of the system response in the same level EME in aircraft cavities such as an avionics bay or cockpit. While MSCs have been accepted as a viable technique for determining system EM susceptibility, the link with system response in an aircraft compartment has not been demonstrated.

Of the several technical issues that must be resolved before the compliance test sequence can be validated, this test provides a first-order answer to the two specific issues discussed.

1.2 OBJECTIVE

The objectives of this test were to

- Investigate the effects of mode stirring on the EME of compartments/cavities (e.g., avionics bays and cockpits) typical of those in commercial aircraft to internal continuous wave excitation over the frequency range 100 MHz to 18 GHz
- Compare the response of a simulated avionics box in an internally excited aircraft compartment to the response in a MSC

1.3 CONSTRAINTS

1.3.1 Schedule and Funding

The test was conducted within significant scheduling and funding limits. As a result, it was limited to providing first-order answers about the EM responses of commercial aircraft compartments.

1.3.2 Aircraft Availability

The availability of suitable aircraft for the test was a constraint. A number of sources were considered for providing representative avionics bays for this test. These included

- An operational FAA B-727
- An operational National Aeronautics and Space Administration B-737
- An operational but stored, privately owned B-737 at Mohave Airport, California
- The Air Force EMPTAC (B-707) experimental test aircraft at Kirtland Air Force Base (AFB), New Mexico
- A decommissioned B-707 aircraft at the Aerospace Maintenance and Regeneration Center (AMARC), Davis Monthan AFB, Arizona
- A salvaged B-707 aircraft at the Pima Air Museum, Tucson, Arizona

A major selection constraint was potential damage liability for an operational aircraft. Other selection criteria were availability, cost, and ability to make minor modifications for test instrumentation, if necessary.

The selected source was AMARC. There were on the order of 200 B-707 variants available. Since AMARC is a repository for salvaged aircraft, the aircrafts were available in a wide range of structural integrity and equipment configurations. Some aircraft had limited suites of electronics remaining in the bays.

1.3.3 Number of Avionics Bay Types Tested

The test plan indicated that avionics bays in several aircraft would be investigated. The concept was to test different bay configurations. However two factors led to data collection in only one aircraft. The most significant constraint was the time to configure an aircraft for testing. It required more than 10 percent of the total test schedule to set up one aircraft for testing. Use of available test time was the most important factor in the decision to collect data from only one aircraft. The second factor was that although many aircraft were available, at least for the three Boeing 707 variants at AMARC, the avionics bays and cockpits were essentially identical except for the amount of residual equipment. The structural integrity of the aircraft was also a significant variable. Thus it did not appear to the test team that using additional aircraft would provide significant additional data.

The test plan also indicated that different aircraft cavities (e.g., the actuator cavity in the vertical stabilizer) would be investigated. Again, effective use of the available test time led to investigating only the aircraft avionics bay and cockpit.

TABLE 1-1. PROPOSED CERTIFICATION LEVELS

Frequency	Field Strength (V/m) (Peak/Average)
10–100 kHz	50/50
100–500 kHz	50/50
500k–2 MHz	40/40
2–30 MHz	100/100
30–70 MHz	20/20
70–100 MHz	20/30
100–200 MHz	30/30
200–400 MHz	70/70
400–700 MHz	1520/750
700 MHz–1 GHz	950/170
1–2 GHz	2470/180
2–4 GHz	3500/360
4–6 GHz	6800/280
6–8 GHz	1800/330
8–12 GHz	3500/330
12–18 GHz	1700/270

The Certification HIRF Environment above 18 GHz should be used only if the pass/fail criteria are not met in the 12-18 GHz range or if a system that performs a critical function is designed to operate in the 18-40 GHz range.

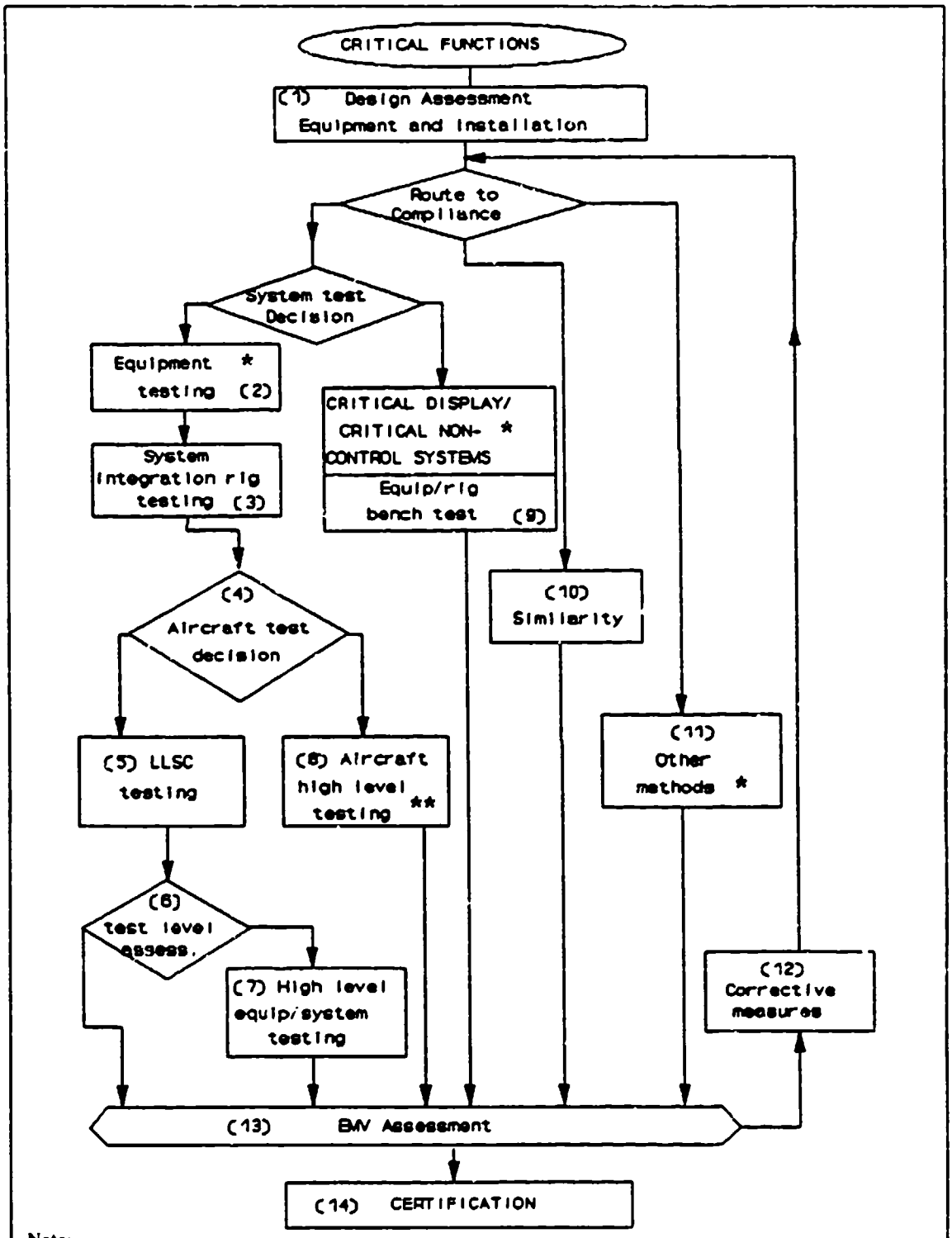

Note:

*Mode-stirring test techniques are permitted.

**Mode-stirring test techniques may be applicable.

FIGURE 1-1. PROPOSED ROUTES TO CERTIFICATION-CRITICAL FUNCTIONS

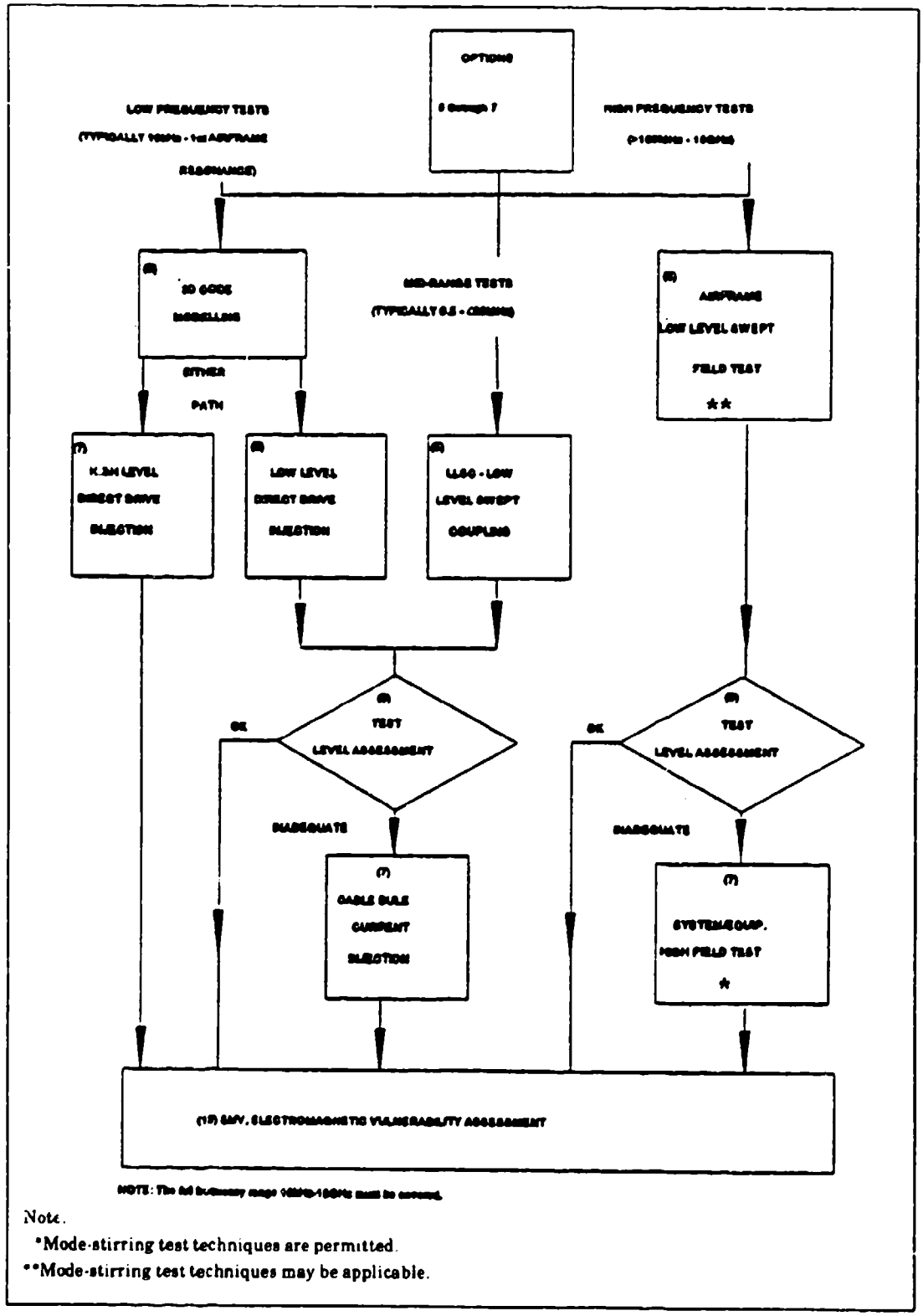

Note.

*Mode-stirring test techniques are permitted.

**Mode-stirring test techniques may be applicable.

FIGURE 1-2. EXPANDED VIEW OF STEP 5, PROPOSED ROUTES TO CERTIFICATION-CRITICAL SYSTEMS

2.0 APPROACH

2.1 AIRCRAFT DESCRIPTION

The AMARC had approximately 200 aircraft in three variants of the basic Boeing 707 aircraft. Figure 2-1 shows a portion of the 707 aircraft stored at AMARC. The aircraft covered a wide range of states of preservation.

Nine aircraft were surveyed by the test team. Factors considered were general condition, residual electronics boxes and cable runs, conditions of access panels and doors, and general EM shielding integrity.

The aircraft recommended by AMARC personnel was selected as the test aircraft. The aircraft was a Boeing 707-720B. It was constructed in 1965, had over 50,000 hr of flight time, and was last flown in September 1990. The aircraft had a substantial suite of equipment. The major equipment racks in the avionics bay had over 50 percent of the equipment remaining. With the exception of the center control console that was removed, most of the cockpit was intact. The passenger compartment was essentially intact, and the aircraft structural integrity was good.

Figure 2-2, extracted from the Boeing maintenance manual, shows the profile of the aircraft with the various antenna locations. For emphasis, the avionics bay and cockpit have been highlighted with dotted lines.

Figure 2-3 shows a schematic outline of the avionics bay with pertinent EM features. The most significant feature is that the bay is not a closed metallic structure. Note the large area, approximately 5 by 11 ft, directly above the two major equipment racks that have a non-metallic cover. A phenolic and/or masonite type material separated the avionics bay from the passenger compartment. The passenger compartment was essentially intact including the seats, galleys, lavatories, overhead bins, and all wiring bundles. The metal floor between the cockpit and the avionics bay had many penetrations. The access hatch from the cockpit to the avionics bay, which had a 3/8-in. wire mesh, was closed during all testing. The center pilot's console area in the cockpit as well as the access ports for manual landing gear extension were covered by aluminum foil and conductive tape to reduce these major open interfaces between the cockpit and the avionics bay. There were many penetrations of the avionics bay topology including wire bundles, air conditioning ducts, etc. Figure 2-4 shows a schematic of the location of major equipment racks in the avionics bay.

Figure 2-5 shows a schematic outline of the cockpit with features pertinent to EM shielding. For the cockpit, the windows were the major violation of a complete metal enclosure, although they had a coating that may have been conductive.

Figure 2-6 shows a schematic of the avionics bay and cockpit and the location of the tuners and the simulated avionics box provided by the Lawrence Livermore National Laboratory (LLNL). Figure 2-7 is a photo of the starboard equipment rack with the simulated avionics box. The box was a metal enclosure with no attempt made to enhance the box SE. An external 6-ft cable bundle with approximately 12 in. of unshielded wire, penetrated the metal enclosure. Figure 2-8 is a photo of the interior of the box showing the cable bundle and a circuit card. The cable bundle is attached to the circuit card in several locations. The center conductor of a semi-rigid coaxial cable was soldered to a single trace on the card. The semi-rigid cable was connected to a Type SMA connector on the enclosure for monitoring the box response.

2.2 INSTRUMENTATION

The test setup is shown schematically in Figure 2-9. Sweep frequency synthesizers drove a wire antenna and a broad-band, dual-ridged horn antenna at +10 dBm from 100 MHz to 18 GHz. Initial measurements showed that, as a result of the system noise floor, the effective frequency range was limited to 10 GHz or less.

Both a broad-band, dual-ridged horn and a wire were used as receiving antennas. The received signal drove a spectrum analyzer. Data collection with the spectrum analyzer was automated and under computer control. Normally 600 data points per spectrum-analyzer sweep were available. The data were stored on disks.

When collecting data from the simulated avionics box, a preamplifier was added to the circuit before the spectrum analyzer. The preamplifier provided approximately 17 dB of gain and was linear over the frequency range of interest.

Two aluminum foil tuners were constructed on a wire/rod frame. The direct current (DC) tuner motors were shielded to minimize the noise associated with the tuner operation. One tuner was placed in the avionics bay and the other in the cockpit, as shown in Figure 2-6. In many MSC tests, the tuner is stepped through precisely controlled repeatable steps. However, step control was not possible in this field test and the tuner rotated continuously.

The discrete frequency stirring ratio (SR) measurements required data collection over at least one complete tuner rotation. The statistical analysis by LLNL required statistically independent data that restricted their useful data set to one complete tuner rotation. To accommodate both requirements, while assuring that the measurement was stable and repeatable, the spectrum analyzer sweep rate and the tuner rotation rate were adjusted to provide data collection over 1.25 rotations of the tuner. The LLNL analysis used the first 80 percent of the data sample as their set of independent data points.

In one configuration, which had the transmitting (TX) antennas in the cockpit and the receiving (RX) antennas in the avionics bay, two tuners operated simultaneously. In this case, the data collection ideally should have occurred over an interval that would assure the capture of all received power variations for tuner rotation rates related as two prime numbers. For this test, based on the limited time available, such a rigorous data collection technique was not practical. Instead after observing the general pattern of the discrete frequency stirring data, a representative plot was selected for the file. The actual stirring ratio will be equal to or greater than that derived from the limited data.

Swept frequency measurements were normally performed in two overlapping frequency bands; i.e., 0.1 to 2.9 GHz and 2.75 to 18 GHz. For swept frequency measurements with mode stirring, both the synthesizer and spectrum analyzer were sweeping repetitively. By varying the two sweep rates, the tuner rotation rate and sampling the data with the spectrum analyzer maximum hold feature, the optimum combination was found to collect reasonably complete data in the minimum time. The measure of reasonableness was a subjective evaluation of when the spectrum analyzer data no longer appeared to be changing with time. This typically required data collection runs of 15 to 25 min. The equipment list for the test is shown in Table 2-1.

The equipment external to the aircraft (e.g., synthesizer, spectrum analyzer, etc.) was mounted in a 14-ft truck. This arrangement provided some protection from the sun and wind and maintained the equipment in a relatively fixed configuration. Figure 2-10 shows a photograph of the vehicle in a typical location with respect to the aircraft. It also shows typical cable runs to the bay. Figure 2-11 shows the equipment arrangement within the vehicle.

2.3 TEST PROCEDURES

The ambient EME in the FM band (88-108 MHz) and the very high frequency (VHF)/ultra high frequency (UHF) band (100-1000 MHz) was measured using the wire receive antenna. The ambient field was rechecked at the end of the test.

Five 1/4-in. holes were drilled in the aircraft pressure hull in the nose landing gear well and SMA feedthrough connectors were inserted in the holes. The five penetrations provided connections for two TX and two RX antennas, and power for one tuner motor. The physical arrangement for these connections is shown in the photo of Figure 2-12, which shows the landing gear wheel well looking aft.

The required semi-rigid cables were fabricated on-site to provide the cable lengths necessary to reach all points of interest in the avionics bay and cockpit. The frequency synthesizer-cable-spectrum analyzer system was calibrated by direct connection of the transmit and receive cables inside the bay. These data were stored on disk and were used to correct all raw test data. For verification the system was recalibrated after completion of the test and again within the Naval Surface Warfare Center, Dahlgren Division (NSWCDD) MSC.

A configuration is defined as the unique combination of a specific location, orientation, and polarization for the set of two TX antennas and the two RX antennas. Note that one of the *receive antennas* may be the simulated avionics box. As with all MSC testing, direct line-of-sight between the TX and RX antennas was avoided. Further in some cases, the antennas did not have a direct line-of-sight to the tuner.

FIGURE 2-1. BOEING 707 AIRCRAFT AT AMARC, DAVIS MONTHAN AFB, AZ

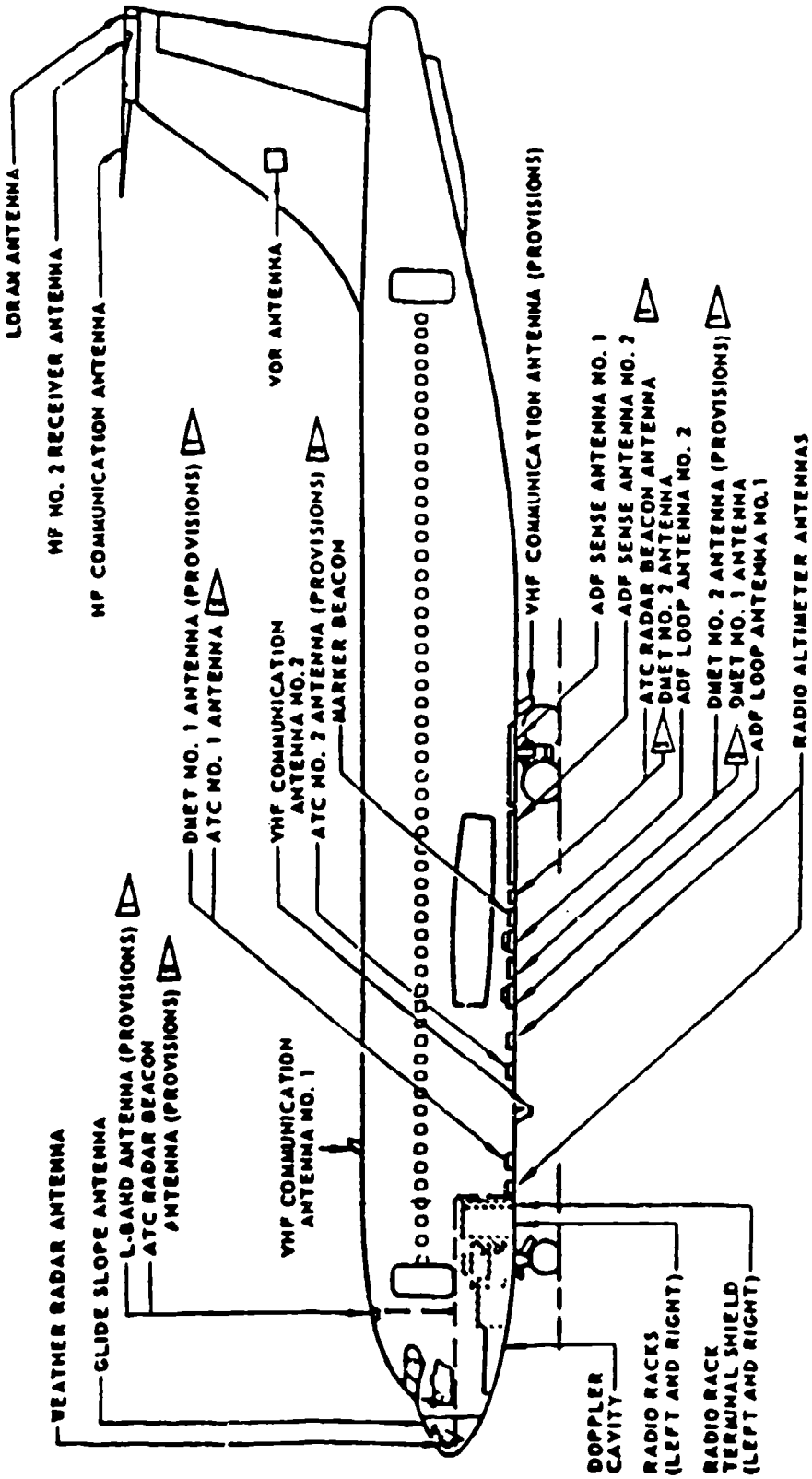

FIGURE 2-2. PROFILE OF BOEING 707 AIRCRAFT

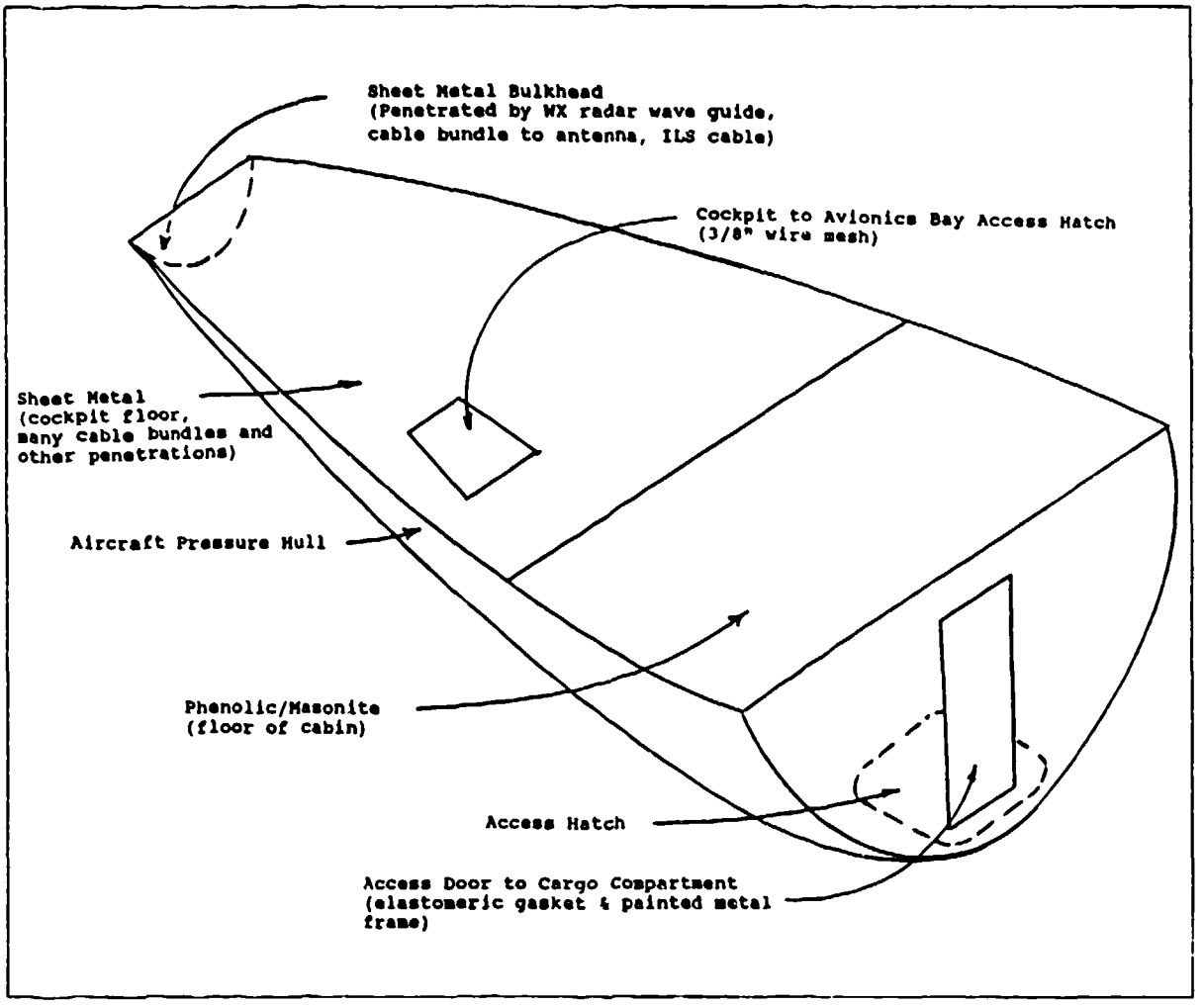

FIGURE 2-3. SCHEMATIC OF ELECTROMAGNETIC TOPOLOGY OF AVIONICS BAY

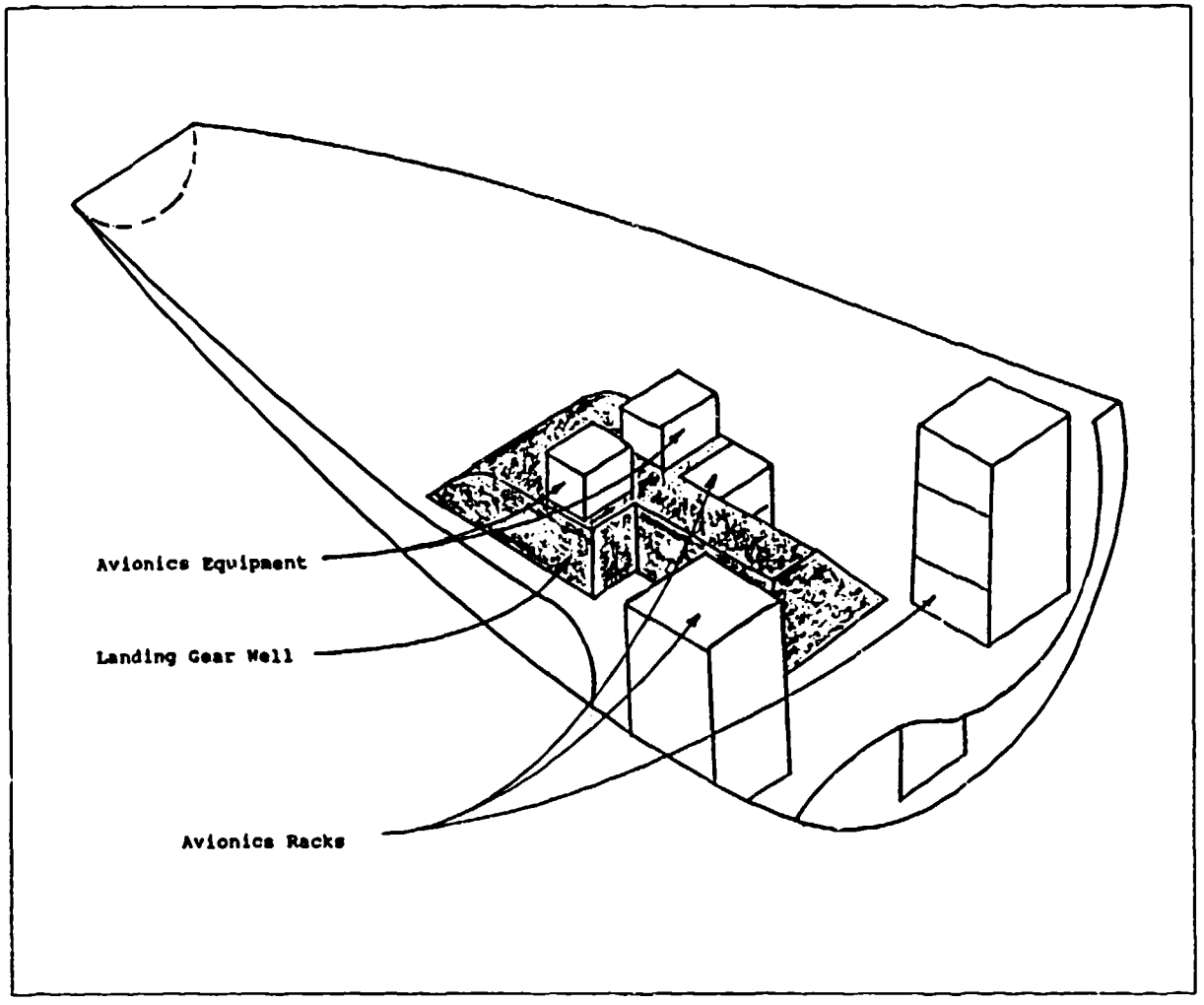

FIGURE 2-4. LOCATION OF MAJOR EQUIPMENT RACKS IN AVIONICS BAY

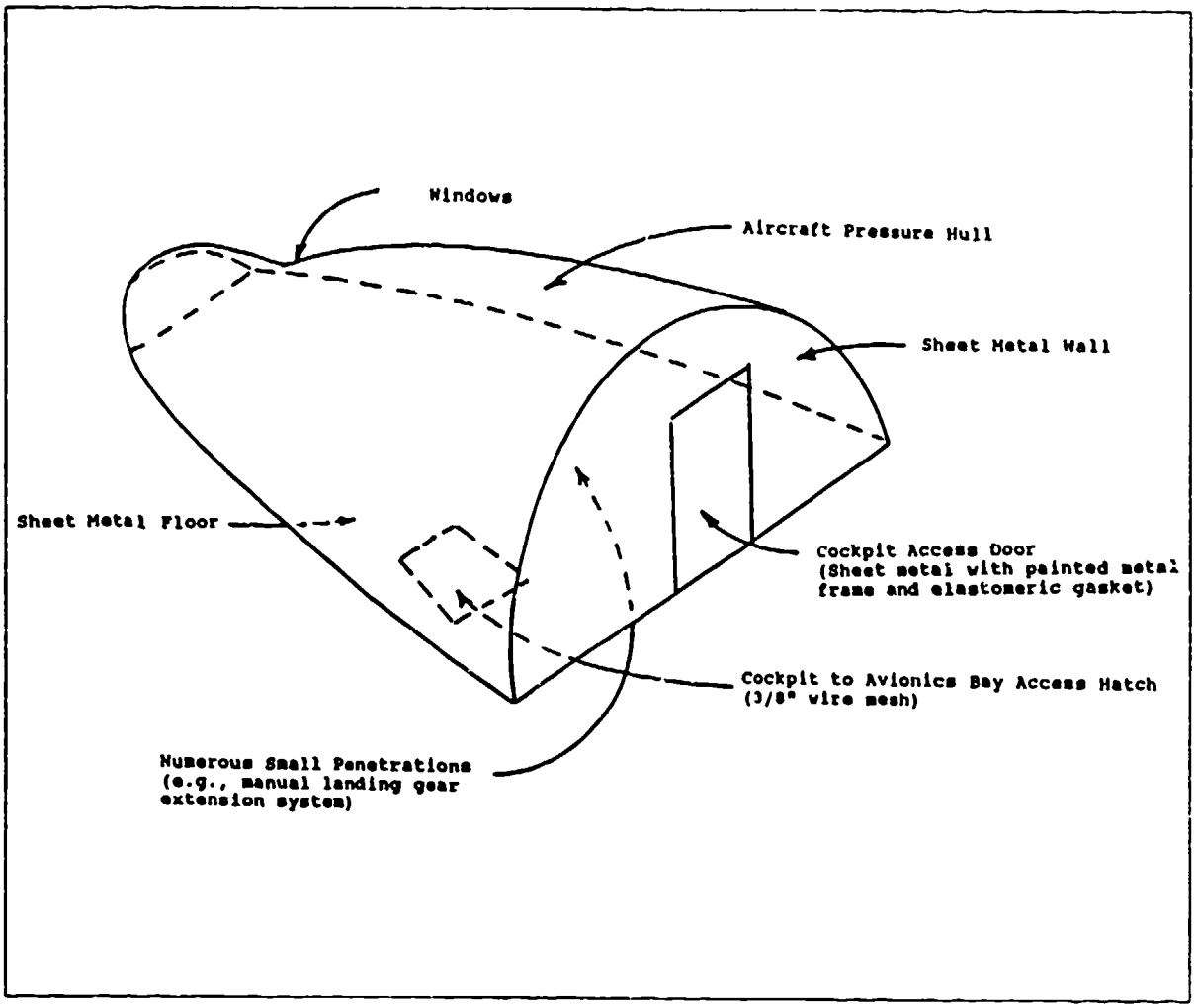

FIGURE 2-5. SCHEMATIC OF ELECTROMAGNETIC TOPOLOGY OF COCKPIT

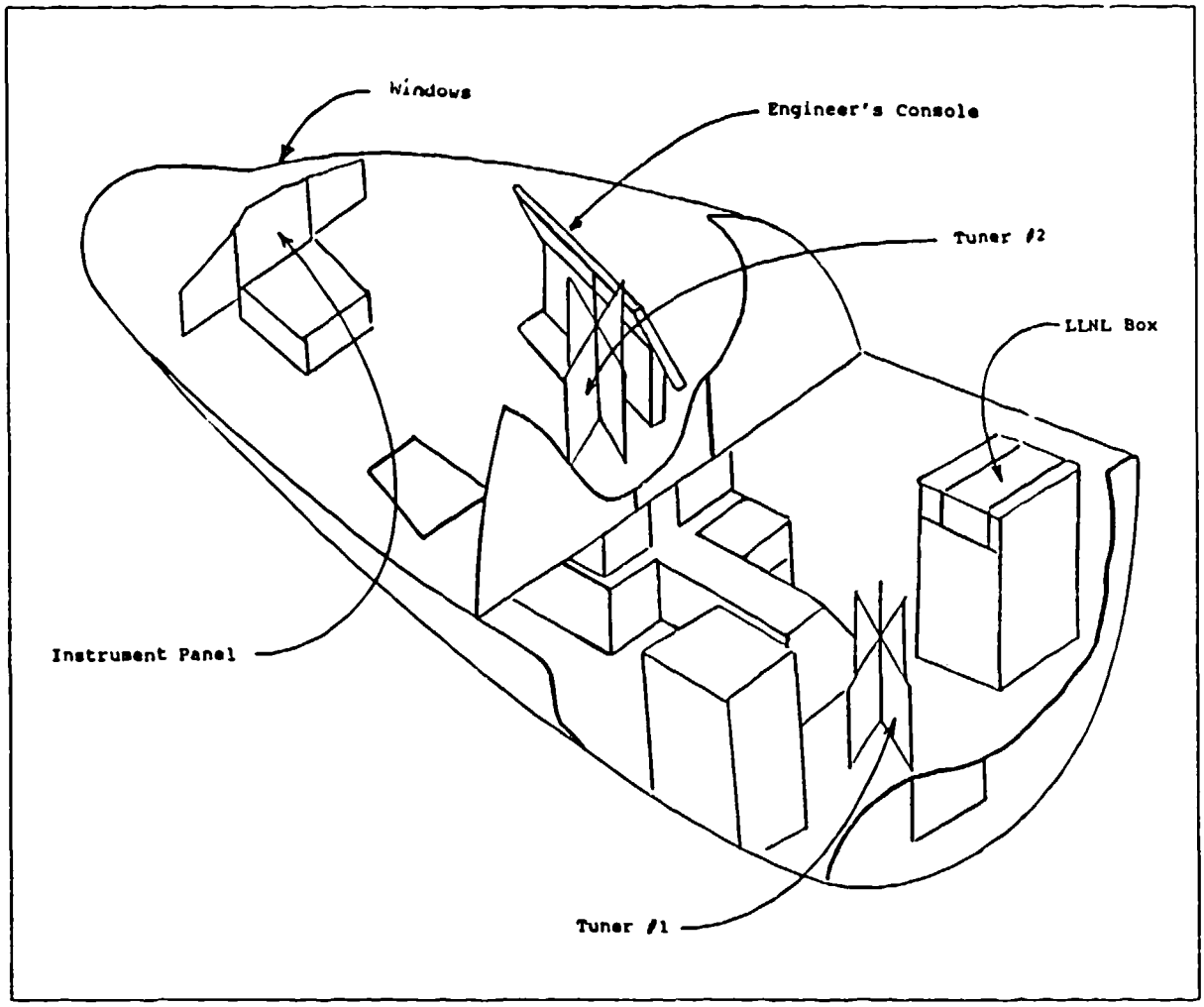

FIGURE 2-6. LOCATION OF TUNERS AND SIMULATED AVIONICS BOX

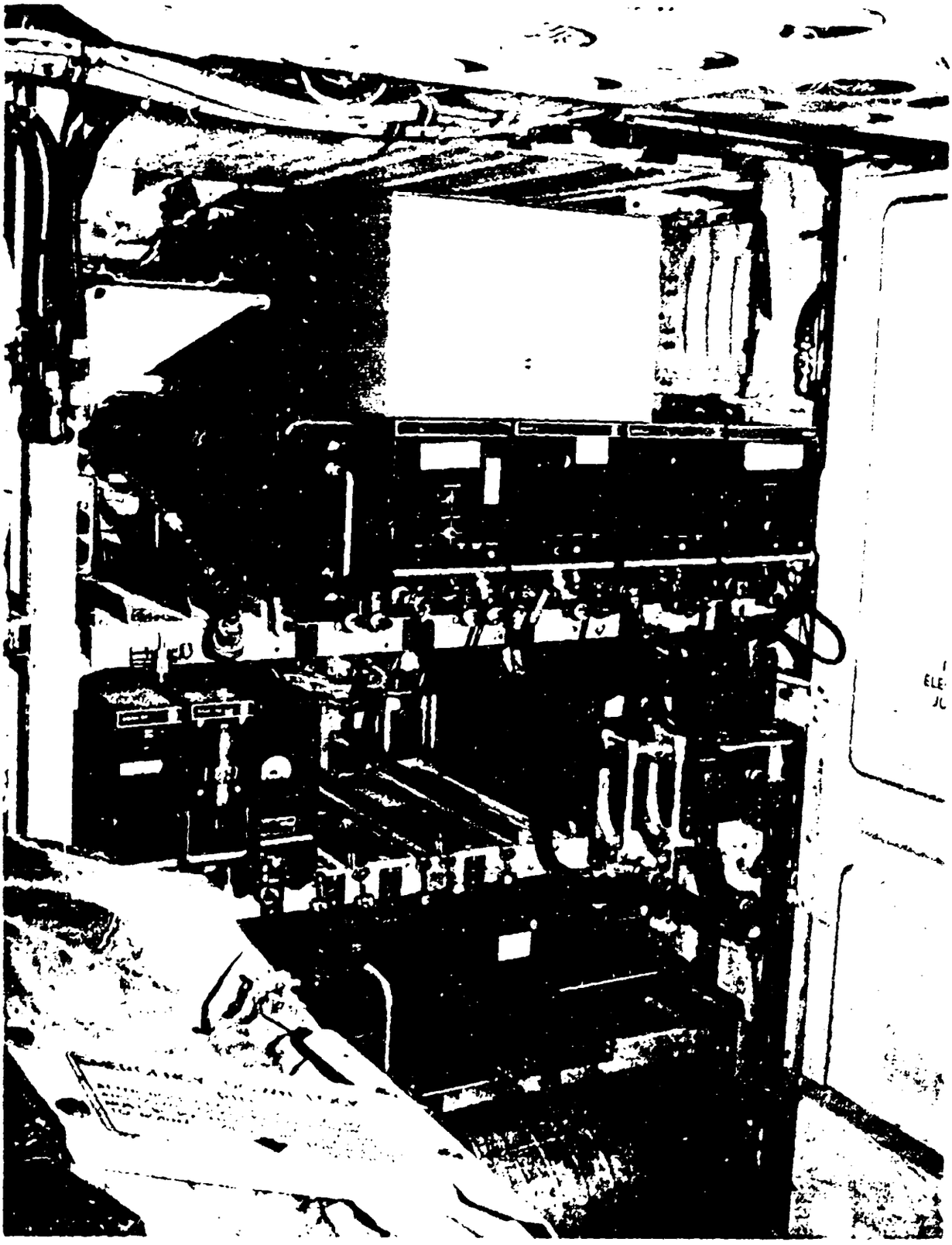

FIGURE 2-7. LOCATION OF SIMULATED AVIONICS BOX IN AIRCRAFT EQUIPM T RACK

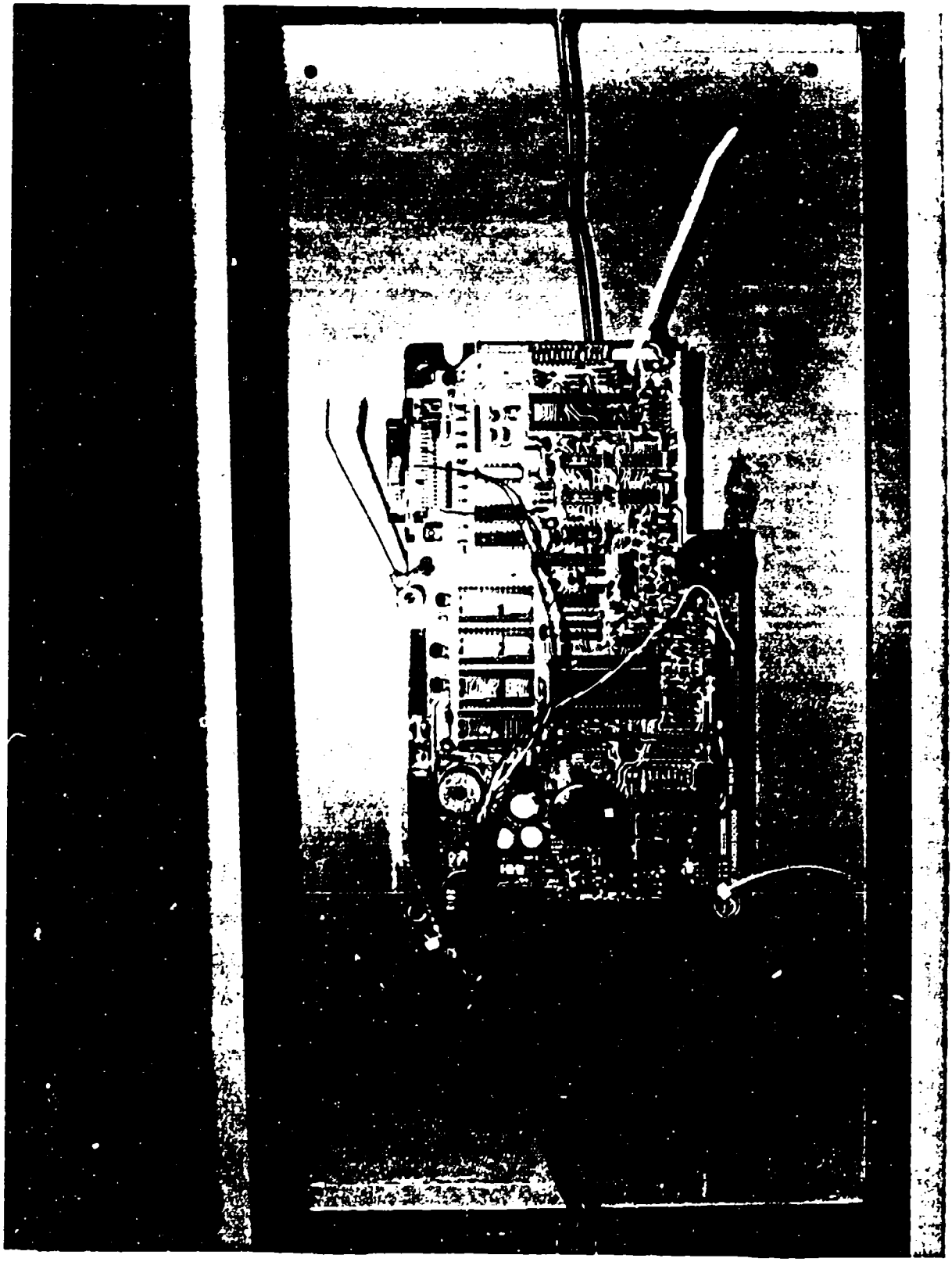

FIGURE 2-8. CIRCUIT CARD IN SIMULATED AVIONICS BOX

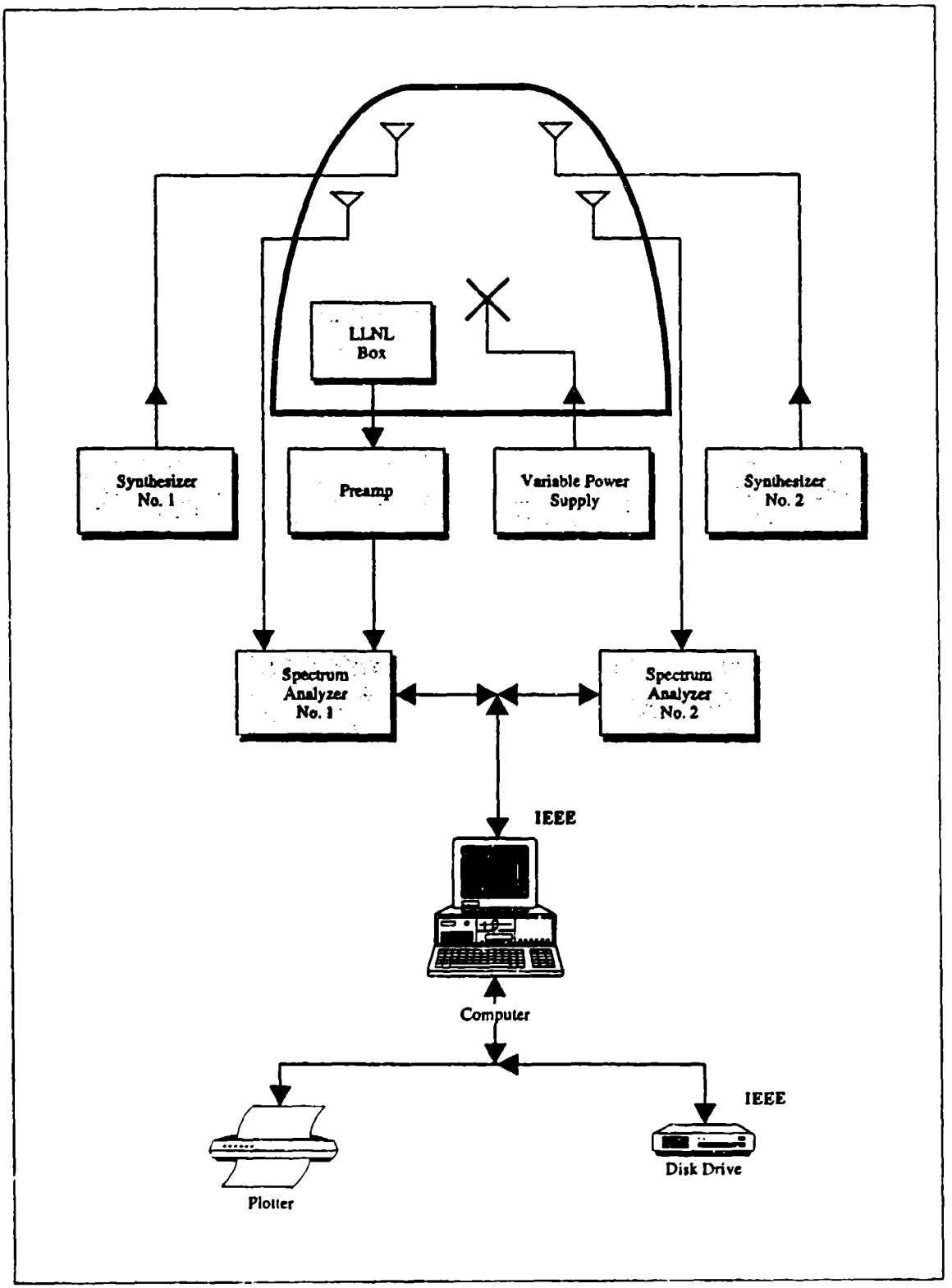

FIGURE 2-9 SCHEMATIC OF TEST SETUP

TABLE 2-1. TEST EQUIPMENT

Equipment	Amount
HP 8341 Sweep Frequency Synthesizer	2
HP 8562A Spectrum Analyzer	2
B&H AC260 83H20 Preamplifier	1
EMCO 18 GHz Dual-Ridged Horn Antenna	1
Eaton 18 GHz Dual-Ridged Horn Antenna	1
Wire Antenna	1 (14 in.) 1 (6 in.)
Tuner (24 x 24 in.)	2
Variable DC Power Supply for Tuner Motor Drive	2
Shielded Tuner Motor Drive	2
Miscellaneous Cables, Connectors, etc.	
Computer and Associated Peripherals	

FIGURE 2-10. LOCATION OF INSTRUMENTATION VEHICLE WITH RESPECT TO AIRCRAFT

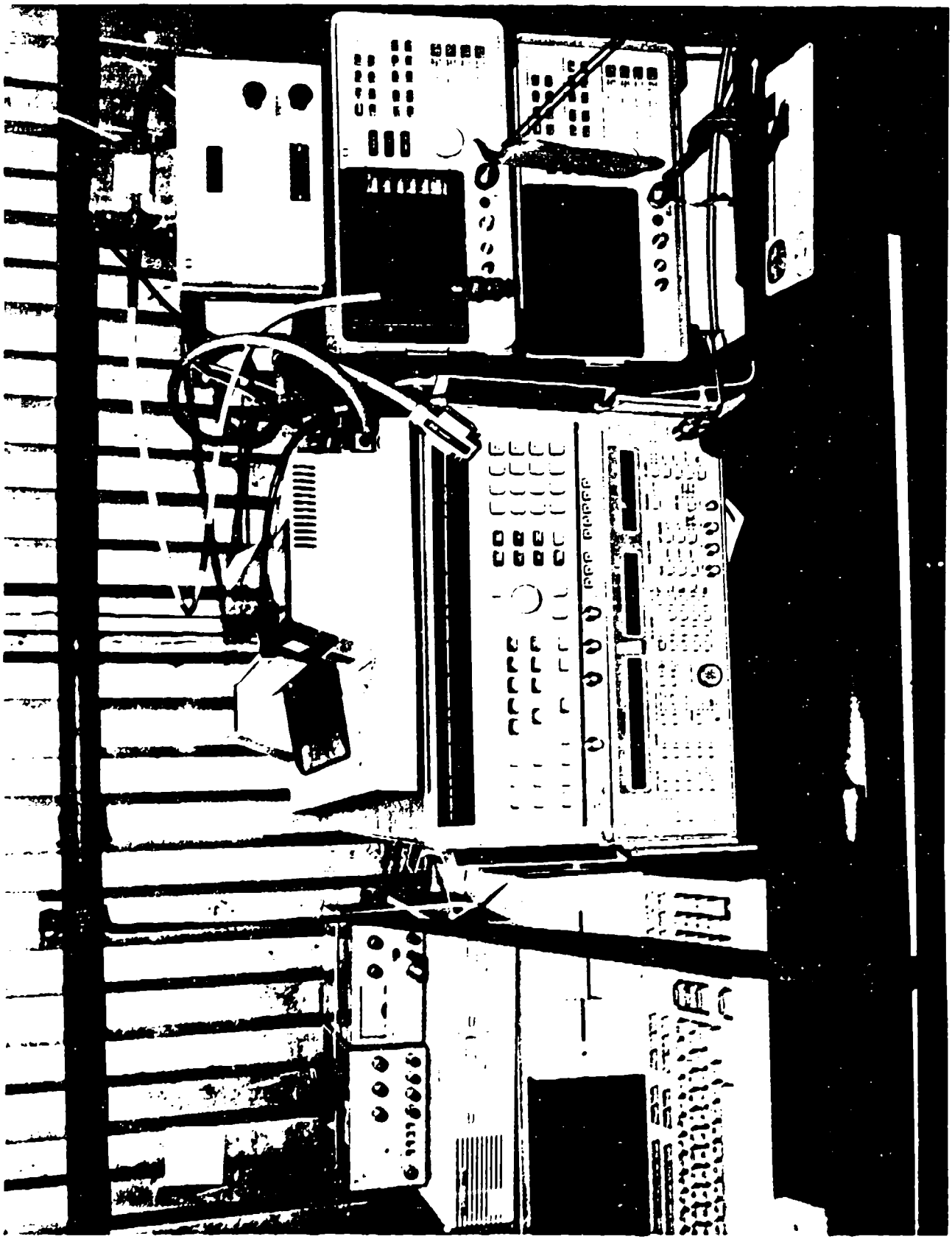

FIGURE 2-11. TEST INSTRUMENTATION

FIGURE 2-12. INSTRUMENTATION CABLE PENETRATIONS OF AIRCRAFT PRESSURE HULL

3.0 SUMMARY OF DATA

3.1 CALIBRATION DATA

Calibration runs were obtained before and after the data collection activity. The input cable port at the location of the TX antenna was directly connected to the output cable port at the location of the RX antenna. These calibration runs provided the end-to-end measurement system losses, less antenna losses, as a function of frequency. One pretest calibration curve is shown in Figure 3-1. The post-test calibration curve was within 1 dB of Figure 3-1 over the entire frequency range. Since test measurements were performed using the same measurement system at the NSWCDD MSC after the field test, additional system calibration runs were performed. The calibration curve for the NSWCDD MSC was also within about 1 dB of Figure 3-1 over the frequency range 0.1 - 18 GHz. These data indicate the stability of the measurement system throughout the test. Figure 3-1 data were used for correcting all the data runs except those using the ambient radio frequency (RF) environment as the source.

As discussed earlier, a preamplifier was used when data were collected from the simulated avionics box. The amplifier gain over the lower frequency sweep band (0.1 to 2.9 GHz) is shown in Figure 3-2. The preamplifier had a relatively constant gain over the frequency range of interest in this test. All raw box data were corrected for the amplifier gain.

Limited external ambient EME data in the FM and VHF/UHF bands are available in single sweep data. The external ambient environment measured with a wire RX antenna is shown in Figure 3-3 for the FM band and in Figure 3-4 for the VHF/UHF band. No attempt was made to vary the RX antenna position with respect to the truck or the aircraft to maximize the ambient signal. Also, no attempt was made to investigate the temporal variability of the ambient signals.

3.2 CONFIGURATION DATA

A total of 10 configurations were investigated. Five configurations had both the TX and RX antennas in the avionics bay. Two configurations had the TX antennas in the cockpit and the RX antennas in the avionics bay, and three configurations had both the TX and RX antennas in the cockpit. The placement of the TX and RX antennas for each of the 10 configurations are shown in the

schematics of Figures 3-5 through 3-14. For each of the 10 configurations, one or more of the following types of measurements were obtained.

- Cavity EME due to external ambient EME without stirring
- Cavity EME due to external ambient EME with stirring
- Cavity EME due to internal swept frequency excitation without stirring
- Cavity EME due to internal swept frequency excitation with stirring
- Cavity EME due to internal discrete frequency excitation with stirring

Figure 3-15 shows a typical data run for the internal cockpit EME resulting from the ambient external FM band. Since this type of data did not support the primary test objective, only a limited number of data runs were obtained for the FM and VHF/UHF bands. However, the data provide an indication of the potential SE of the aircraft structure and will be discussed in Section 4.7.

Figure 3-16 shows swept frequency data without stirring obtained in Configuration 3 during Run 62. The excitation was provided by the wire TX antenna and the bay EME was measured with the wire RX antenna. Figure 3-17 shows data from Run 66 for the same conditions but with stirring. These data are typical of the general frequency response of the avionics bay.

Figure 3-18 shows discrete frequency data with stirring for Configuration 2 obtained in Run 233. As described in Section 2.2, the tuner rotation rate and the spectrum analyzer sweep rate were adjusted to provide data over approximately 1.25 revolutions of the tuner. The pattern repetition can be seen by comparing the data trace for times greater than approximately 3.75 sec (the rotation period) with the start of the trace. This type of data addressed the primary objective of the project, determination of the effects of mode stirring on the EME in the avionics bay and the cockpit.

Over 700 individual data runs were performed with 600 data points per run. The measurements are summarized in the test matrix shown in Table 3-1. Runs are sequential except for the discrete frequency data. To provide a consistent reference for the SR evaluation, a structured pattern of about 60 runs, called the discrete frequency matrix, was defined for the discrete frequency measurements. Wire TX data were obtained from 0.1 to 2 GHz. The upper limit was invoked based on the low effectiveness of the wire TX antenna compared to the horn antenna at higher frequencies and the need to limit data collection time. Horn TX and RX data were obtained from 0.5 to 10 GHz. The lower limit was invoked because the horn efficiency dropped significantly below 1 GHz. This can be seen in Figure 3-19, which shows the received power data for Run 37 in the avionics bay. A comparison of the low frequency data for horn and wire antennas can be seen in Figures 3-19 and 3-17, respectively. The 10 GHz upper limit was invoked because, as will be seen in

Figure 4-1, system noise limited the use of data above approximately 6 GHz. Although discrete frequency measurements were obtained up to 10 GHz, most data analysis were limited to 6 GHz. The simulated avionics box was sampled from 0.9 to 10 GHz. The lower limit was based on an early observation that when using the horn TX antenna, the box response was generally at the system noise floor below about 900 MHz. The discrete frequency data were collected in blocks starting with even hundreds (e.g., Runs 200 to 269, 300 to 361, etc). Over 500 data runs were allocated to discrete frequency measurements since these data supported the primary test objective.

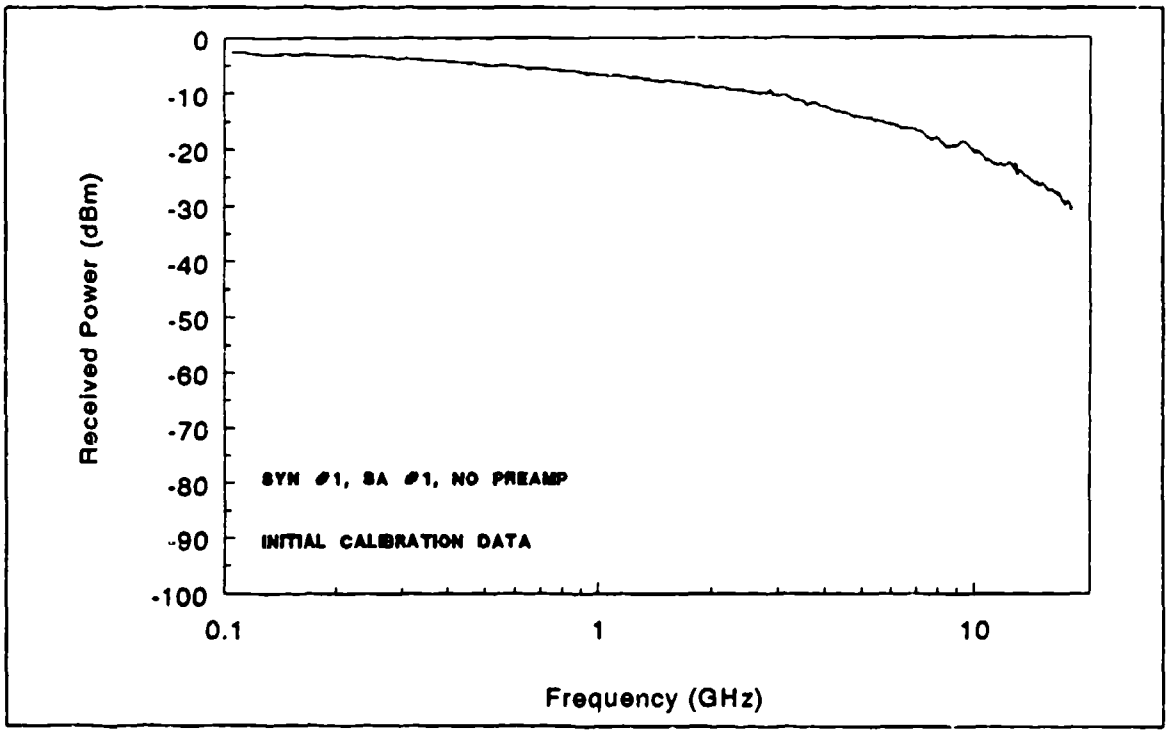

FIGURE 3-1. PRETEST SYSTEM CALIBRATION DATA

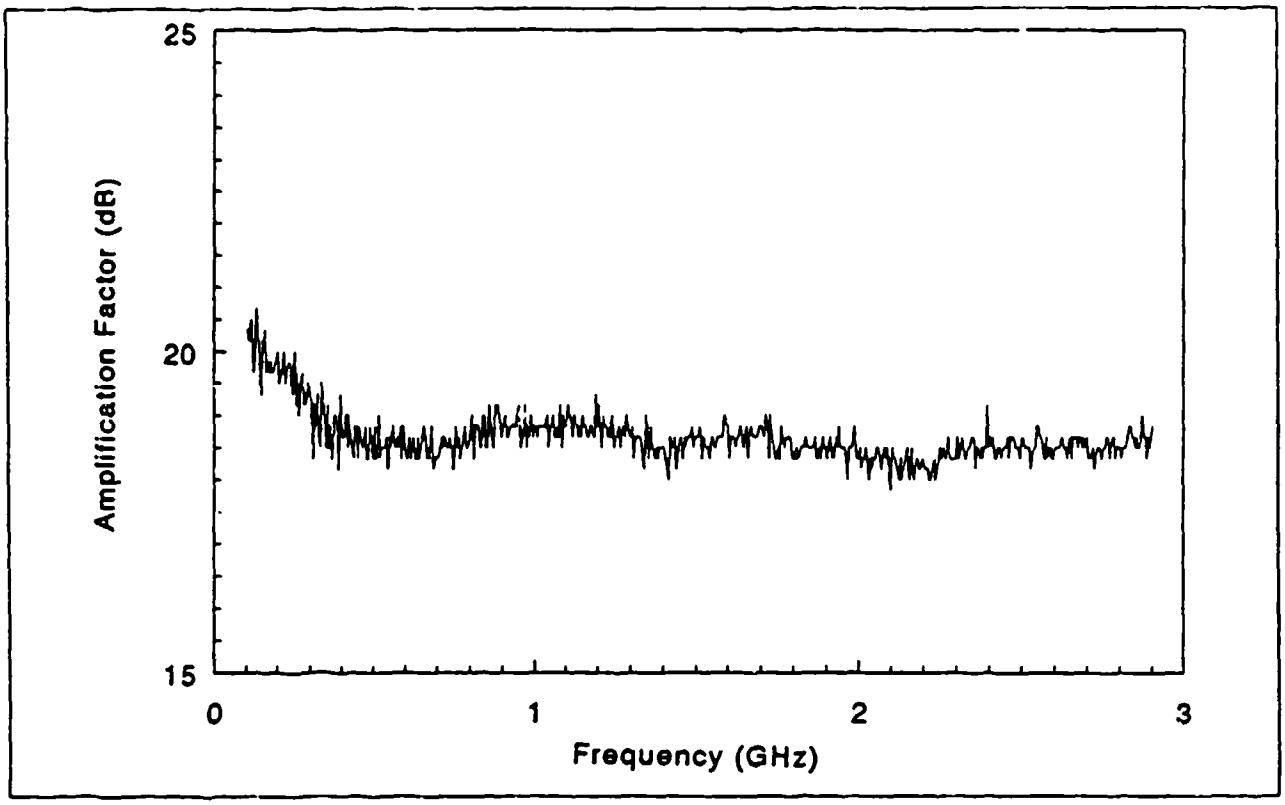

FIGURE 3-2. PREAMPLIFIER PERFORMANCE

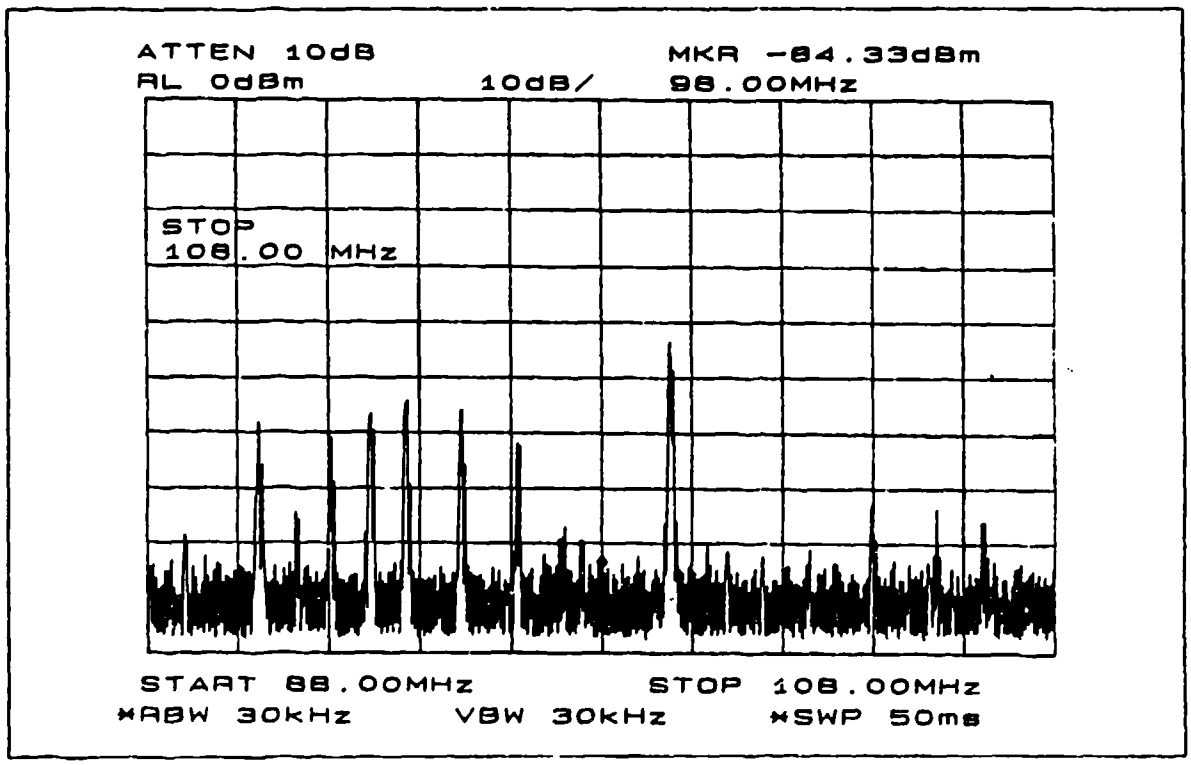

FIGURE 3-3. AMBIENT ENVIRONMENT-FM BAND

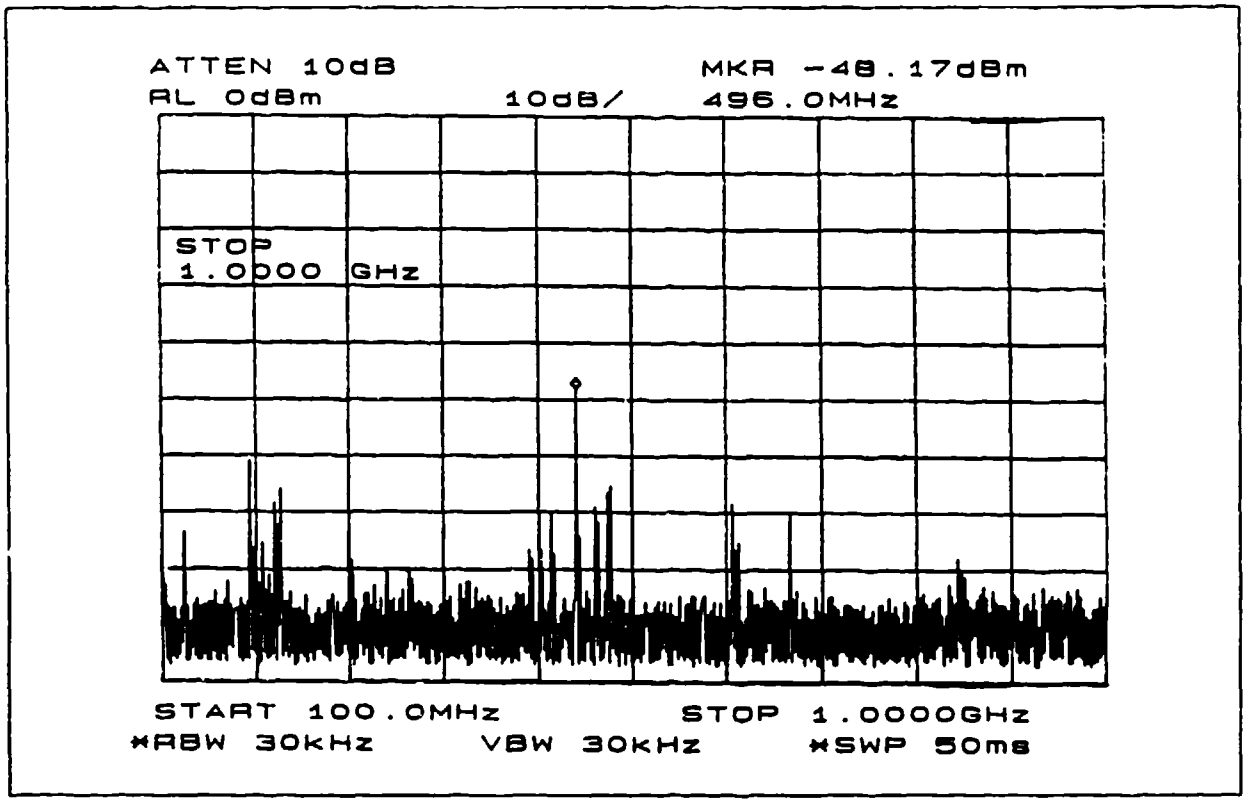

FIGURE 3-4. AMBIENT ENVIRONMENT-VHF/UHF BANDS

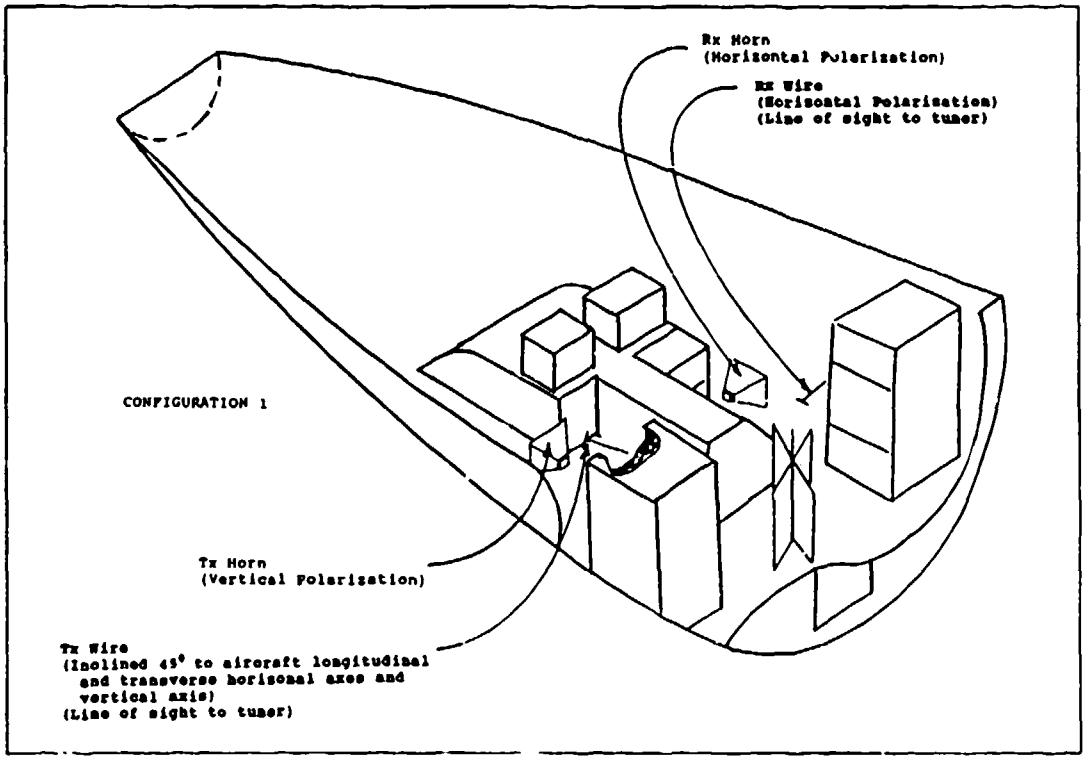

FIGURE 3-5. SCHEMATIC OF CONFIGURATION 1

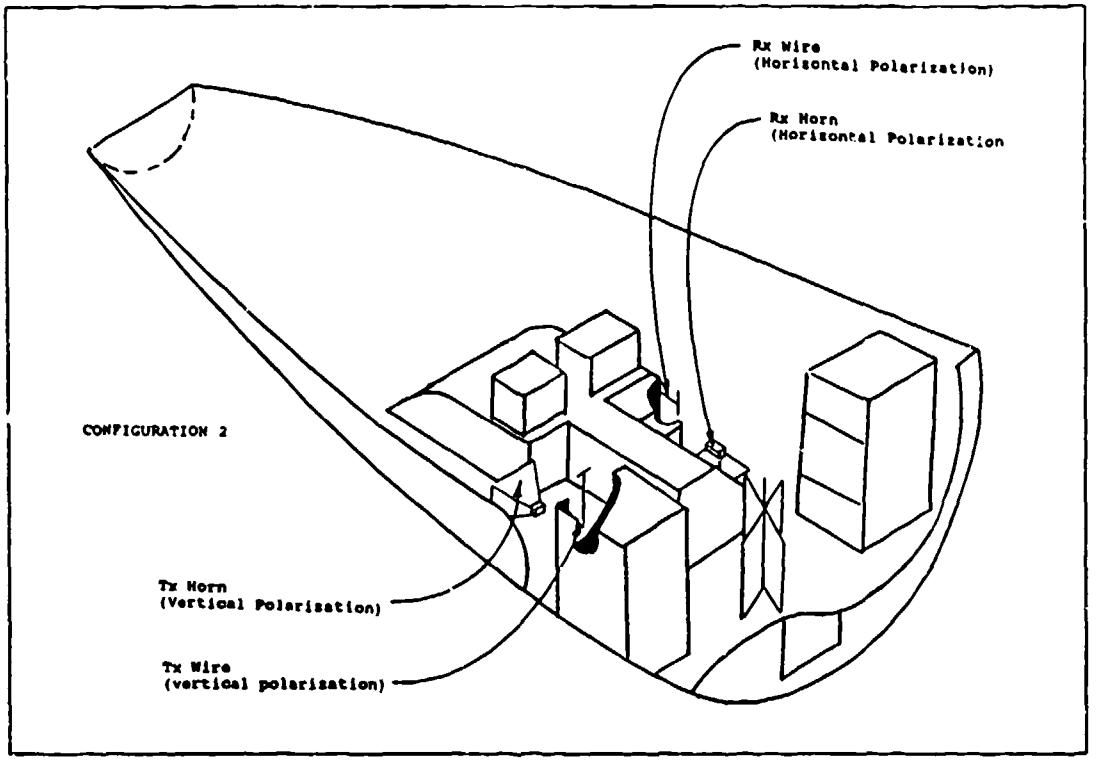

FIGURE 3-6. SCHEMATIC OF CONFIGURATION 2

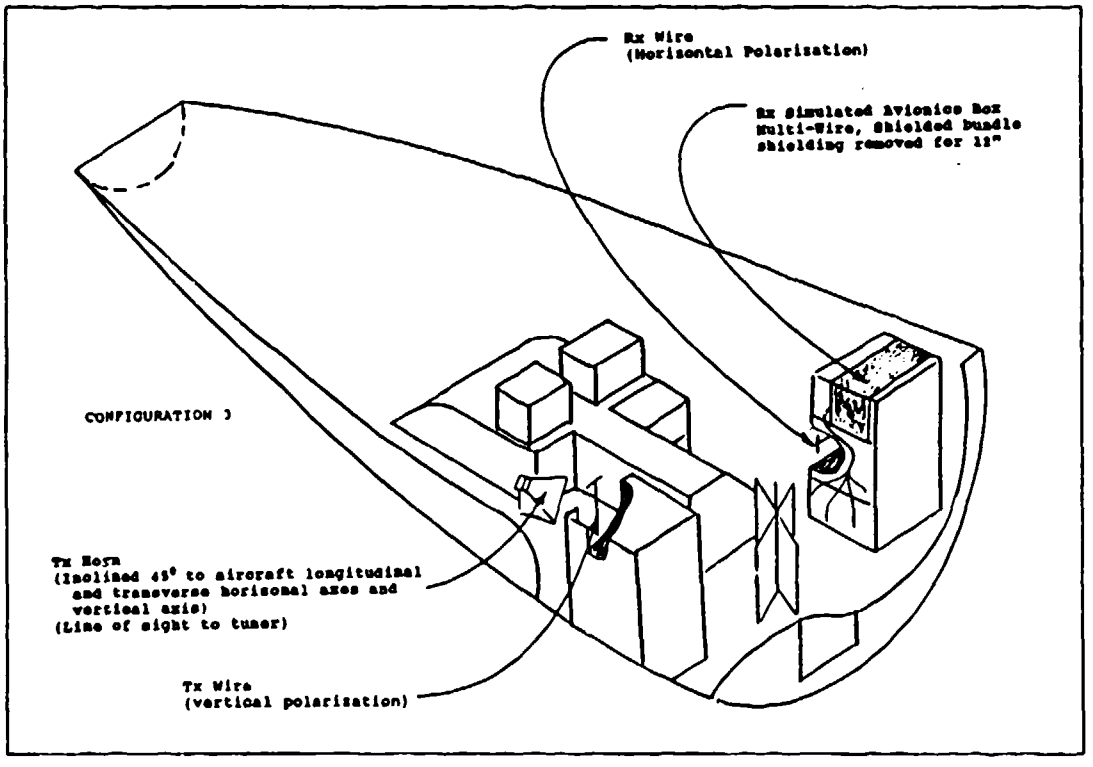

FIGURE 3-7. SCHEMATIC OF CONFIGURATION 3

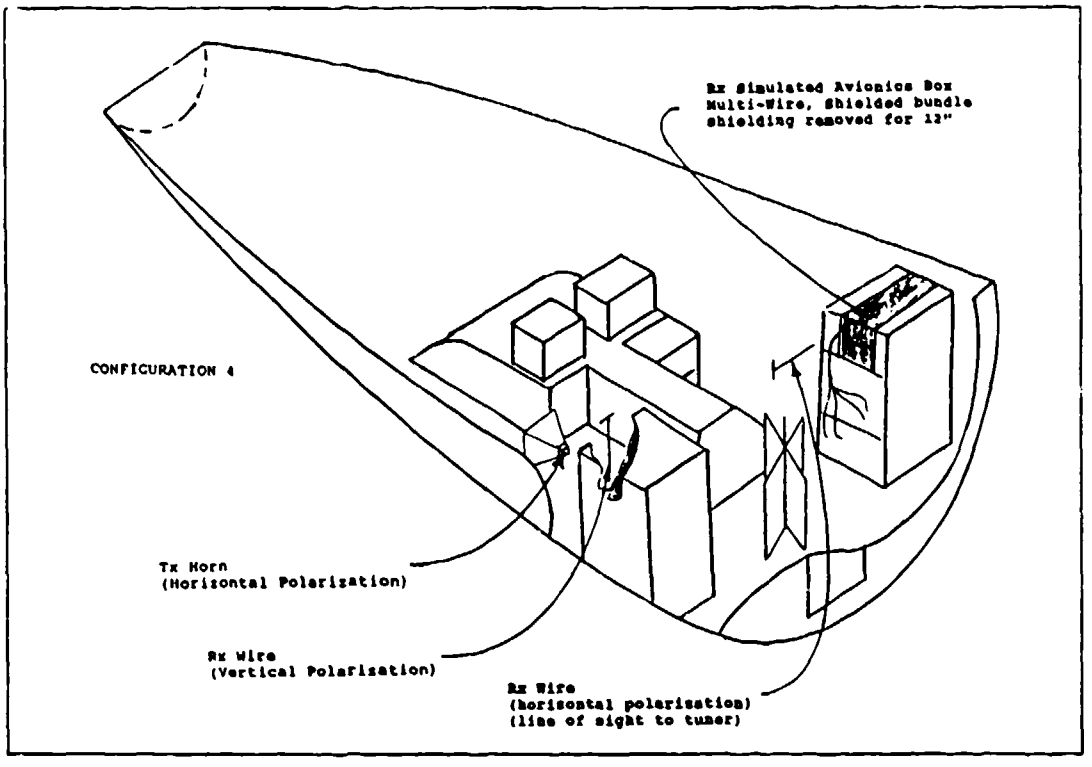

FIGURE 3-8. SCHEMATIC OF CONFIGURATION 4

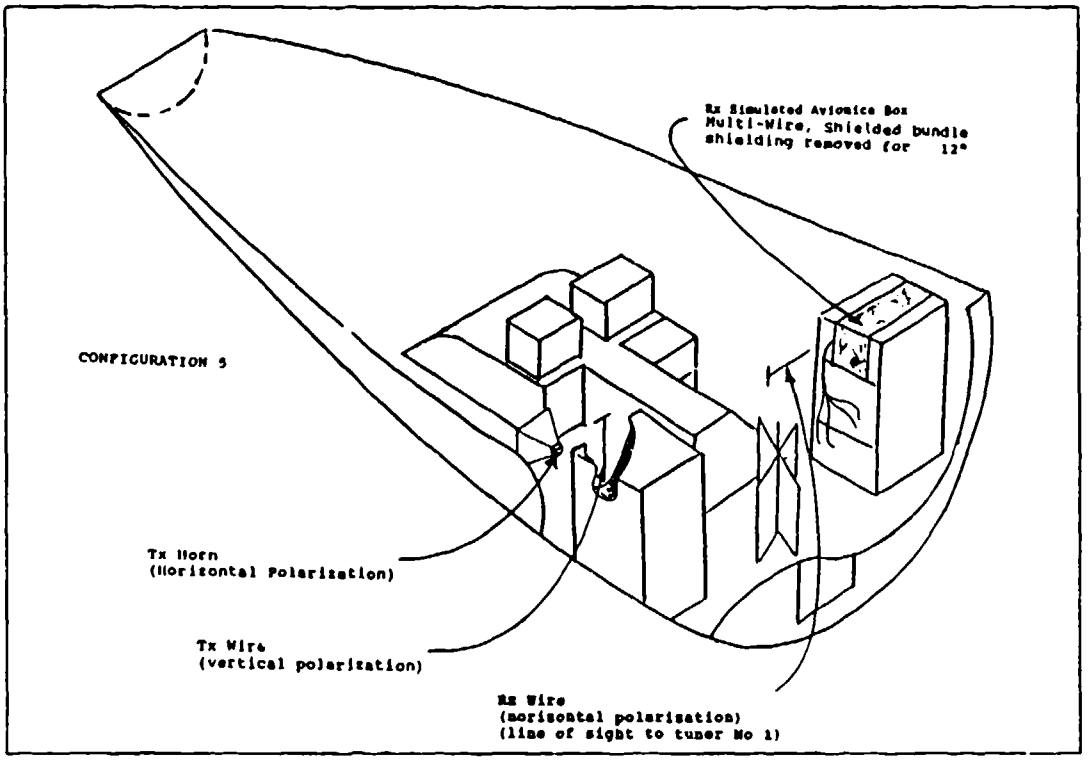

FIGURE 3-9. SCHEMATIC OF CONFIGURATION 5

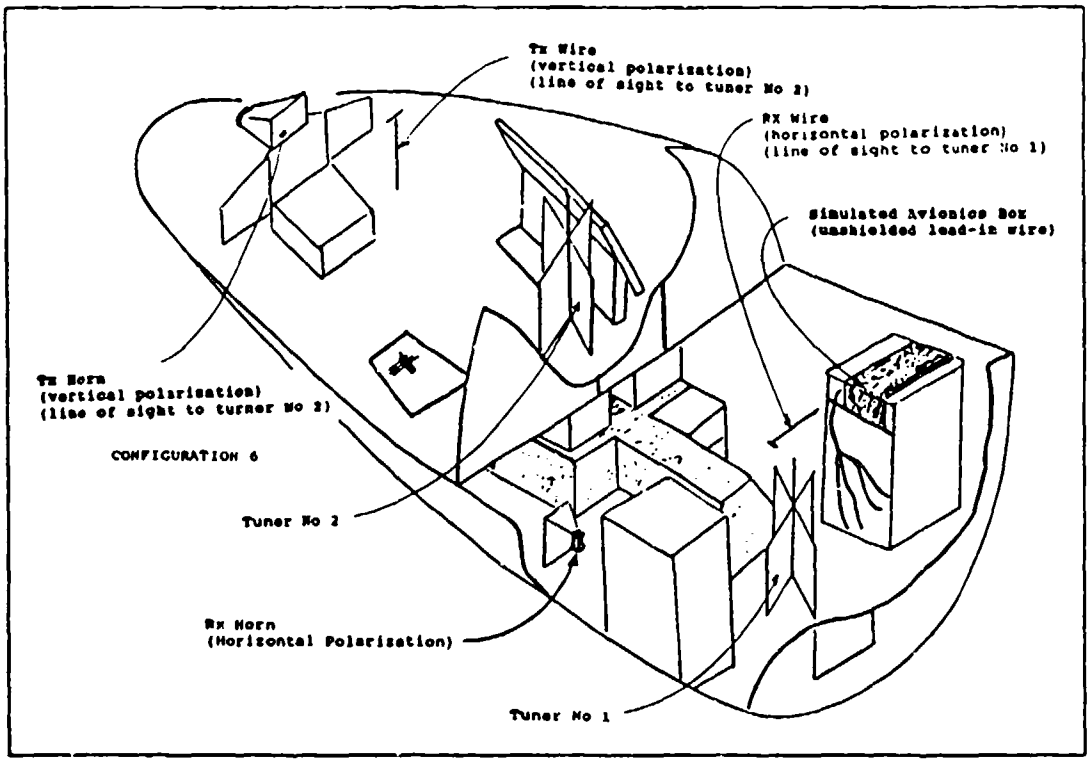

FIGURE 3-10. SCHEMATIC OF CONFIGURATION 6

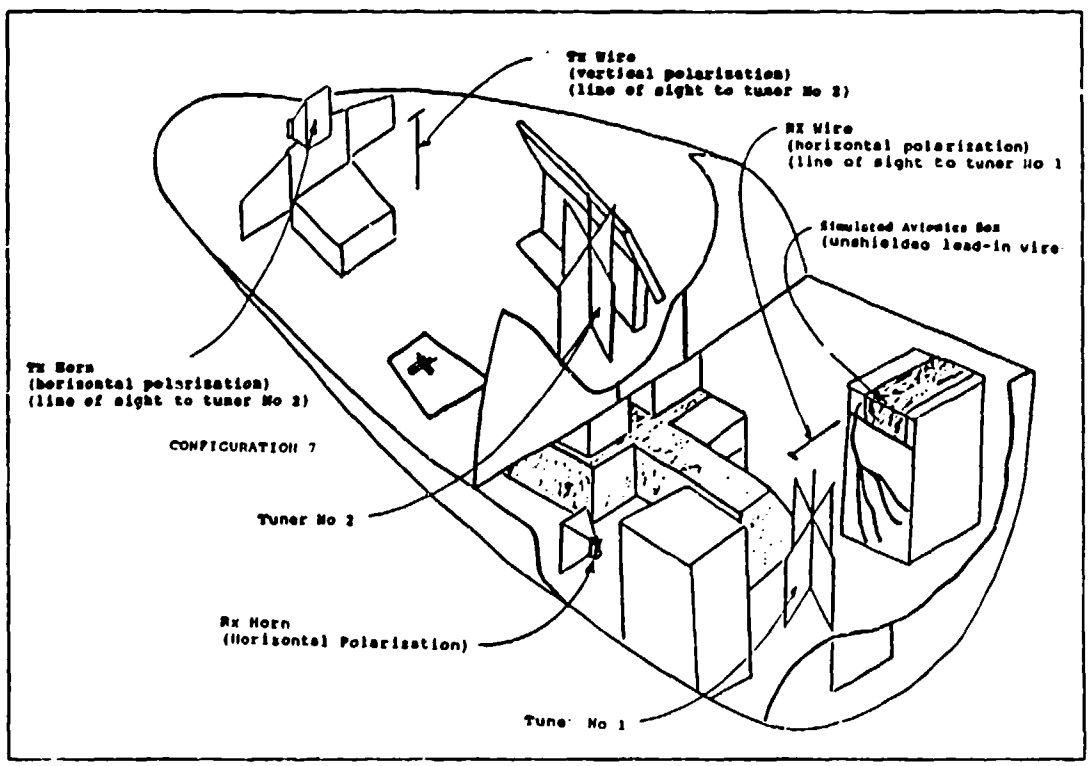

FIGURE 3-11. SCHEMATIC OF CONFIGURATION 7

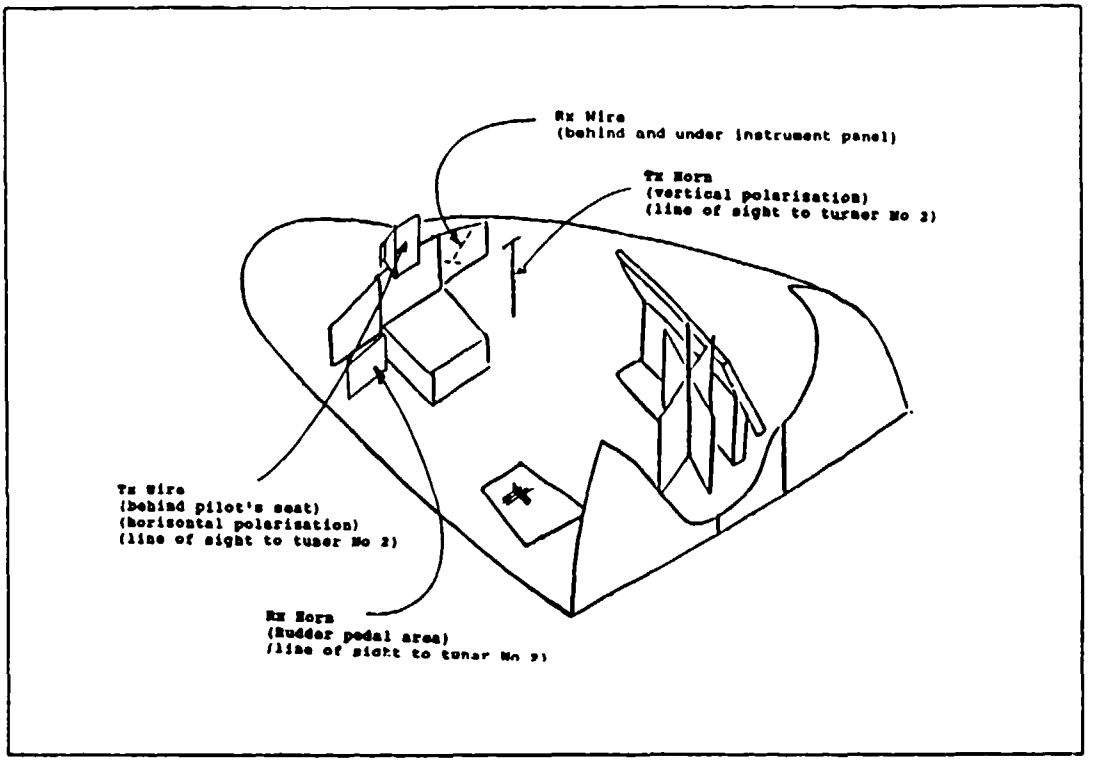

FIGURE 3-12. SCHEMATIC OF CONFIGURATION 8

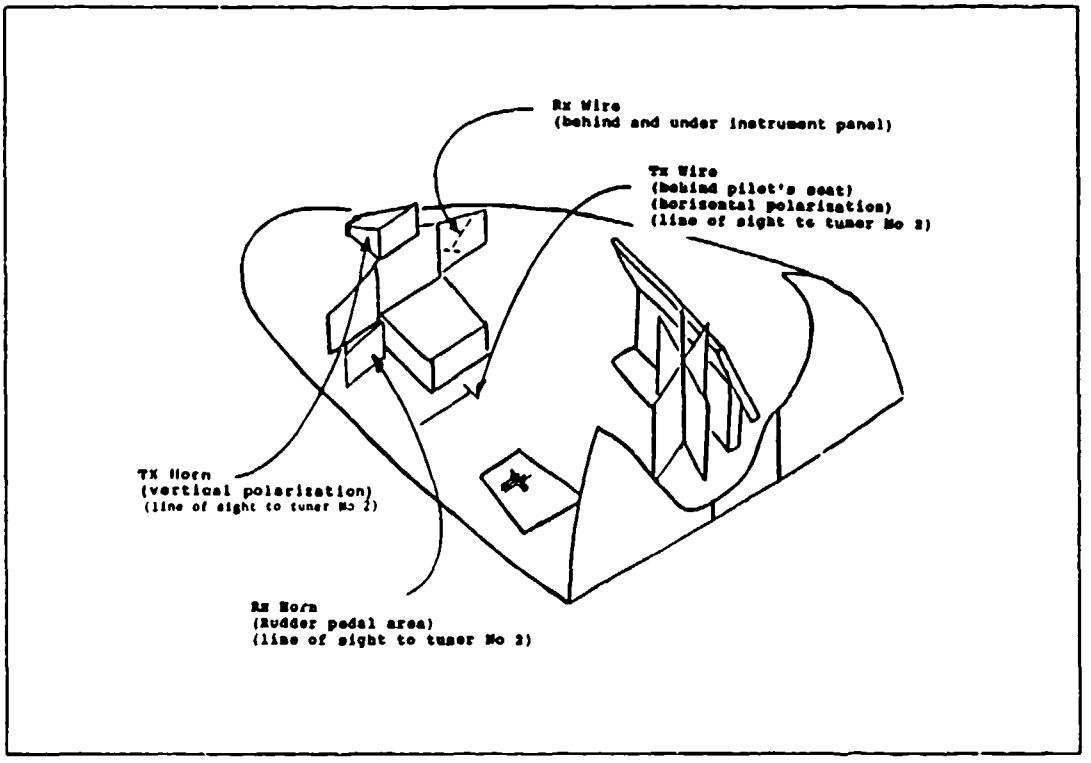

FIGURE 3-13. SCHEMATIC OF CONFIGURATION 9

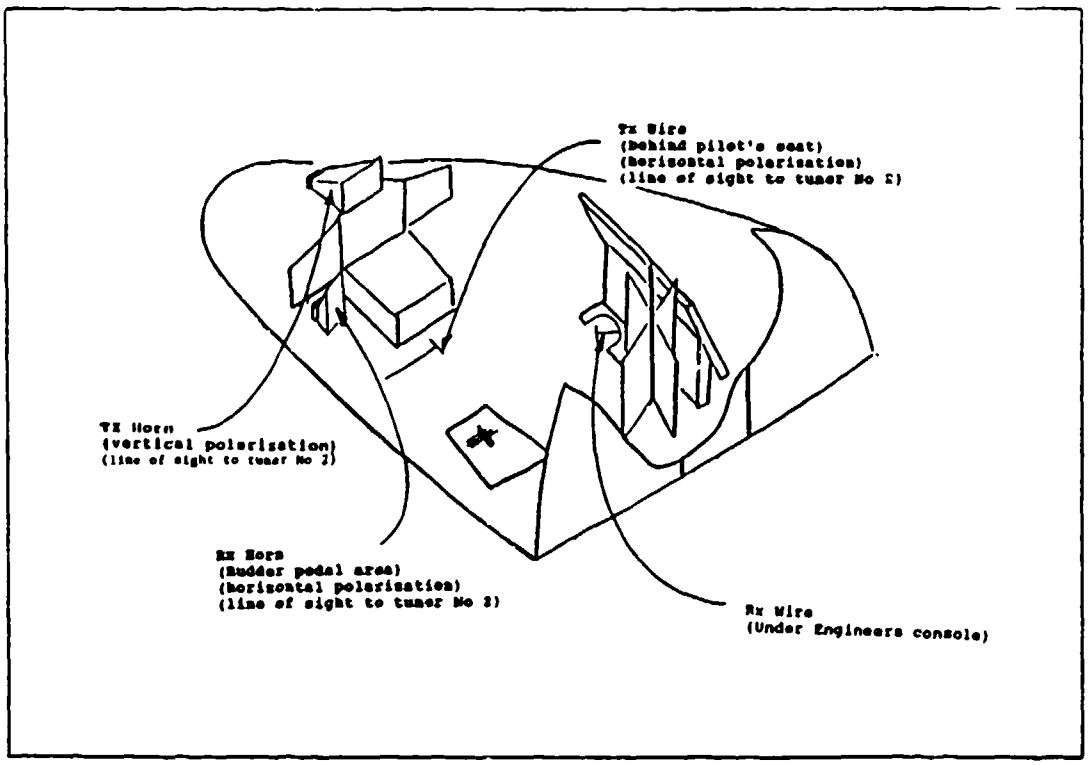

FIGURE 3-14. SCHEMATIC OF CONFIGURATION 10

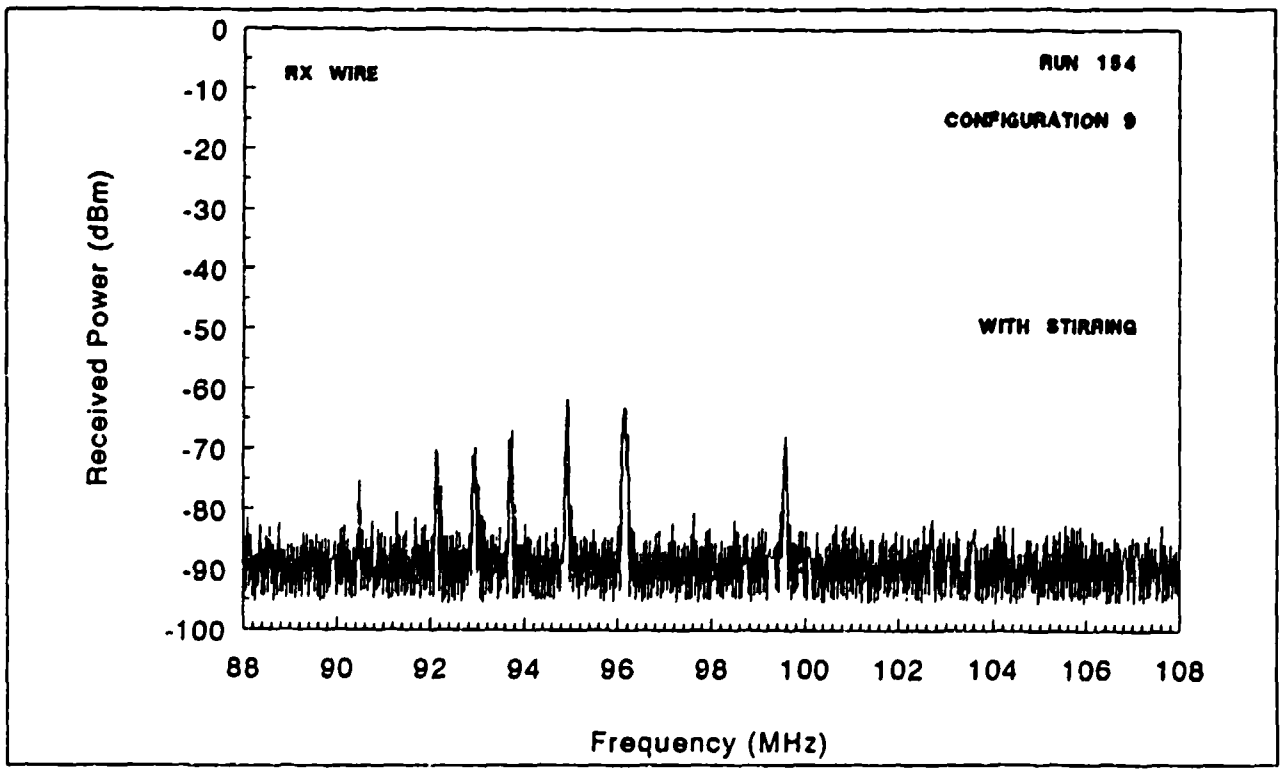

FIGURE 3-15. POWER RECEIVED IN COCKPIT DUE TO EXTERNAL AMBIENT FM BAND

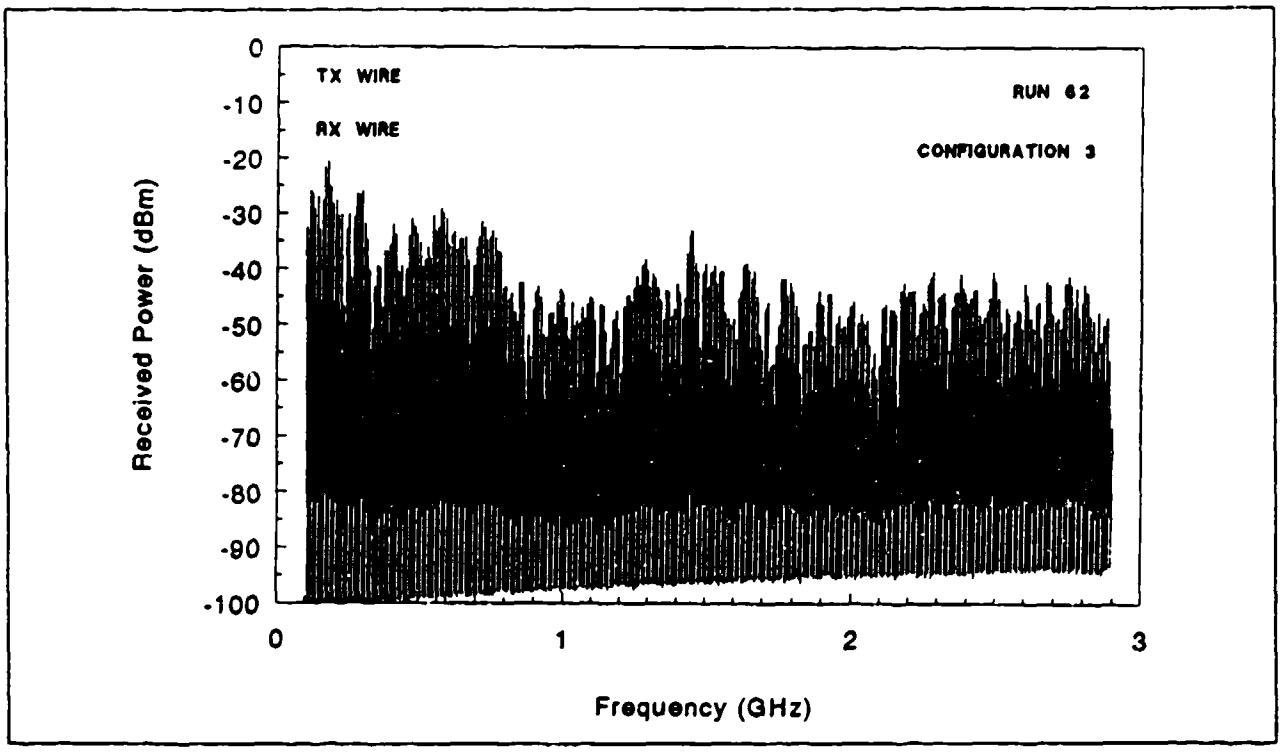

FIGURE 3-16. POWER RECEIVED IN AVIONICS BAY WITHOUT STIRRING FOR TX WIRE/RX WIRE FOR CONFIGURATION 3

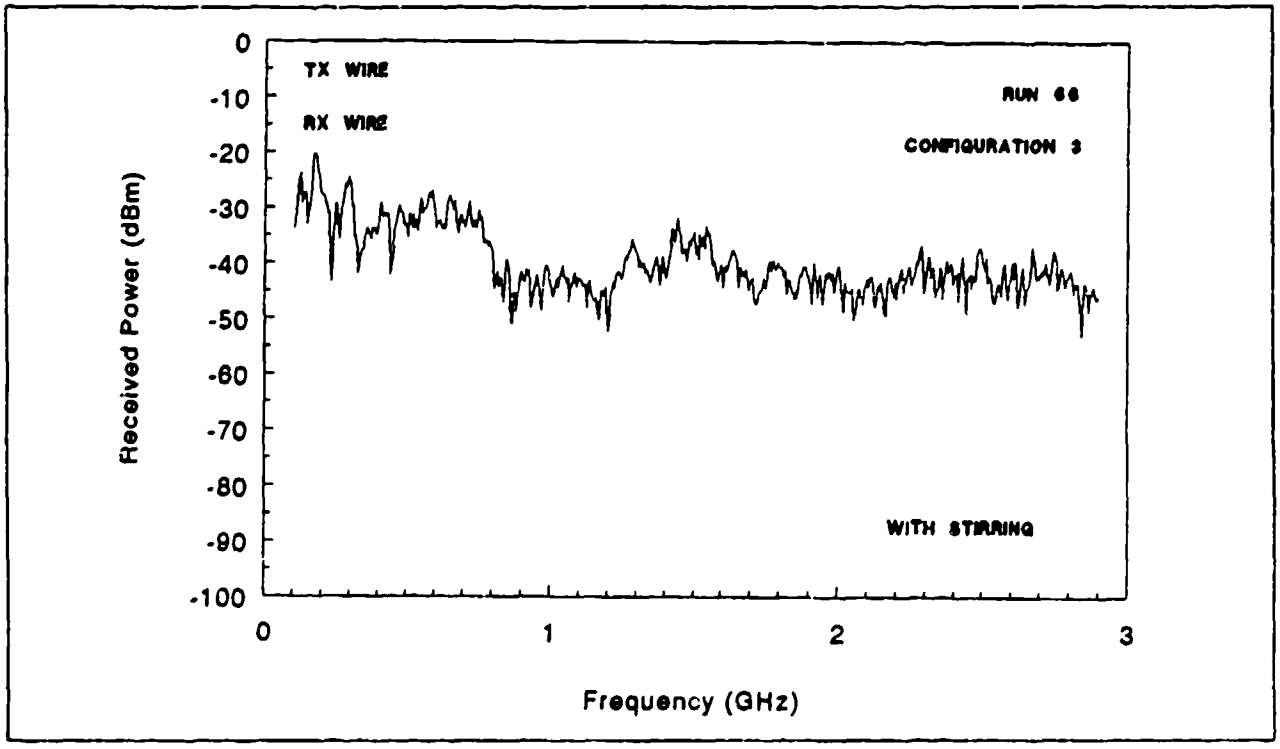

FIGURE 3-17. PEAK POWER RECEIVED IN AVIONICS BAY WITH STIRRING FOR TX WIRE/RX WIRE FOR CONFIGURATION 3

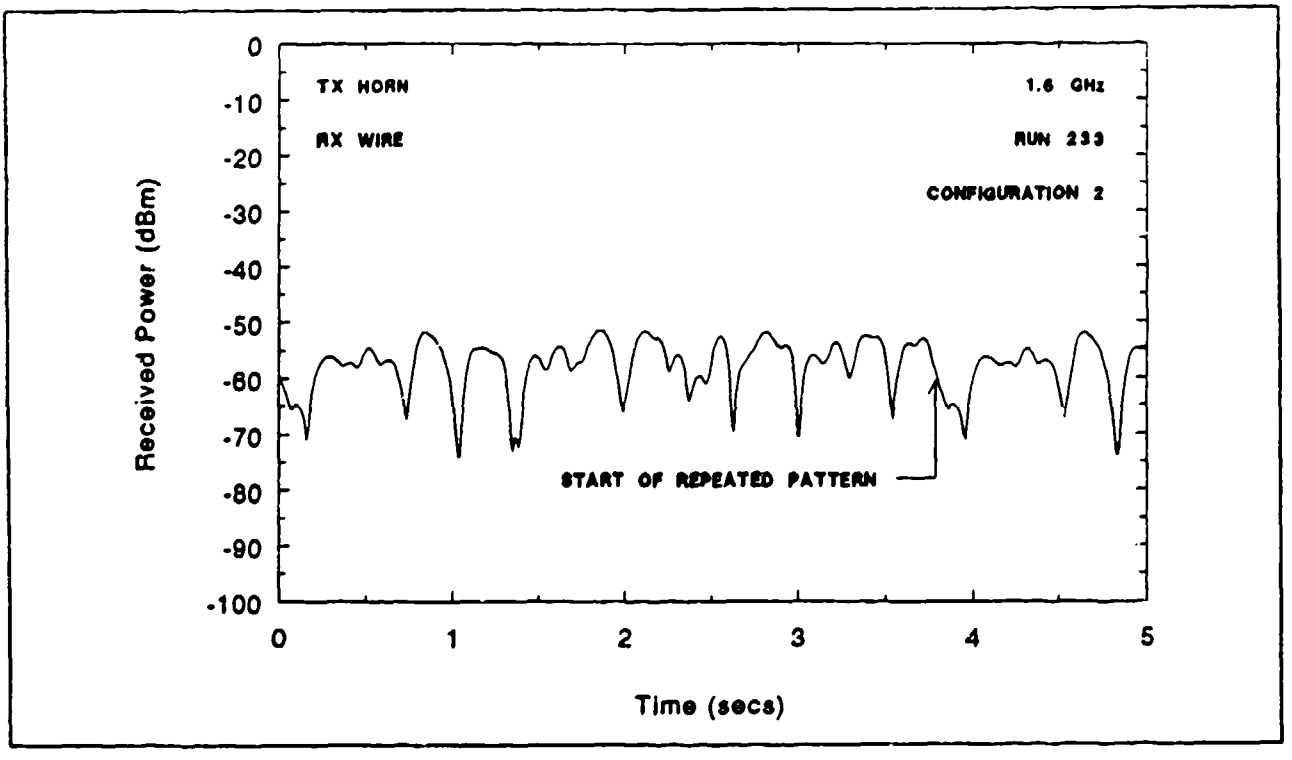

FIGURE 3-18. AVIONICS BAY DISCRETE FREQUENCY DATA (1.6 GHz) FOR CONFIGURATION 2

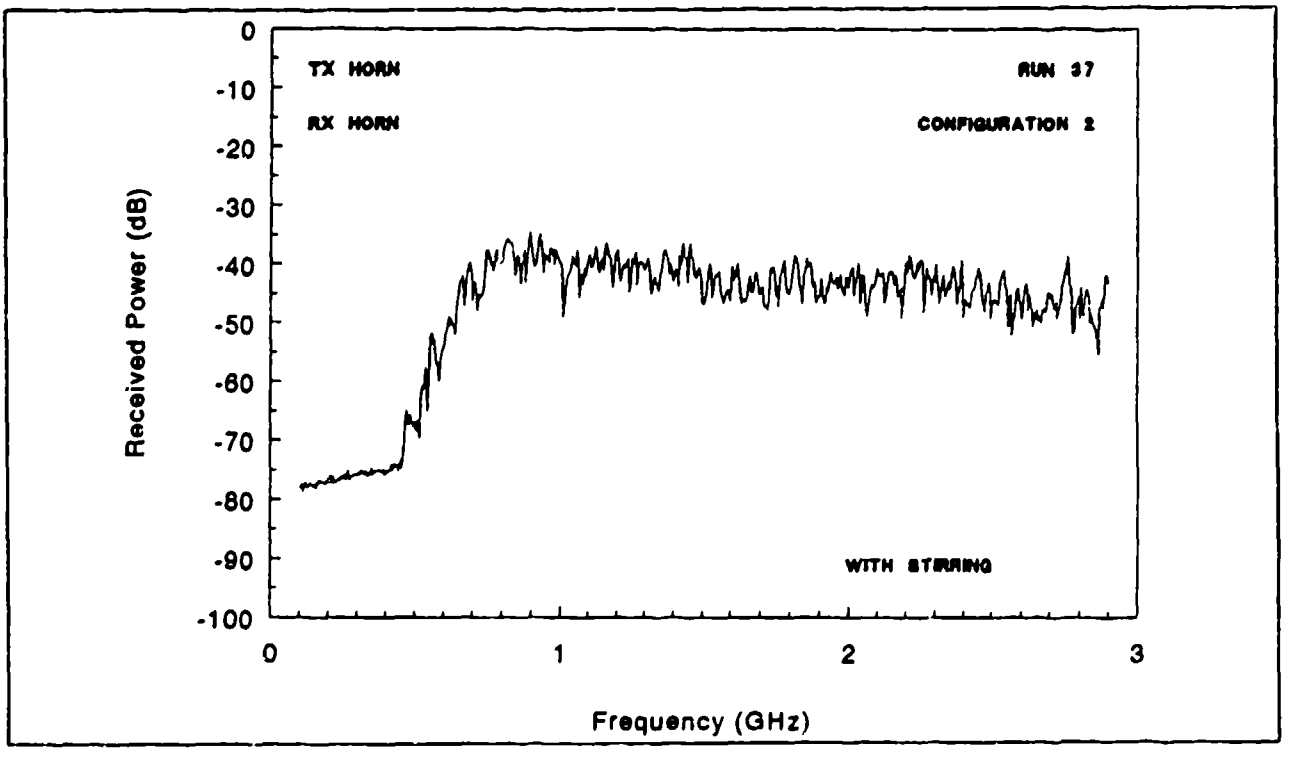

FIGURE 3-19. PEAK POWER RECEIVED IN AVIONICS BAY WITH STIRRING FOR TX HORN/RX HORN FOR CONFIGURATION 3

TABLE 3-1. TEST MATRIX

Data Type	Configurations						
	NSWCDD MSC	1	2	3A[1]	3B[1]	4A[3]	4B[3]
Calibration	1-6[2] 180-183 192-195						
Ambient without Stirring	176-179					73, 74, 76	
Ambient with Stirring						75 77	
Swept Frequency without Stirring		7-14			59-62	71 72	90
Swept Frequency with Stirring	184-191	15-22	37-44 47-50	51-58E	63-66	78-85	89
Discrete Frequency with Stirring	900-969	23-36	200-269 45, 46	300-361	67-70	400-461 86-88	
	5	6	7	8	9	10	11
Calibration							
Ambient without Stirring						156,158,162 163	
Ambient with Stirring		105, 106	112, 113	118, 119		153-155,157 159-161 164-165	166, 167
Swept Frequency without Stirring	91	93		122, 124	130-133		170-171 174, 175
Swept Frequency with Stirring	92	94-104E 107-108	114E, 115E 116, 117	120,121,123, 125-127	128-129 134-143	144-152	168, 169 172, 173
Discrete Frequency with Stirring		109-111 500-569		600-669	700-769	800-869	

[1]Prior to recheck of Configuration 3 data, a physical check of the bay found the support tie for the TX horn had broken and horn orientation was changed from original Configuration 3. Since it cannot be determined when orientation changed, will consider Configuration 3A and 3B, which may or may not be the same.
[2]Numbers identify specific data files.
[3]Rx horn removed from Configuration 4A to obtain Configuration 4B.

4.0 ANALYSIS OF DATA

The National Institute of Science and Technology (NIST) has empirically identified several conditions for a shielded enclosure to operate effectively as a reverberation or MSC.[1] First, the enclosure must be large compared to wavelengths of interest to provide a sufficient number of modes and mode density. Thus, cavity size sets a lower frequency limit on reverberation effectiveness.

Second, the enclosure losses should be low or equivalently Q should be high. The enclosure losses influence the field levels inside the enclosure for a given level of excitation, the spatial field uniformity, and the response to pulse excitation.

Finally, the tuner should be designed to perturb the modal structure and effectively distribute the EM energy over the available modes (mode stirring). The tuner should be metal, electrically large, and shaped and/or oriented to maximize randomization of the energy within the enclosure.

The tuner used in this test was constrained to on-site fabrication because of uncertainties about the size and accessibility of potential tuner locations. The tuner was approximately 0.6 by 0.6 by 0.6 m and was relatively symmetric compared to tuners in most MSCs. NIST recommends the tuner be at least $\lambda/2$ at the lowest frequency of operation.[1] Other work indicates the desirability of tuner dimensions equal to or greater than a wavelength.[2] For example, the NSWCDD tuner has its largest dimension equal to a wavelength for the lowest operational frequency. The NIST guideline suggests a potential minimum usable frequency of 250 MHz based on tuner dimensions. However the data show little mode mixing below about 800 MHz, which suggests the possibility that a larger tuner is required.

The original test plan proposed varying the tuner size to evaluate the tuner effectiveness dependence on size in the avionics bay. Time constraints prevented this investigation. Thus, with the data available, it cannot be determined if the lack of mode mixing below 500 MHz was the result of tuner effectiveness or the intrinsic mode structure characteristics of the avionics bay and cockpit.

---

[2]Wu, D. I. and Chang, D. C., "Effects of an Electrically Large Stirrer in a Mode-Stirred Chamber," *IEEE Trans. on EMC*, Vol. 31, No. 2, May 1989.

4.1 CAVITY LOSSES

Losses in an enclosure can be characterized by comparing the received power to the input power. Figure 4-1 shows the received power referenced to 0 dBm input power for the avionics bay in Configuration 2 as obtained in Runs 40 and 44 with wire TX and RX antennas. (Note that all the figures for this section can be found following the text.) The two runs are swept frequency data with stirring, and cover the two bands 0.1 to 2.9 and 2.5 to 18 GHz. The plot is referenced to 0-dBm input and corrected for measurement system losses but not for antenna response. The impact of the system measurement capability is apparent in that above approximately 6 GHz, the noise floor of the spectrum analyzers becomes a measurement limitation. Some data were observed above the noise floor up to about 9 GHz. The step response at about 13 GHz is an uncorrected, internal instrumentation band change.

Figure 4-2 overlays received power data for three wire-to-wire runs for 0.1 to 2.9 GHz, and Figure 4-3 overlays two runs for 2.75 to 18 GHz. These runs were obtained for different configurations of the TX and RX antennas in the avionics bay. A review of all the avionics bay data indicates an average variability between runs of about 8 dB with a maximum variation of 18 dB.

For comparison, Figure 4-4 shows the peak of the data from Figure 4-3 plus the received power in the NWSCDD MSC using the same measurement system. Above about 200 MHz, the difference between the received power in the two cavities for the same input power averages about 15 dB. Thus the data show that the avionics bay had approximately 15 dB greater losses than the low loss, high *Q*, NSWCDD MSC. As indicated in Section 2-1, the avionics bay was electromagnetically open to the passenger compartment and had many potential sources of energy absorption or leakage.

Figure 4-5 shows the received power for the cockpit in Configurations 9 and 10 obtained in Runs 135 and 145 for 0.1 to 2.9 GHz. Figure 4-6 shows similar data from Run 139 for 2.5 to 18 GHz. In reviewing all the cockpit data, it was found that the average variability in the received power was about 5 dB with a maximum variation of 15 dB. Figure 4-7 shows the peak data from Figure 4-5 and the received power data in the NWSCDD MSC with both referenced to 0-dBm input power. The cockpit loss is somewhat less than that of the avionics bay and averages approximately 12 dB greater loss than the NWSCDD MSC.

4.2 COCKPIT TO AVIONICS BAY COUPLING/ISOLATION

In Configurations 6 and 7, the horn and wire TX antennas were located in the cockpit while the horn and wire RX antennas remained in the avionics bay. Data were collected for combinations of tuner 1 (avionics bay) and tuner 2 (cockpit) operations. Operation of both tuners yielded a bounding condition for the energy received in the avionics bay. Figure 4-8 indicates the power received in the avionics

bay for an input power in the cockpit referenced to 0 dBm. Both tuners were operating when these data were collected.

The coupling/isolation of the cockpit and avionics bay can be evaluated by performing an energy balance analyses for the cavities using data collected during the test. The energy balance analysis is based on

$$(Power\ In)_{cavity} = (Power\ Out)_{cavity} \tag{4-1}$$

As shown in Figure 4-9, the energy balance in the cockpit when the cockpit is internally excited by the TX antennas can be described by

$$P_{in/c} + \sigma_{ab} \cdot PD_{ab/c} = P_{rec/c} + L_c \cdot PD_c + \sigma_c \cdot PD_c \tag{4-2}$$

where

$P_{in/c}$ = Power injected into the cockpit by the TX antenna
σ_{ab} = Coupling coefficient from the avionics bay to the cockpit
$PD_{ab/c}$ = Power density in the avionics bay due to coupling from the cockpit
$P_{rec/c}$ = Power extracted from the cockpit by RX antennas in the cockpit
L_c = Loss coefficient that includes all power losses from the cockpit other than that coupled to the avionics bay or extracted by the RX antenna
PD_c = Power density in the cockpit
σ_c = Coupling coefficient from the cockpit to the avionics bay

The data in Figure 4-5 show the $P_{rec/c}$ of equation (4-2) when the cockpit is internally excited.

The energy balance in the avionics bay can be described by a similar expression

$$P_{in/ab} + \sigma_c \cdot PD_{c/ab} = P_{rec/ab} + L_{ab} \cdot PD_{ab} + \sigma_{ab} \cdot PD_{ab} \tag{4-3}$$

where the terms are equivalent to those previously defined. The data in Figure 4-2 show the $P_{rec/ab}$ of equation (4-3) when the avionics bay is internally excited.

Note the terms $\sigma_{ab} * PD_{ab/c}$ and $\sigma_c * PD_{c/ab}$ as power input terms in equations (4-2) and (4-3) are second-order effects and will be neglected in the following analysis.

Finally, the energy balance in the avionics bay due to excitation in the cockpit can be described by

$$\sigma_c \cdot PD_c = P_{rec\,ab\,c} + L_{ab} \cdot PD_{ab\,c} + \sigma_{ab} \cdot PD_{ab\,c} \tag{4-4}$$

The data in Figure 4-8 show the $P_{rec\,ab\,c}$ of equation (4-4) when the cockpit is internally excited.

It is assumed by symmetry that the coupling coefficients σ_c and σ_{ab} are the same and the subscripts will be dropped.

The power density can be expressed in terms of the measured received power

$$P_{rec} = A_{eff} \cdot \eta \cdot PD \tag{4-5}$$

where A_{eff} is the effective area of the antenna and is $\lambda^2/8\pi$ for an antenna with Gain = 1, and η is the antenna efficiency.

Equations (4-3) and (4-4) can be solved for σ by eliminating L_{ab} and using the value of PD_c obtained from the data of Figure 4-5 in equation (4-5).

$$\sigma = (\eta \cdot \lambda^2/8 \cdot \pi)(P_{rec/ab/c}/P_{in/c})/(P_{rec/c}/P_{in/c})(P_{rec/ab}/P_{in/ab}) \tag{4-6}$$

The three received power ratios are available from measured data shown in Figures 4-8, 4-7, and 4-4, respectively.

Figure 4-10 shows the coupling coefficient, σ(dB-m^2), as a function of frequency based on equation (4-6) and the data in Figures 4-4, 4-7, and 4-8 assuming the wire antenna efficiency is 0.75 and constant with frequency. A linear fit to the data above 800 MHz where mode stirring begins to become effective indicates the average value of the coupling coefficient varies from about -9 dB-m^2 at 800 MHz to -14 dB-m^2 at 2.9 GHz.

Another way to quantify the coupling/isolation between the cavities is to consider the ratio of the coupling coefficient to the loss coefficient. The loss coefficient, L_c, can be evaluated using the energy balance equation (4-6). Figure 4-11 shows the ratio σ/L_c. This parameter quantifies the fraction of the energy introduced into the cockpit that will couple to the avionics bay. From an operational point of view, the quantity of most interest is the maximum energy that can be coupled between the two aircraft cavities. A bounding envelope on the coupling/loss coefficient curve indicates that over the frequency range 800 MHz to 2.9 GHz the ratio varies from -12 dB to -6 dB with the maximum coupling near 2.5 GHz. Thus over this frequency range up to approximately 25 percent of the energy entering the cockpit could couple to the avionics bay.

4.3 STIRRING RATIO

The SR is defined as the maximum received power to minimum received power (or the noise floor whichever is highest) for discrete frequency measurements over a complete rotation of the tuner.

The SR is a qualitative measure of the effectiveness of the randomization of the EME in the enclosure. Although many factors will influence the SR, the enclosure Q and the tuner effectiveness are substantial contributors. Note that a valid measurement of the SR requires care in positioning the TX and RX antennas to avoid direct line of sight. A SR of at least 20 dB is an empirical guideline defined by NIST,[1] which implies that the tuner is operating effectively and that the field spatial uniformity and peak-to-average values are consistent with the expected characteristics of a MSC.

For each configuration, up to four received power measurements could be available at each discrete frequency. The four measurements are obtained from the permutations of two TX and two RX antennas.

Figure 4-12 shows discrete frequency data of Run 226 for 1.0 GHz for the wire TX and the horn RX antenna combination in Configuration 2. Figure 4-12 shows the effect of the tuner rotation on the received power. The pattern repetition can be seen to start at about 4 sec. The maximum and minimum received power are -45.2 dB and -78.5 dB, respectively, for a SR ratio of 33 dB. All the SR data for the wire TX and horn RX antenna combinations for Configuration 2 are shown in Figure 4-13. At 500 MHz, the lowest discrete frequency sampled for a horn antenna, the SR is about 9 dB. Most of the remaining data points are above 20 dB. Figure 4-14 shows another example of a discrete frequency measurement. The data are below the noise floor of the measurement system at about -78 dB. In these cases, the SR is determined by using the noise level as the minimum received power. Thus in noise limited data, the actual SR is equal to or greater than the reported value. Figure 4-15 shows the SR for the combination of horn TX and wire RX antennas for Configuration 2. Note that the bold symbols indicate the minimum power received was limited by the noise floor so that the plotted data are a minimum SR. Figure 4-16 shows the wire TX and wire RX antenna SR data, and Figure 4-17 shows the horn TX and horn RX SR data for Configuration 2. Figure 4-18 summarizes all the SR data for Configuration 2. A substantial number of the data points exceed the commonly accepted 20 dB guideline for effective stirring in a MSC.

Figure 4-19 shows the SR data for Configuration 1. A discrete frequency matrix was not obtained for Configuration 1 so the available data are considerably less than that available for Configuration 2. In Configurations 3 and 4, the simulated avionics box replaced the horn as the RX antenna. The box results will be presented in Sections 4.5 and 4.6 . The available SR data for Configurations 3 and 4 are shown in Figures 4-20 and 4-21, respectively. No SR data were obtained in Configuration 5.

The SR data for Configuration 6 are shown in Figure 4-22 with the TX antennas in the cockpit and the RX antennas in the avionics bay. Both tuners were operating. At 500 MHz and below, the SR is less than 10 dB. Above about 600 MHz, the data generally exceed 10 dB and a substantial number of the data points exceed 20 dB. No SR data were obtained for Configuration 7.

Configurations 8, 9, and 10 had all the antennas in the cockpit. The SR data for these configurations are shown in Figures 4-23, 4-24, and 4-25, respectively. The cockpit data appear to have a somewhat lower SR than the avionics bay up to about 1 GHz. Above 1 GHz, a substantial number of data points exceed 20 dB.

An analysis of the SR data was performed to determine if there was a correlation between SR and peaks and nulls in the swept frequency data. Figure 4-26 shows the swept frequency data for Run 40, which was obtained in Configuration 2 with stirring. At the peak at 2.295 GHz, noted with a marker, the received power as a function of tuner position (i.e., time) is shown in Figure 4-27. The SR is about 8 dB, which from Figure 4-18 is one of the lowest values for the SR obtained in that configuration and combination of antennas. At the narrow minimum at 1.96 GHz, the received power as a function of tuner position is shown in Figure 4-28. These data yield a noise-limited SR of about 14 dB. As another example, a discrete frequency measurement was obtained at the marker frequency of 787 MHz shown in Figure 4-29. The SR data for 787 MHz are noise limited at about 28 dB. Note that in each of these examples, the same antenna combination was used for both the swept and discrete frequency data. Figures 4-30 and 4-31 show typical swept frequency data and the SR obtained at the discrete frequencies indicated by the markers. For these frequencies, there is no correlation between the SR and the received power. From analysis of these examples and other data, no correlation was found between the SR and peaks or nulls or the magnitude of the received power.

In summary, the SR data indicate

- Stirring effectiveness is limited below 800 MHz
- A significant number of data points with SR over 20 dB occurred for the frequency range 800 MHz to 10 GHz for all configurations
- No general SR correlation was observed with peaks, nulls, or received power levels

The data indicate that both the avionics bay and cockpit approach, and in many cases exceed, the commonly accepted 20 dB guideline for stirring effectiveness. Both the intrinsic EM properties of the avionics bay and the cockpit as well as the tuner contribute to the observed SR. Insufficient time was available to characterize the tuner dependence. However, it is quite probable that the tuner effectiveness could be improved by making the paddles more asymmetric as well as larger. Thus, it is possible that the promising SR reported may be improved by additional attention

to tuner configuration. A corollary is that the test data indicate that the intrinsic characteristics of the aircraft satisfy a necessary condition; that is, a reasonable SR, for behavior as a MSC.

4.4 STIRRING STATISTICS

The statistical properties of the EME provide a more rigorous basis for comparison of the EME in aircraft cavities and MSCs. A number of the statistical properties of the EME in a highly moded, complex cavity are predicted by theory.[3,4] The probability density function for the power density at a discrete frequency in a complex cavity where the fields are isotropic and randomly polarized is given by[4]

$$[exp\{(P_{rec} - \mu)/\Sigma - exp((P_{rec} - \mu)/\Sigma)\}]/\Sigma \qquad (4\text{-}7)$$

where μ is the arithmetic mean of the power density expressed in decibels and $\Sigma = 10 \; Log \; e = 4.34 \; dB$

Figure 4-32 shows the data for Run 87 in Configuration 4 for a discrete frequency of 2.0 GHz. These data and those to be discussed for Runs 205 and 441 were selected from over 400 data runs to show specific statistical attributes. Figure 4-32 shows the stirring effects for one rotation of approximately 4 sec. It also shows the pattern repetition discussed in Section 4.3 in the interval between 4 to 5 sec. Run 87 data yielded a SR of 21 dB and therefore based on the empirical 20 dB guideline discussed in Section 4.3, implies sufficient stirring to be representative of a MSC EME.

The probability density distribution for the experimental data is quite sensitive to the received power interval, or bin size, used to collect the experimental data. The arbitrary selection of a bin size can be avoided by using the cumulative probability density. The theoretical cumulative distribution function is obtained by integrating the probability density function, equation (4-7) given above. The theoretical and experimental cumulative distributions for Run 87 are shown in Figure 4-33. At values of the received power higher than the average value (the region of most significance), the agreement between the two distributions appears quite good. However the full distribution fails a statistical test at a reasonable level of significance. Statistical parameters like the standard deviation (SD) of the received power data and the peak-to-average ratio can also be considered. The SD of these data is 4.1 dB versus the theoretically predicted value of 5.7 dB. The peak-to-average value is 5.9 dB based on the arithmetic mean of the data. The peak-to-average ratio based on the geometric mean can be determined from the data in Figure 4-33. The statistical parameters suggest the avionics bay EME may not be completely isotropic and randomly polarized even though the 20-dB SR guideline is satisfied.

---

[3]Lehman, T. H., *Private Communication*, Consultant, Albuquerque, NM. Oct 1992.

[4]Lehman, T. H., Paper presented at the Anechoic Chamber and Reverberation Chamber Operators Group Meeting, NSWCDD, Dahlgren, VA, Nov 1992.

Figure 4-34 shows the data for Run 205 for a discrete frequency of 500 MHz in Configuration 2. The data indicate a SR of 9 dB, a peak-to-average ratio of 2.8 dB, and a SD of 2.4 dB. Figure 4-35 shows poor agreement between the theoretical and experimental cumulative distributions for Run 205. Thus the statistical parameters of the measured data imply a significantly greater departure from the theoretical predictions than the previous case. This implies that SR values lower than 20 dB reflect EME conditions where the cavity fields are not isotropic and randomly polarized.

Figure 4-36 shows another example of discrete frequency stirring data. In this case, Run 238 at 2.5 GHz in Configuration 2, there is a deep null in the data. The null is actually below the noise floor at about -78 dBm. The large SR derived from the deep null does not necessarily reflect a better test environment that depends on achieving the maximum (as opposed to minimum) values of all three field components. All the SR data presented in this report have been corrected for the noise floor. The corrected value for Run 238 is 29 dB. The cumulative probability distribution for the received power is shown in Figure 4-37. In this case, the distribution of the measured data passes the statistical test for equivalence to the theoretical distribution. The SD for Run 238 is 4.9 dB, which is a better match to the theoretical SD of 5.7 dB than was observed for Run 87. The peak-to-average ratio is 7.7 dB.

Figure 4-38 shows the cumulative probability distribution for the received power in the cockpit for Run 628 at 1.2 GHz in Configuration 8. The run was selected because the SR is approximately 30 dB. The abscissa in Figure 4-38 is the received power referenced to the mean of the run. This normalized parameter can be used to directly compare different data runs as well as compare measured data to the theoretical distribution. The data suggest that for a given average power density in an aircraft cavity, the bounding EME is isotropic and randomly polarized.

Also shown in Figure 4-38 are data from the NSWCDD MSC at 1.2 GHz using the same measurement system as was used in the aircraft and the theoretical distribution. The agreement between the data runs is an indication of how well the EME in an adequately stirred aircraft cavity is represented by a MSC test. Note that the mean value of the received power for a cavity can be adjusted by varying the input power so that the test EME in a MSC can be adjusted to match that specified for the aircraft cavity certification level.

In summary, three examples of discrete frequency stirring data runs were shown in Figures 4-32, 4-34, and 4-36. The agreement between the measured data and the theoretical predictions for an isotropic and randomly polarized EME varies for the three data runs. The parameters compared included the SR, the peak-to-average ratio, the SD of the data, and the cumulative probability distribution. Generally, as the SR increases, the parameter agreement gets better. The data suggest that during a measurement, SRs greater than 30 dB (rather than the 20 dB guideline) may be required to assure an isotropic and randomly polarized EME in a

low Q complex cavity. The agreement between the discrete frequency received power, and therefore the power density, cumulative distribution functions for the aircraft cavities and a MSC suggests that a MSC provides a test EME that is representative of the complex EME in aircraft cavities.

4.5 SIMULATED AVIONICS BOX RESPONSE IN AIRCRAFT

The simulated avionics box provided by LLNL was described in Section 2.1. The results presented in this section characterize the signals on the monitored trace on the circuit board in the box enclosure.

Figure 4-39 shows the box response for Runs 53, 65, and 80 when the bay was excited by a wire antenna. These data are corrected for system losses and the preamplifier, and normalized to 0 dBm input power. The runs were obtained for different locations, orientations, or polarizations of the wire TX antenna with the tuner operating. The run data are consistent in terms of the magnitude as well as the detailed structure of the responses. The average variability between runs is about 4 dB.

The box response data can be described in terms of a transfer function

$$Power\ Received_{box}(f) = Transfer\ Function\ (f) * Power\ Density_{ab}(f) \qquad (4\text{-}8)$$

The transfer function includes the effects of energy coupled to the attached cables or penetrating through the box seams, any internal box resonances or Q effects, the coupling of energy to the circuit board, and the energy distribution to the measured trace. The avionics bay power density was calculated from the average of the received power data of Figure 4-2 using equation (4-5). The peak response of the data in Figure 4-39 represented the box received power. The transfer function is shown in Figure 4-40.

The same transfer function characteristics are evident in Figure 4-41, which shows the data for horn excitation. At low frequencies, the error in the transfer function is large due to the falloff in horn effectiveness below its design range of 1 to 18 GHz. Above about 500 MHz, the two data traces of Figures 4-40 and 4-41 show good agreement.

The first observation from Figure 4-40 (and 4-41) is that the average of the transfer function increases slightly with frequency. The second observation from Figure 4-40 (and 4-41) is that there is frequency-dependent structure overlaid on the average response. As examples, there are the reduced transfer function over the frequency range 500 to 900 MHz, the peak values in the frequency interval 900 MHz to 1.0 GHz, and several structures at higher frequencies. These responses are consistent in the box response data of Figure 4-39 as well as in the transfer function data of Figure 4-40.

4.6 COMPARISON OF SIMULATED AVIONICS BOX RESPONSE IN AIRCRAFT AND MSC

The major issue addressed in this section is whether a MSC test will excite the same internal box response as observed in the avionics bay. The simulated avionics box was also tested in the NSWCDD MSC using the same measurement system. Only one MSC measurement run is available using the wire TX antenna. Data were collected only to 2.5 GHz and are shown in Figure 4-42. The magnitude of the received signal is about 15 dB greater than that received in the avionics bay and shown in Figure 4-39. The 15 dB offset is consistent with the difference in the loss in the MSC and the avionics bay shown in Figure 4-4 where data for both cavities are referenced to 0 dBm input. For a test environment, the MSC power input would be adjusted to provide the same power density as measured in the avionics bay. Figure 4-42 also shows that the simulated avionics box has a frequency-dependent trend of about a 5 dB increase in the received signal. A detailed analysis of the frequency-dependent structure showed that 13 resonance structures over the frequency interval 100 MHz to 2.5 GHz were common in both cavities.

The transfer function for the box in the MSC is shown in the bold trace of Figure 4-43. Also included for reference is the transfer function for the box in the aircraft avionics bay (from Figure 4-40). The transfer functions remove the effects of differences in cavity power densities. Note the agreement in both the structure and magnitude of the transfer functions above about 200 MHz. The difference between the box transfer functions measured in the NSWCDD MSC and the avionics bay for excitation by the wire TX antenna is shown in Figure 4-44. Zero difference indicates an identical box response in the MSC and the avionics bay. A positive difference means the box response was greater in the MSC.

Although the aircraft data available generally cover the frequency range 100 MHz to 10 GHz, the comparisons of this section apply to a restricted frequency range. As mentioned, the MSC reference data are limited to the frequency interval 100 MHz to 2.5 GHz. Low frequency data, below approximately 800 MHz, should be used with caution. It is likely that the tuner size resulted in limited mode stirring in the aircraft below about 800 MHz. While the aircraft data show significant signal structure below 500 MHz, conclusions about the avionics bay EME below 800 MHz are speculative. Therefore, it is believed that an appropriate frequency range for comparing the MSC and avionics bay box response data from this test is about 800 MHz to 2.5 GHz.

One observation is that most of the data are positive. This indicates a MSC test will, in general, excite at least as much response in the box as would be excited when the box was in an avionics bay. This is an important observation for evaluating the feasibility of MSC testing for certification of avionics equipment to operating conditions inside an aircraft avionics bay.

A comparison of the signals at 96.1 and 99.5 MHz in Figures 4-46 and 4-49 yield estimates of both the BCSE and the MSE. For the FM band in the avionics bay, it was found that

$$BCSE_{FM\ avionics\ bay}(99.5\ MHz) = 25\ dB$$
$$MSE_{FM\ avionics\ bay}(96.1\ MHz) = 3\ dB$$

Using an FM signal (92.1 MHz) with considerably less observed variability than that noted for 96.1 MHz, a MSE of 6 dB was obtained. Therefore data other than 96.1 MHz supports low values of the MSE as defined earlier. As a further verification, it was observed that several FM stations could be heard with the receiver in the avionics bay. Stations at 96.1 and 99.5 MHz were particularly noted as *loud and clear*.

For the VHF/UHF band, a comparison of the markers at 496 MHz in Figures 4-45 (avionics bay) and 4-47 (external ambient) show an external to internal attenuation of 15 dB, whereas the data for the 184-MHz signal imply a 3 dB gain. Thus for the VHF/UHF band in the avionics bay it was found that

$$BCSE_{UHF\ avionics\ bay}(496\ MHz) = 15\ dB$$
$$MSE_{VHF\ avionics\ bay}(184\ MHz) = 3\ dB\ gain$$

One of the several internal ambient data runs for the cockpit is shown in Figure 4-50. The change of the spectrum analyzer resolution bandwidth resulted in better than a 10 dB improvement in the noise floor. Comparing the marker value of -58 dBm at 96.1 MHz in Figure 4-50 with the external ambient of approximately -61 dBm in Figure 4-46, the implication of a gain of 3 dB was found. Another data run with a measured signal of -68 dBm at 99.5 MHz was used to define the BCSE. For the FM band in the cockpit it was found that

$$BCSE_{FM/cockpit}(99.5\ MHz) = 25\ dB$$
$$MSE_{FM/cockpit}(96.1\ MHz) = 3\ dB\ gain$$

Other frequency data (e.g., 94.9 MHz) yield a MSE of 4 dB.

For the VHF/UHF band, the cockpit data generally show only a few signals rather than the fairly large number of strong signals observed in the external measurements. The BCSE estimate occurs at 496 MHz.

Figure 4-51 shows an example of an internal signal of -62 dBm at 207 MHz compared to an external signal of -68 dBm in Figure 4-47. The SE bounds for the VHF/UHF band in the cockpit are

$$BCSE_{UHF\ cockpit}(496\ MHz) = 22\ dB$$
$$MSC_{VHF\ cockpit}(207\ MHz) = 6\ dB\ gain$$

Figure 4-51 also shows a common phenomenon observed in the data acquired in the cockpit. The strong signal at 483 MHz was observed several times in the cockpit but was not seen in the external measurement.

Considering all available data for the FM and VHF/UHF bands, it was found that the MSE (as defined) is in the range of 0 dB with variations of a few decibels of gain or attenuation.

In summary, a significant number of relatively strong emitters in the FM and VHF/UHF bands existed in the local area. Most of these are commercial broadcasters although some aeronautical communications frequencies would also be expected. These signals could provide a passive method of investigating aircraft SE over the frequency range 88 to 800 MHz. The local aeronautical radars could also provide a measurable signal over the 1 to 2 GHz frequency interval.

Since the SE data were not a test objective, only limited data were acquired and cannot be used to develop specific SE values. Rather the data were used to develop bounds (a best case and a minimum case) for the SE. The SE range supported by the data is about 25 dB of attenuation to a few decibels of gain.

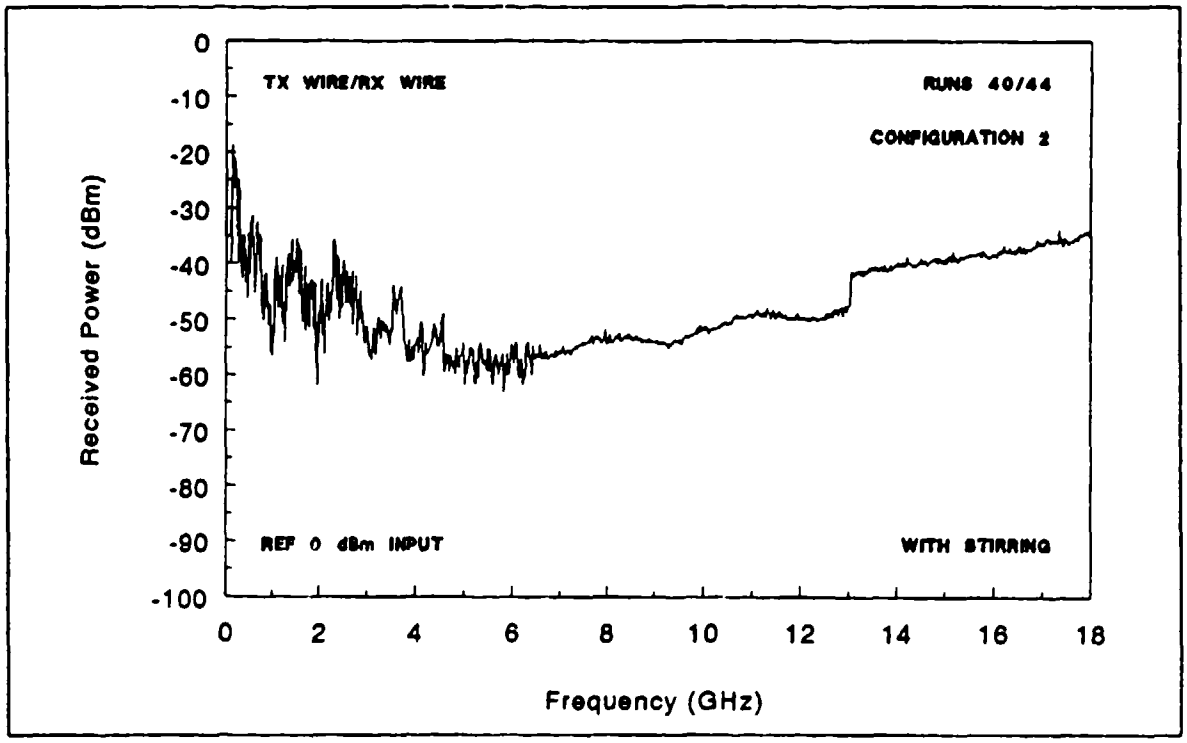

FIGURE 4-1. PEAK POWER RECEIVED IN AVIONICS BAY FOR CONFIGURATION 2 (0.1 TO 18 GHz)

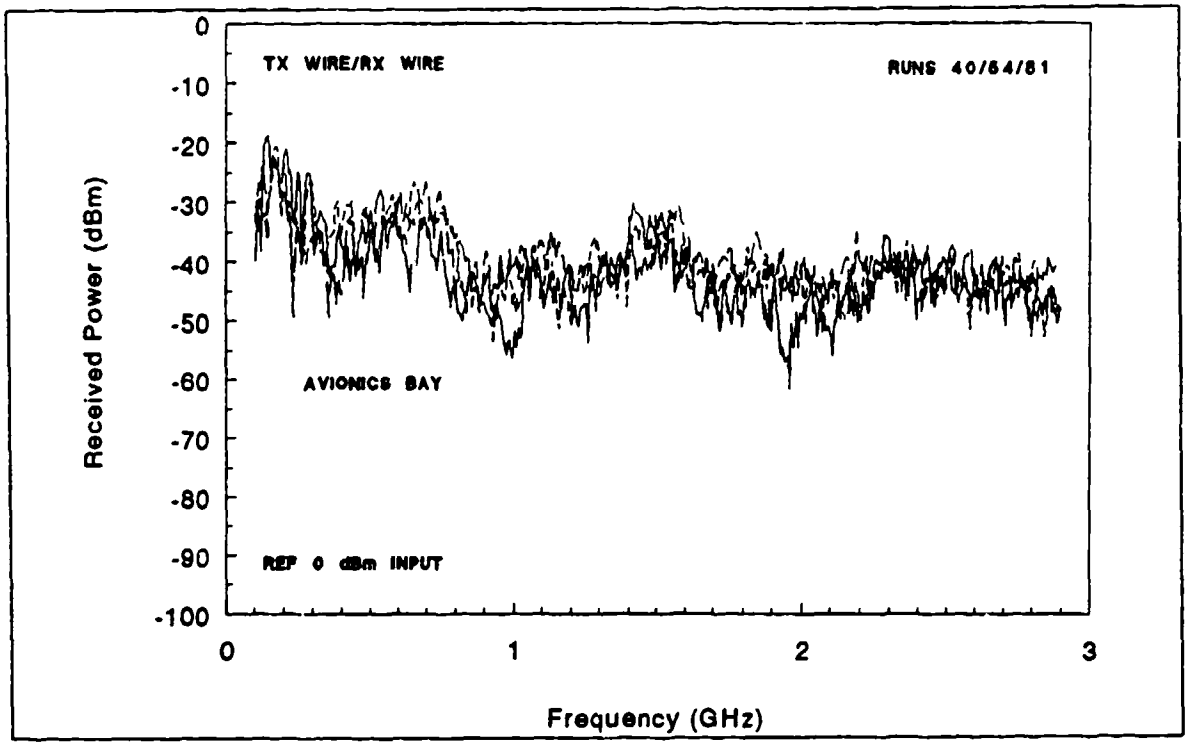

FIGURE 4-2. COMPARISON OF PEAK POWER RECEIVED IN AVIONICS BAY FOR THREE DATA RUNS (0.1 TO 2.9 GHz)

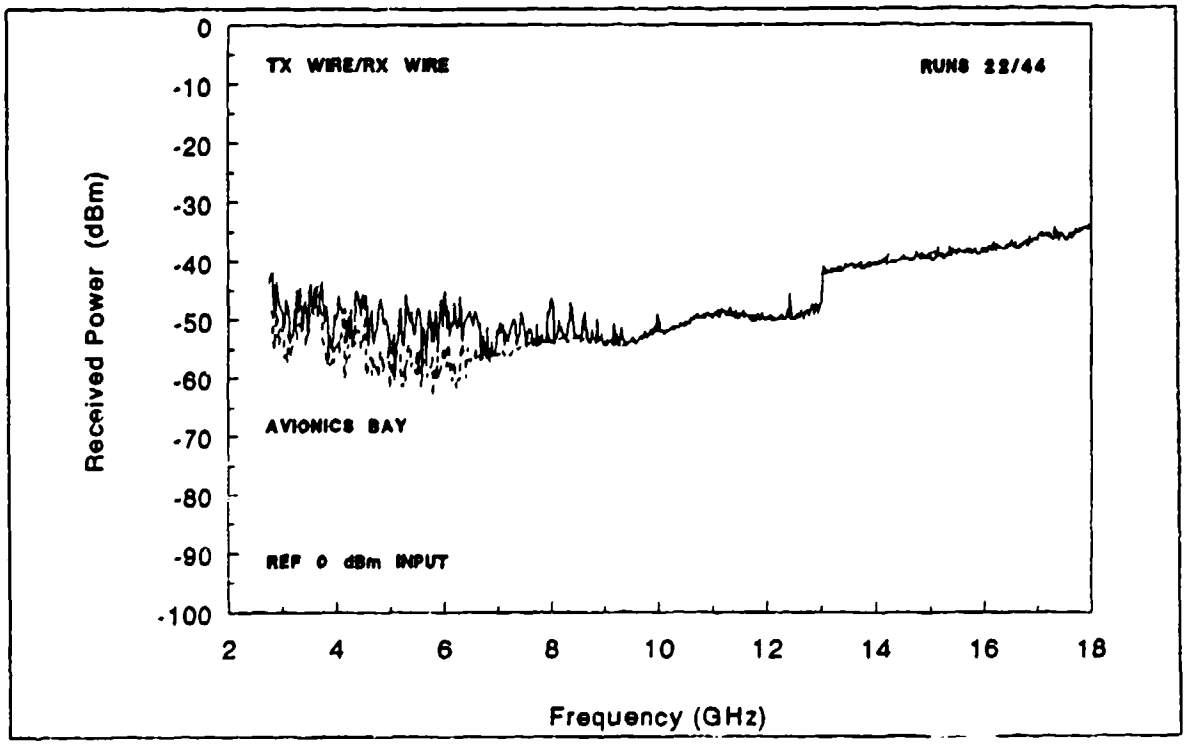

FIGURE 4-3. COMPARISON OF PEAK POWER RECEIVED IN AVIONICS BAY FOR TWO DATA RUNS (2.5 TO 18 GHz)

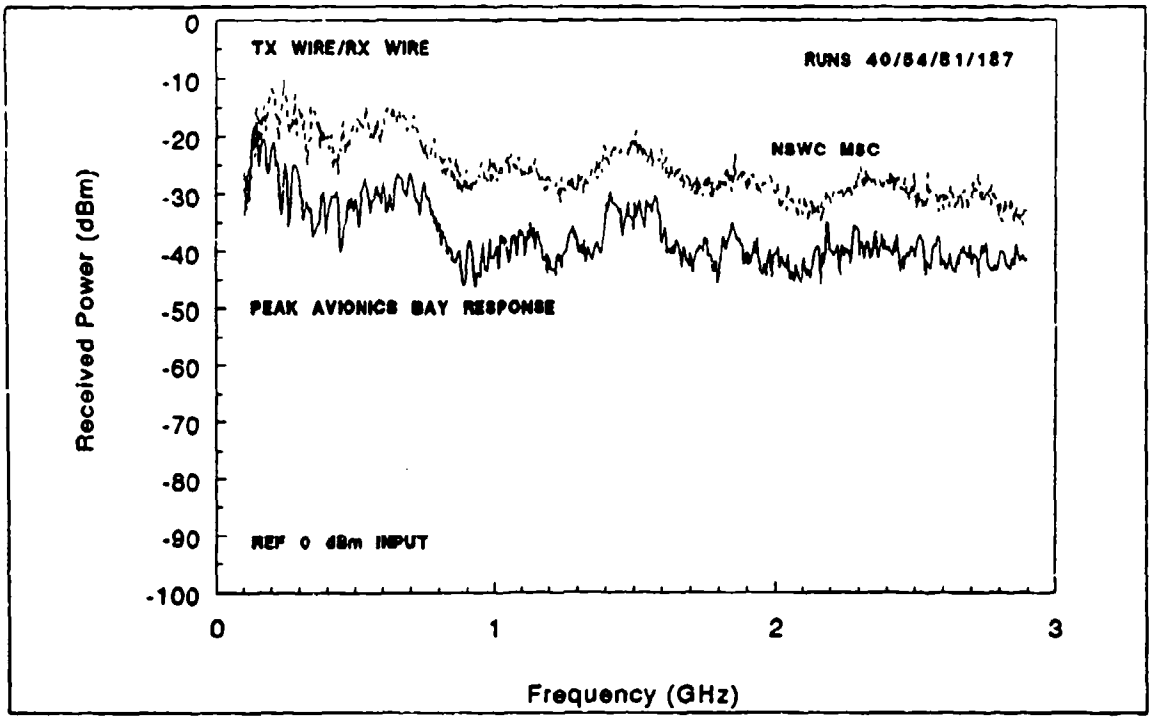

FIGURE 4-4. COMPARISON OF NSWCDD MODE STIRRED CHAMBER AND AVIONICS BAY RECEIVED PEAK POWER (0.1 TO 2.9 GHz)

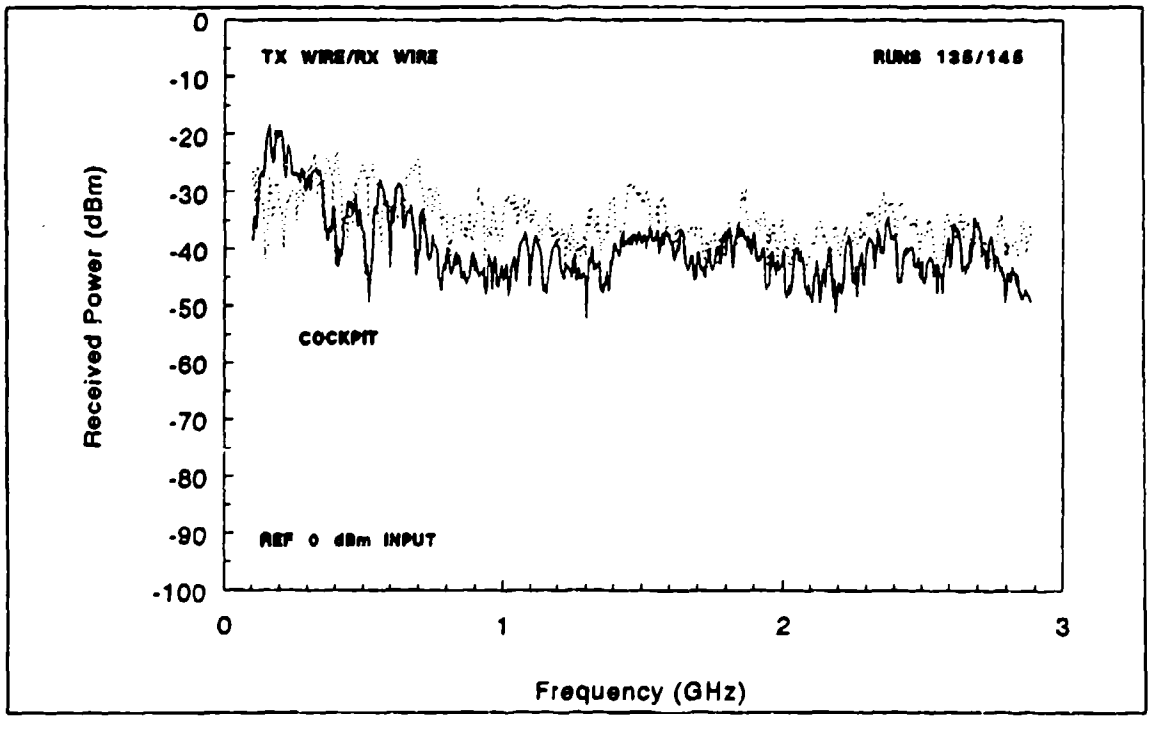

FIGURE 4-5. PEAK POWER RECEIVED IN COCKPIT (0.1 TO 2.9 GHz)

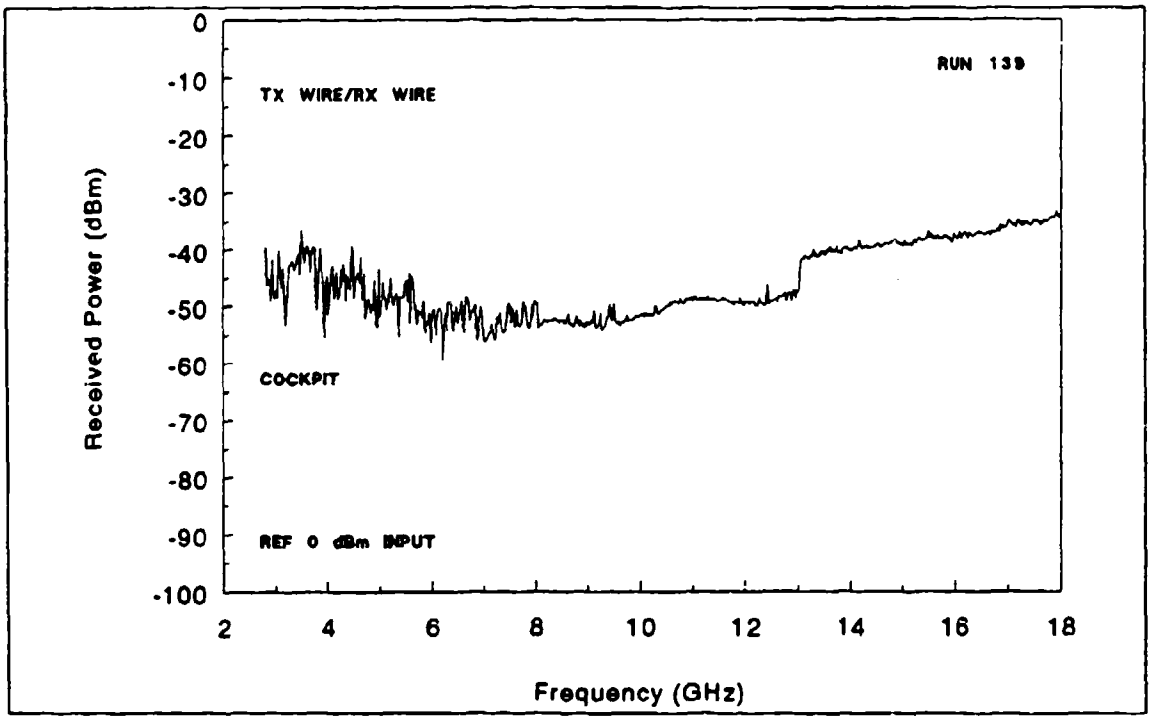

FIGURE 4-6. PEAK POWER RECEIVED IN COCKPIT (2.5 TO 18 GHz)

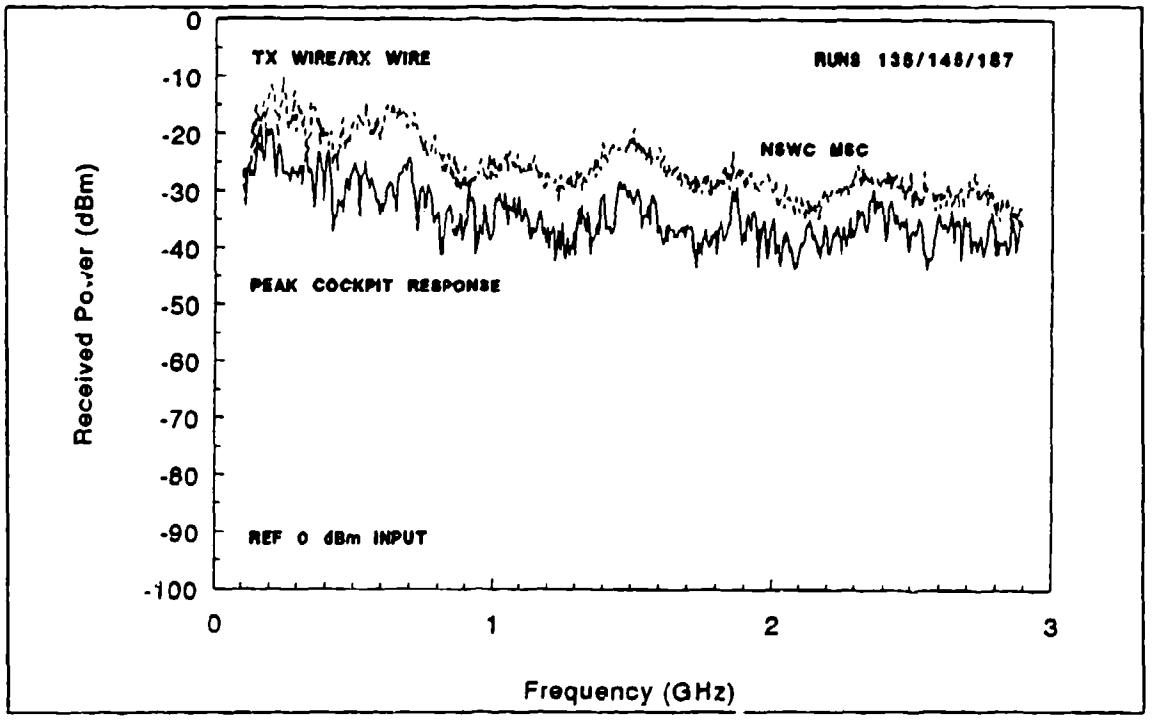

FIGURE 4-7. COMPARISON OF NSWCDD MODE STIRRED CHAMBER AND COCKPIT RECEIVED PEAK POWER (0.1 TO 2.9 GHz)

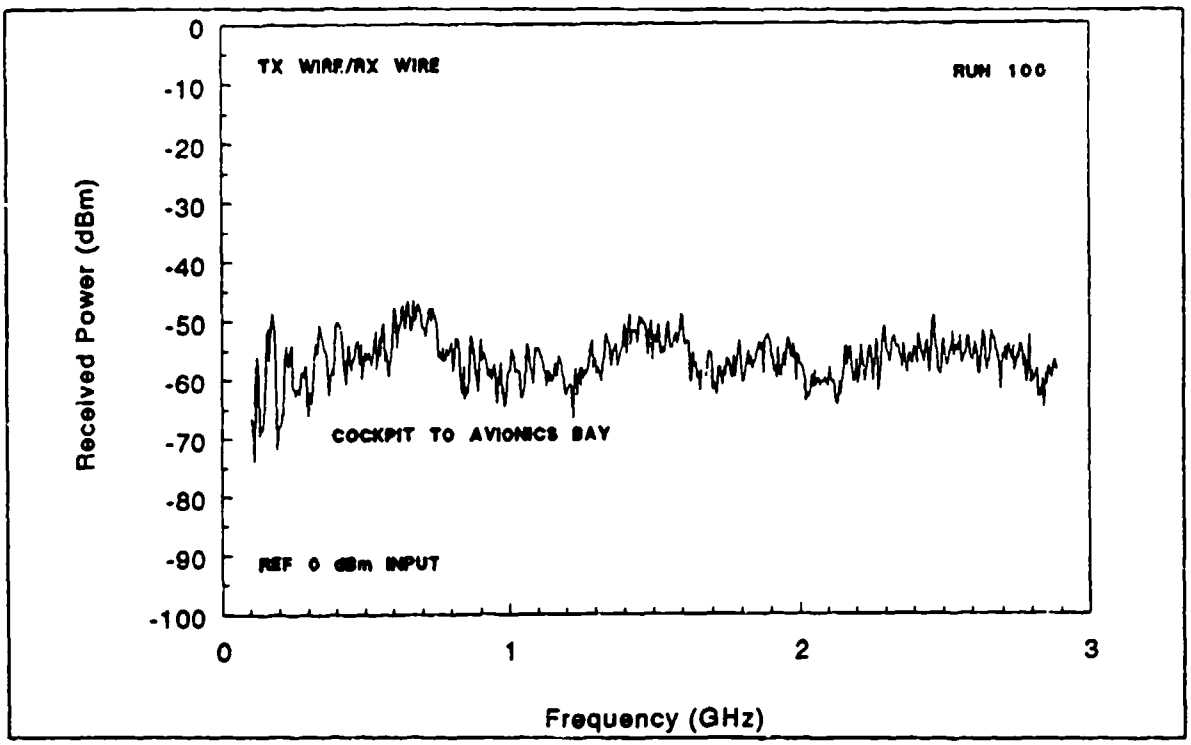

FIGURE 4-8. PEAK POWER RECEIVED IN AVIONICS BAY FOR COCKPIT EXCITATION (0.1 TO 2.9 GHz)

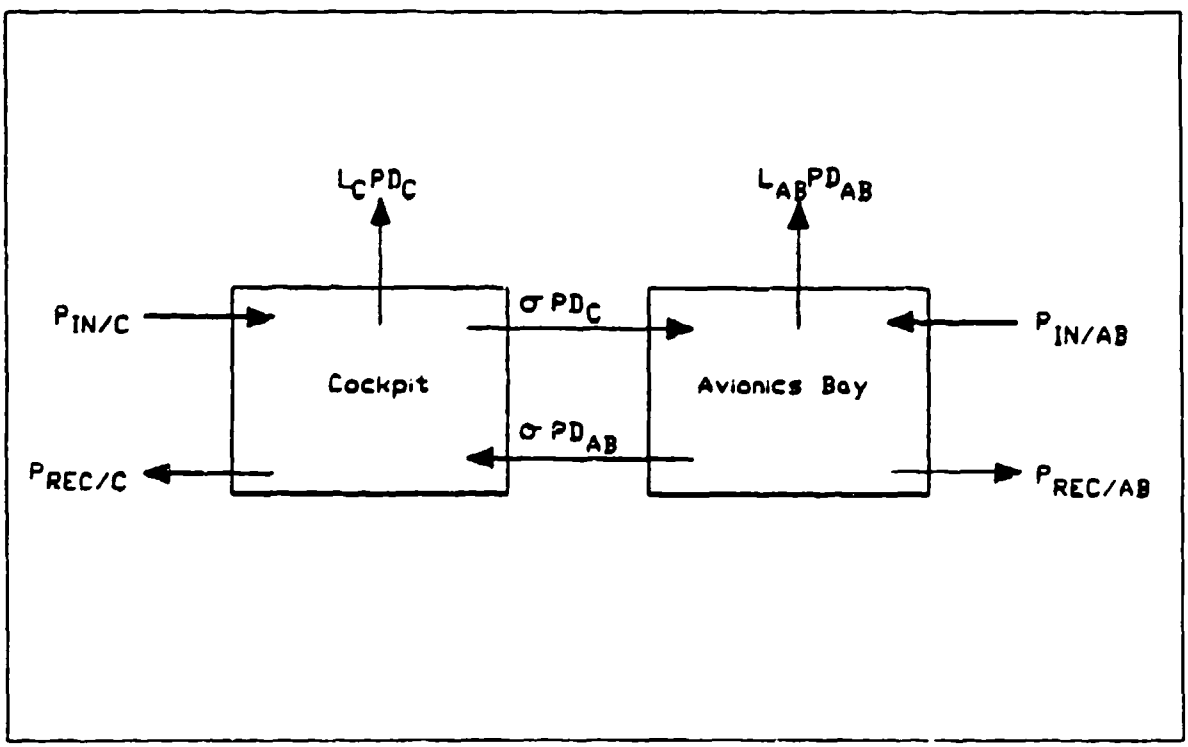

FIGURE 4-9. ENERGY BALANCE FACTORS IN COCKPIT AND AVIONICS BAY

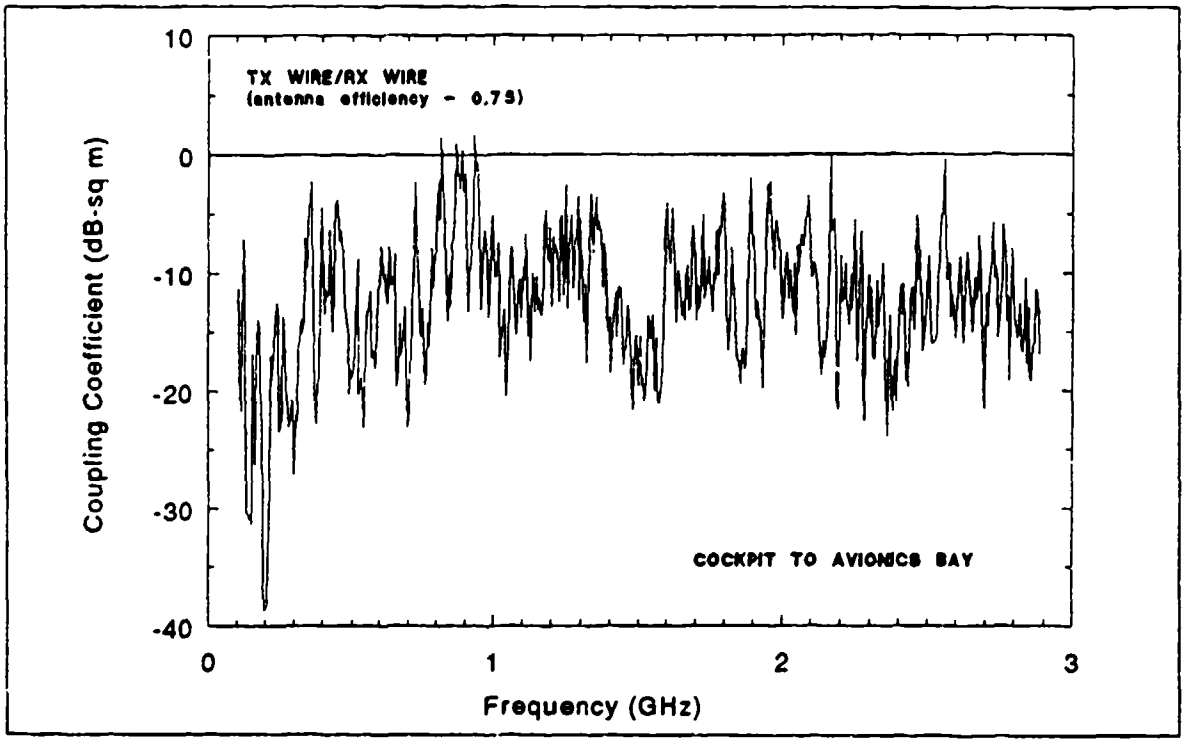

FIGURE 4-10. COCKPIT TO AVIONICS BAY ENERGY COUPLING COEFFICIENT

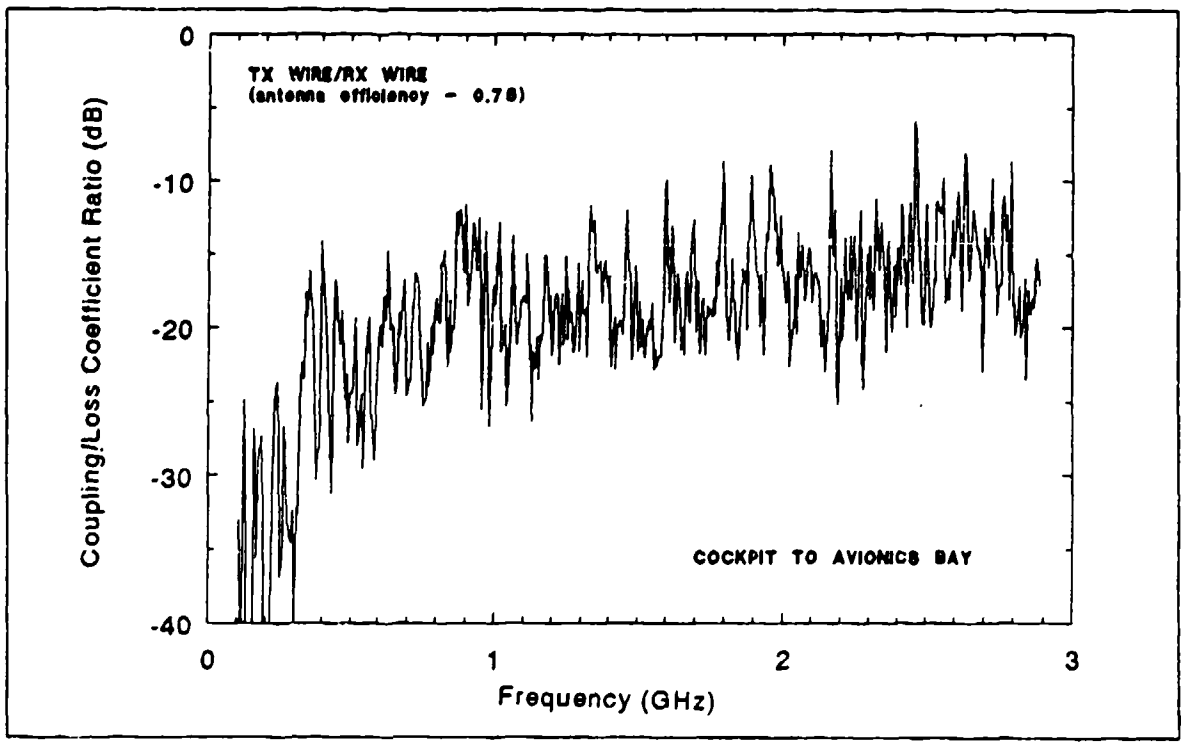

FIGURE 4-11. RATIO OF COCKPIT COUPLING COEFFICIENT TO LOSS COEFFICIENT

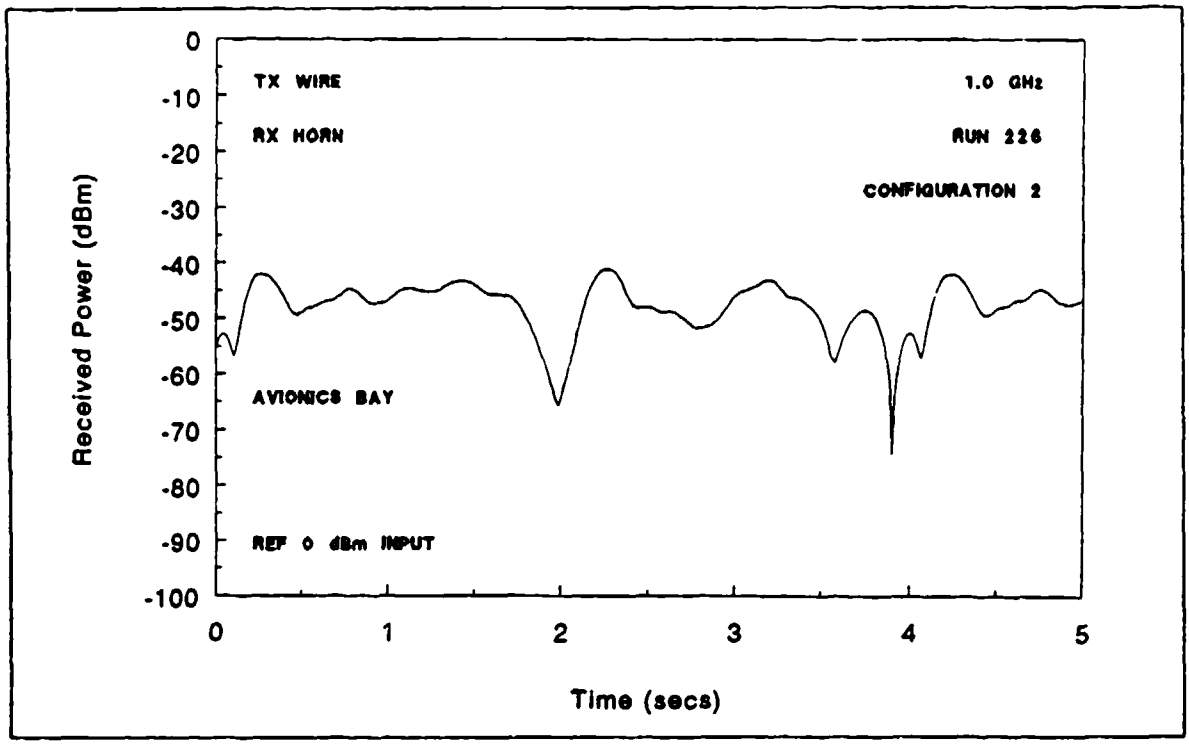

FIGURE 4-12. AVIONICS BAY DISCRETE FREQUENCY DATA (1.0 GHz) FOR CONFIGURATION 2

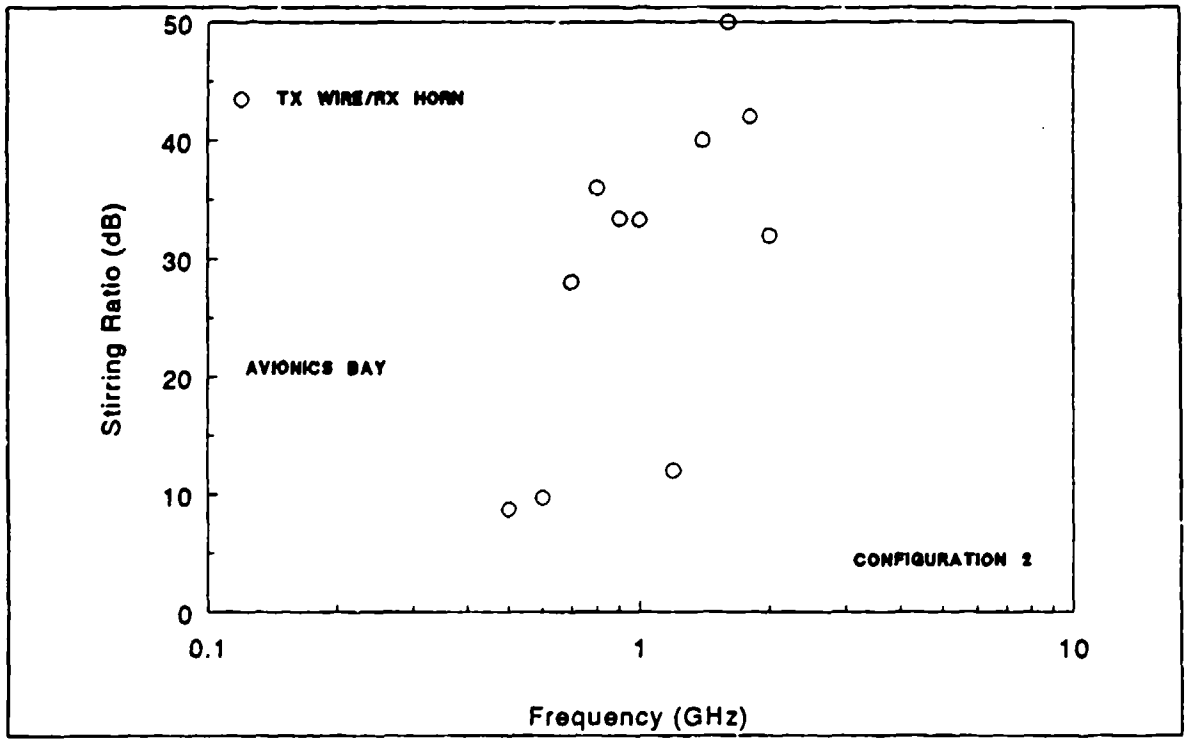

FIGURE 4-13. STIRRING RATIO DATA FOR TX WIRE/RX HORN FOR AVIONICS BAY CONFIGURATION 2

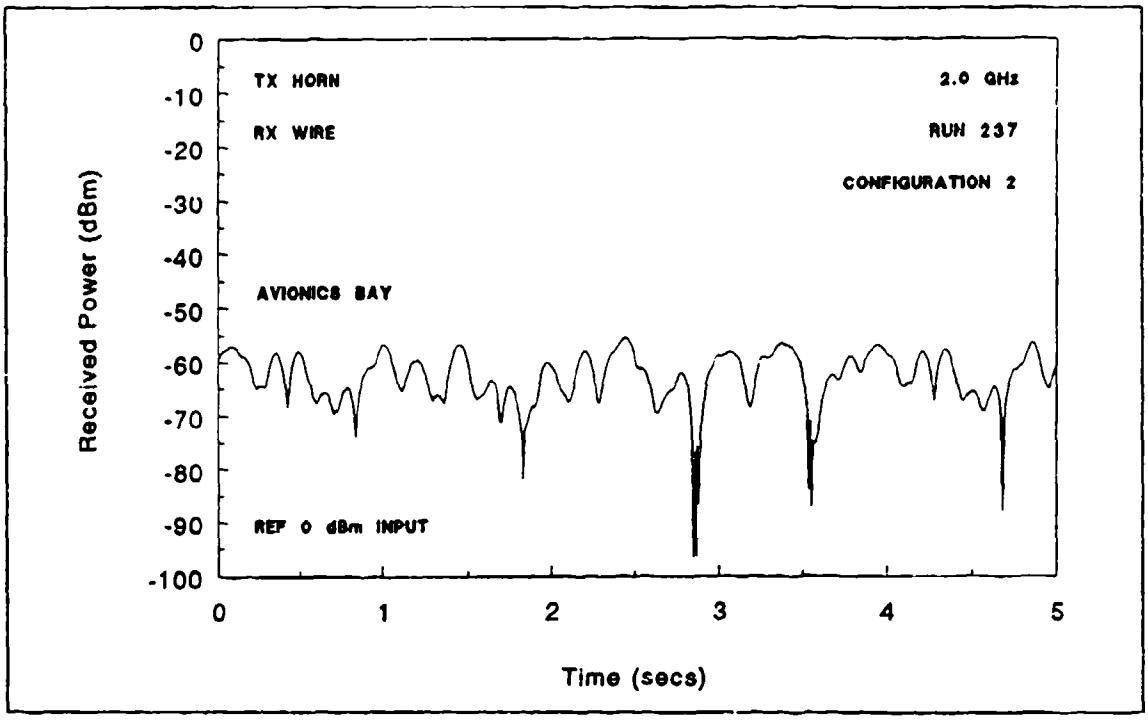

FIGURE 4-14. AVIONICS BAY DISCRETE FREQUENCY DATA (2.0 GHz) FOR CONFIGURATION 2

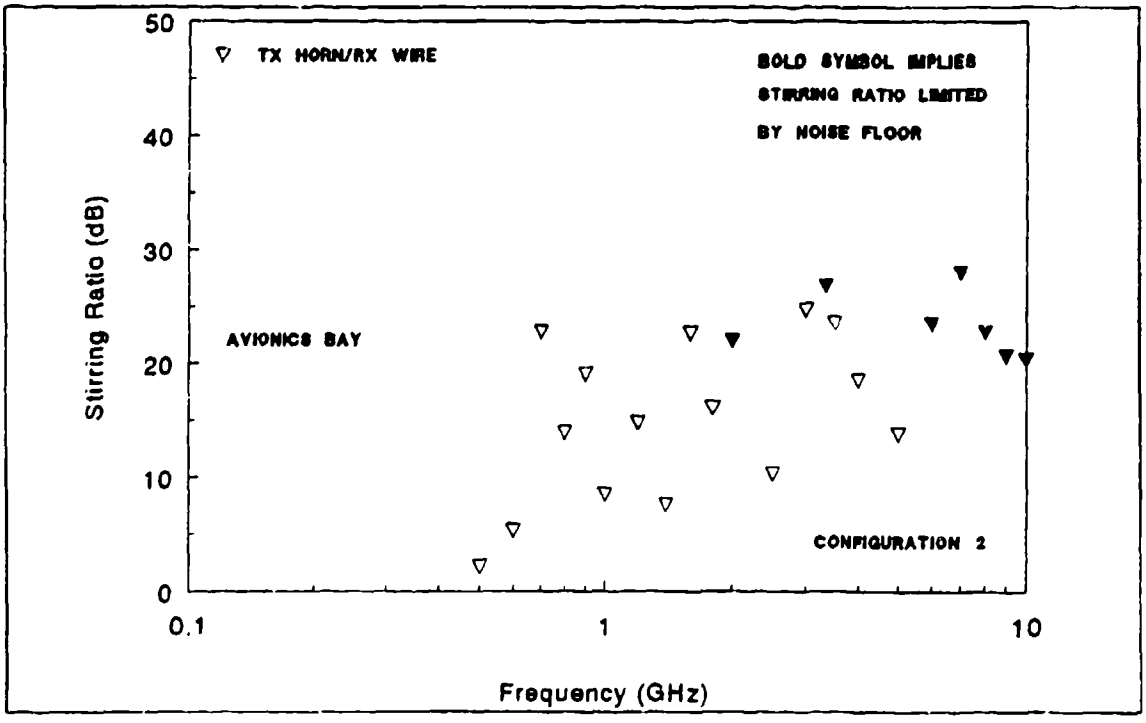

FIGURE 4-15. STIRRING RATIO DATA FOR TX HORN/RX WIRE FOR AVIONICS BAY CONFIGURATION 2

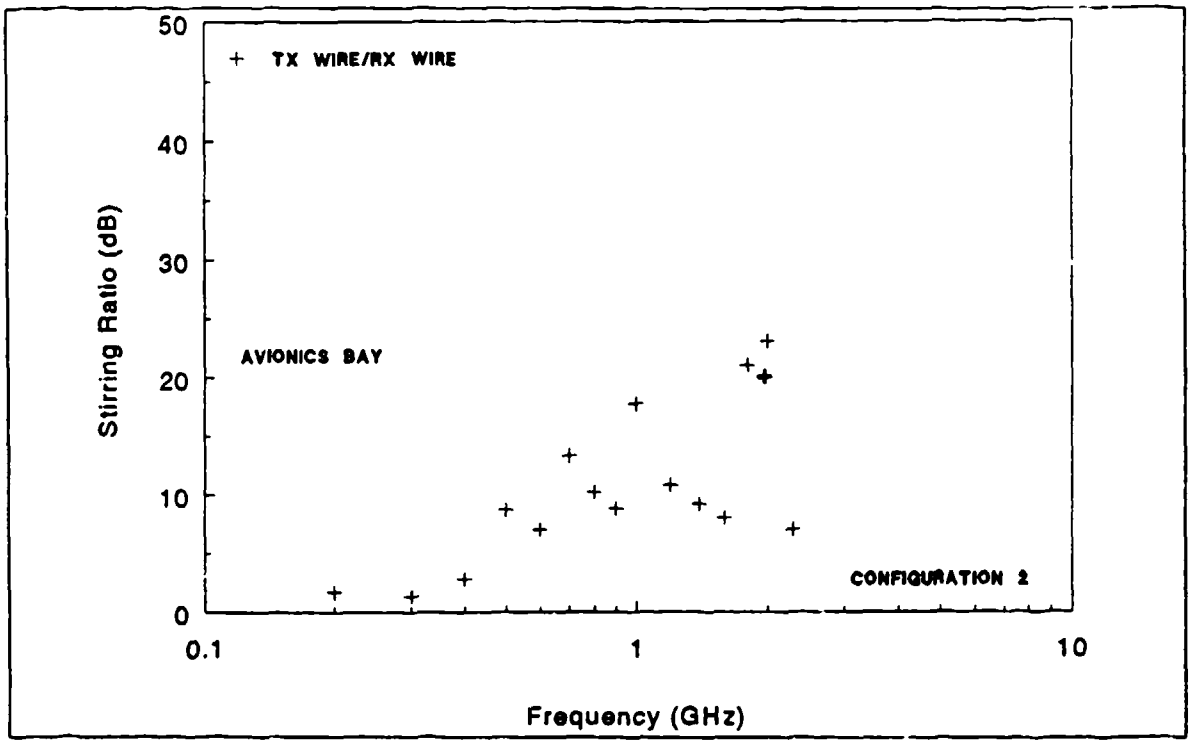

FIGURE 4-16. STIRRING RATIO DATA FOR TX WIRE/RX WIRE FOR AVIONICS BAY CONFIGURATION 2

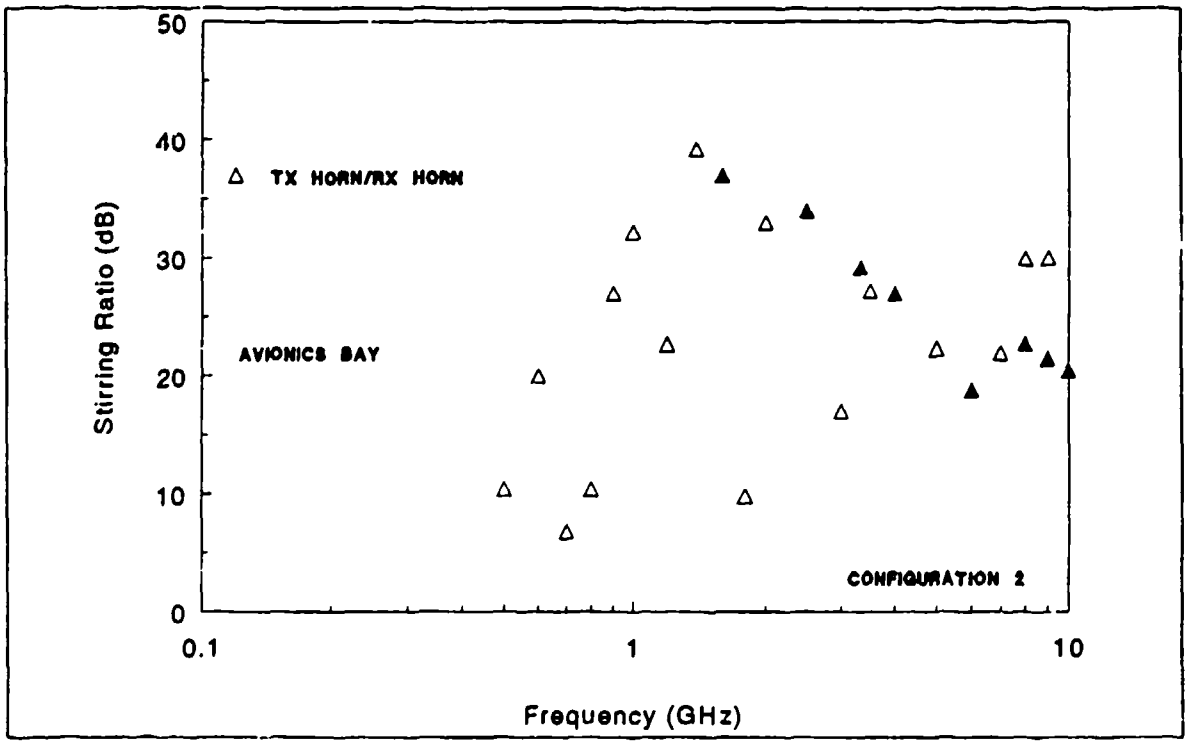

FIGURE 4-17. STIRRING RATIO DATA FOR TX HORN/RX HORN FOR AVIONICS BAY CONFIGURATION 2

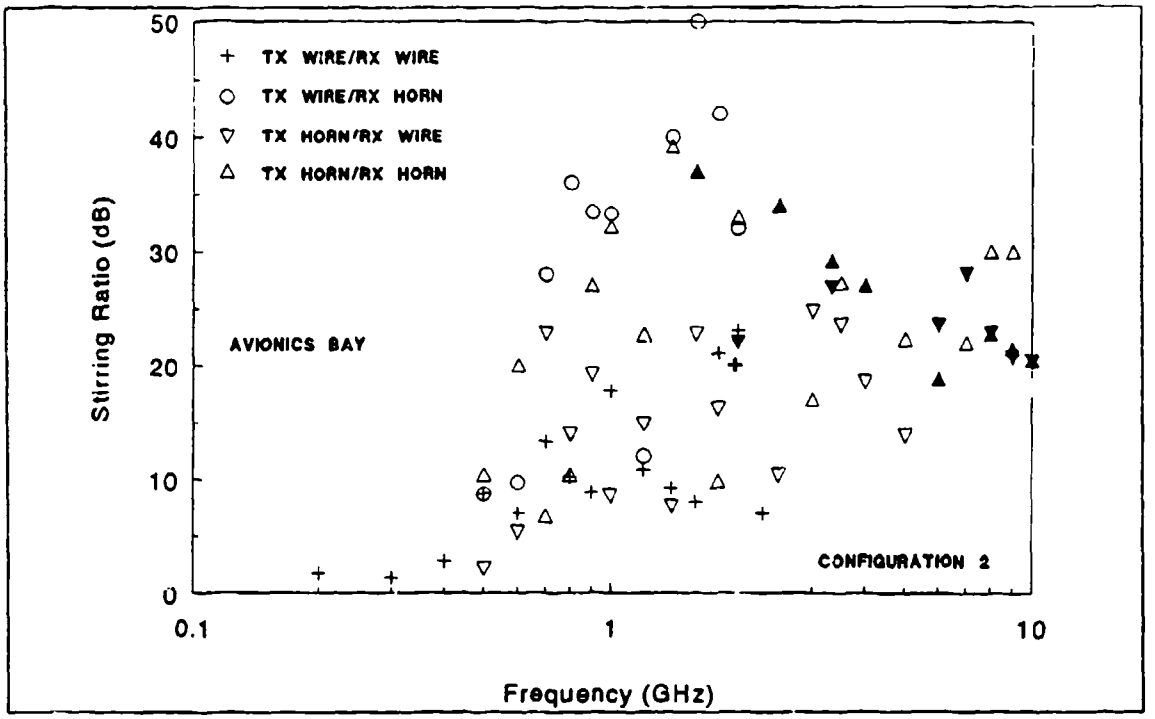

FIGURE 4-18. COMPOSITE OF ALL STIRRING RATIO DATA FOR AVIONICS BAY CONFIGURATION 2

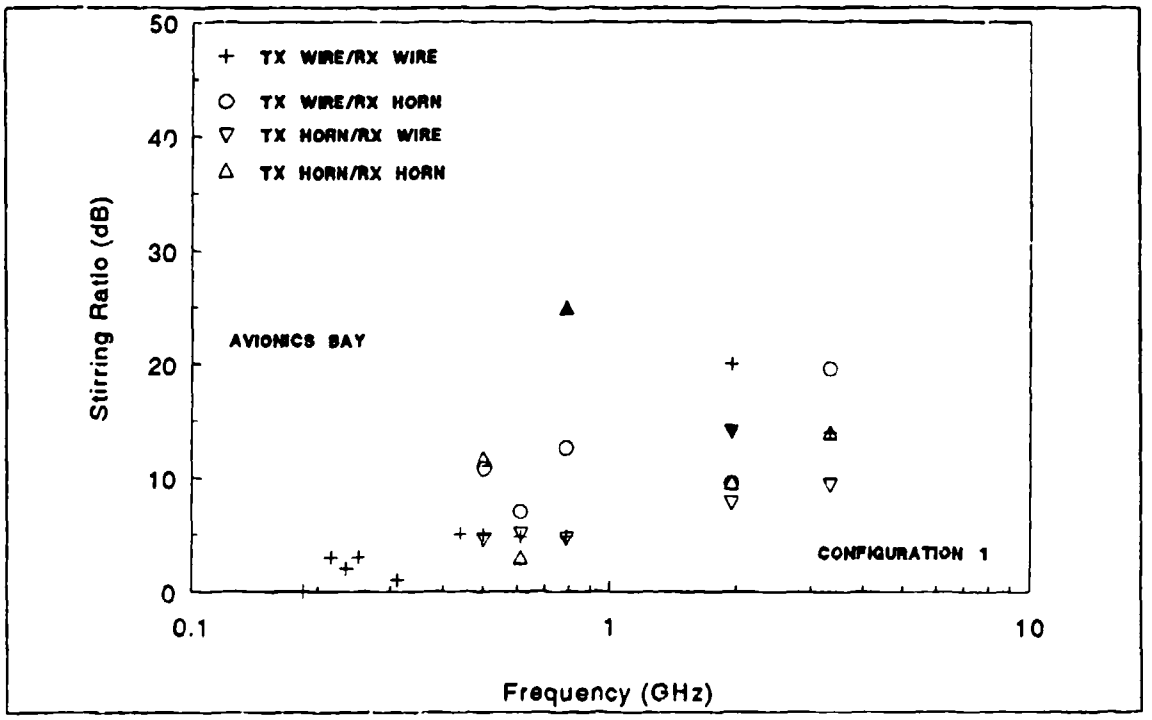

FIGURE 4-19. COMPOSITE OF ALL STIRRING RATIO DATA FOR AVIONICS BAY CONFIGURATION 1

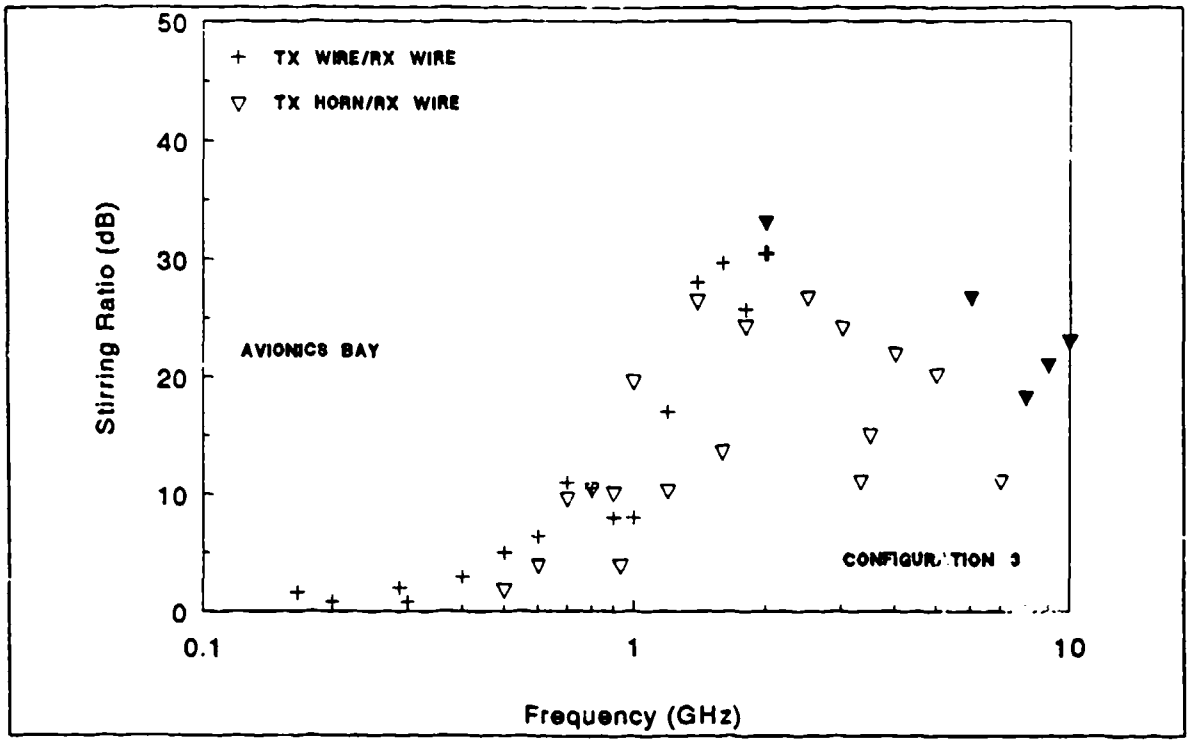

FIGURE 4-20. COMPOSITE OF ALL STIRRING RATIO DATA FOR AVIONICS BAY CONFIGURATION 3

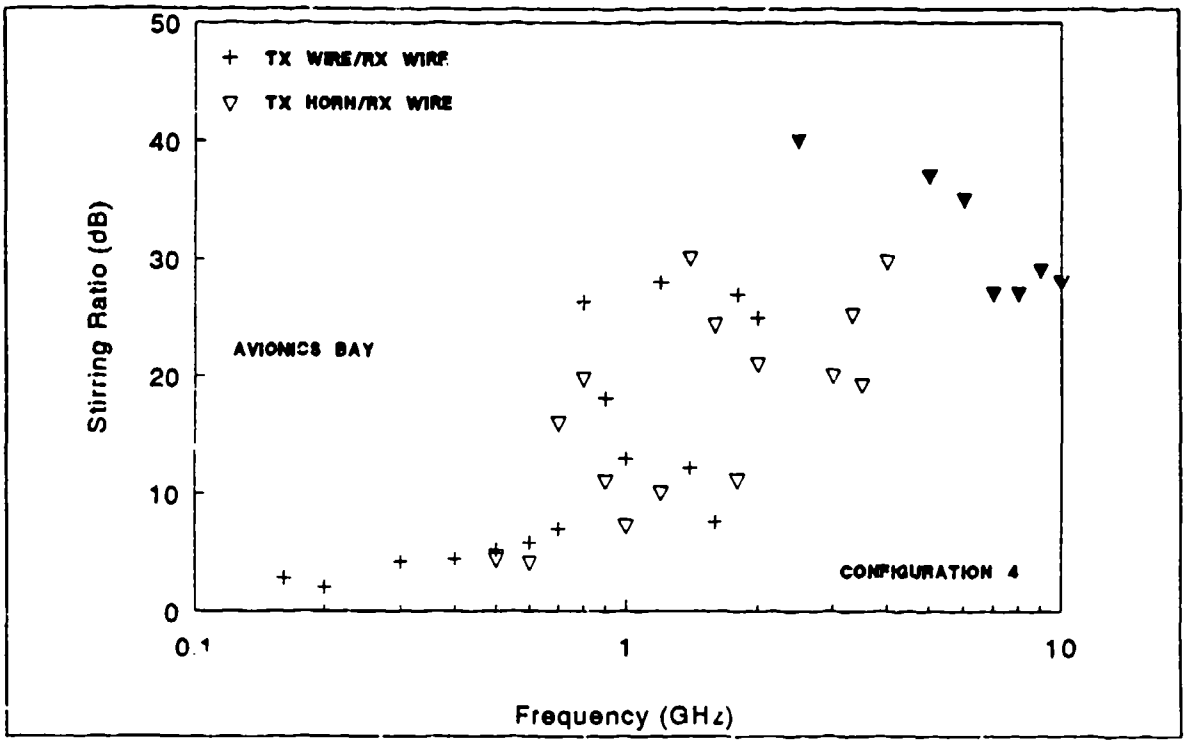

FIGURE 4-21. COMPOSITE OF ALL STIRRING RATIO DATA FOR AVIONICS BAY CONFIGURATION 4

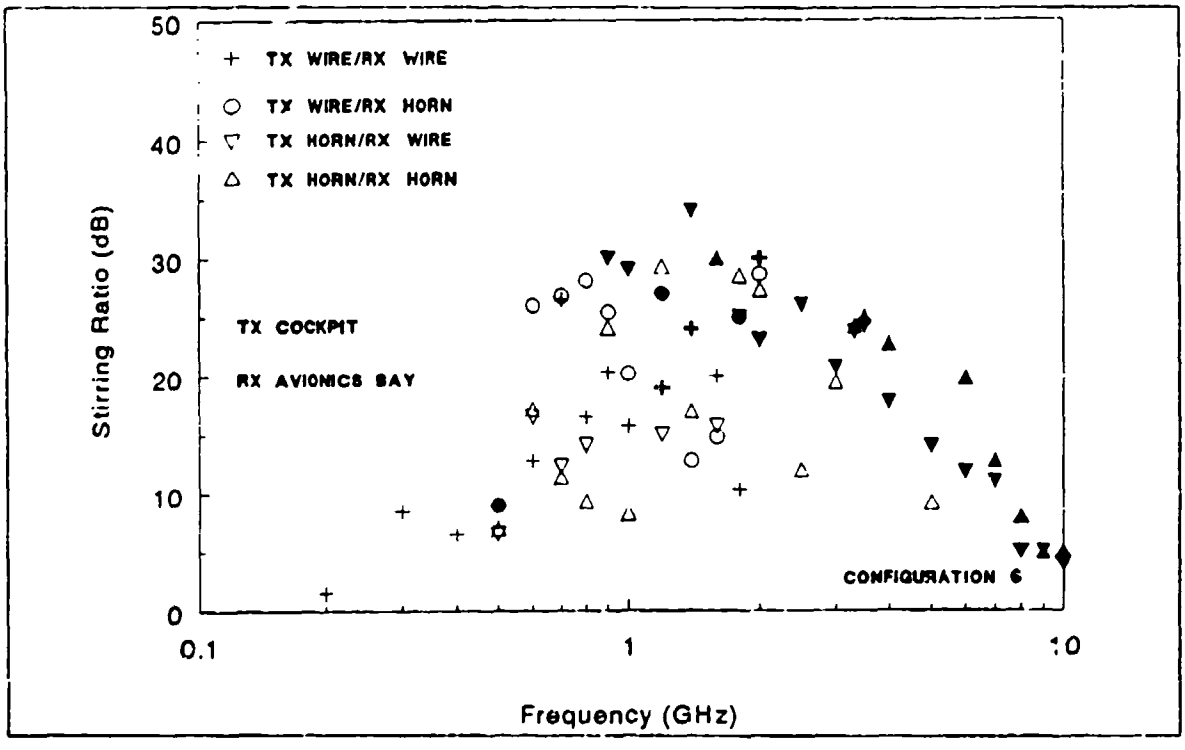

FIGURE 4-22. COMPOSITE OF ALL STIRRING RATIO DATA FOR AVIONICS BAY CONFIGURATION 6

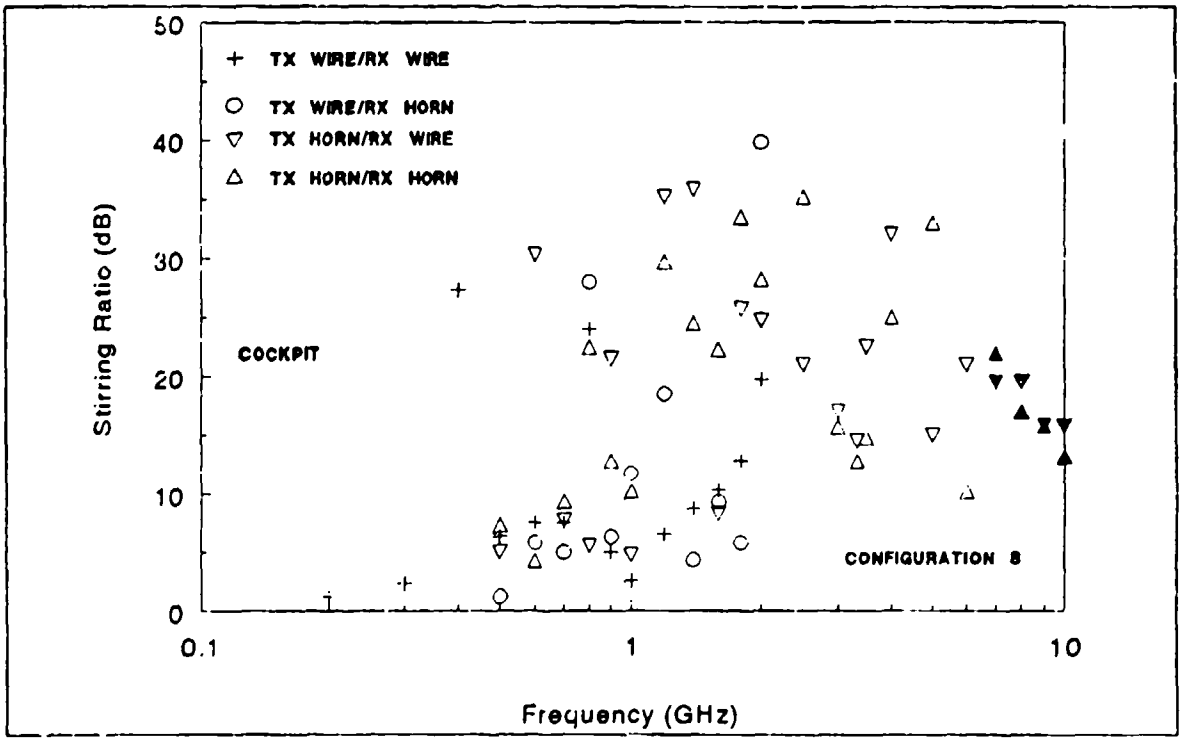

FIGURE 4-23. COMPOSITE OF ALL STIRRING RATIO DATA FOR COCKPIT CONFIGURATION 8

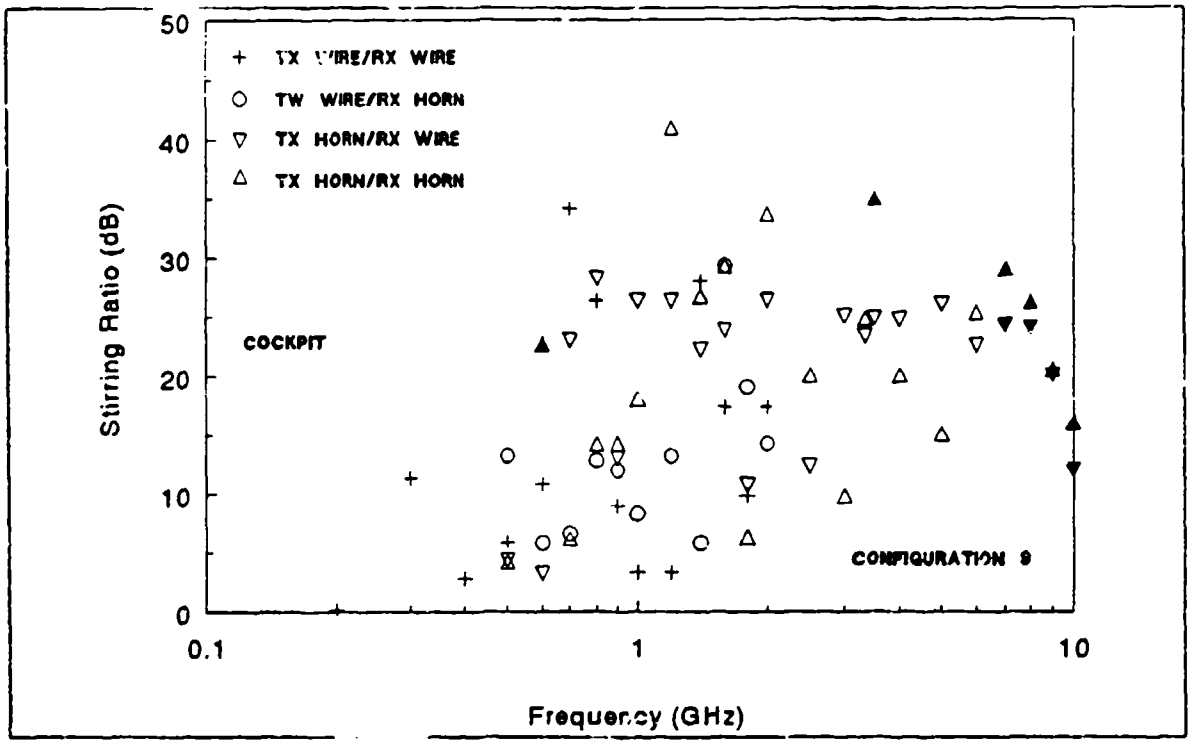

FIGURE 4-24. COMPOSITE OF ALL STIRRING RATIO DATA FOR COCKPIT CONFIGURATION 9

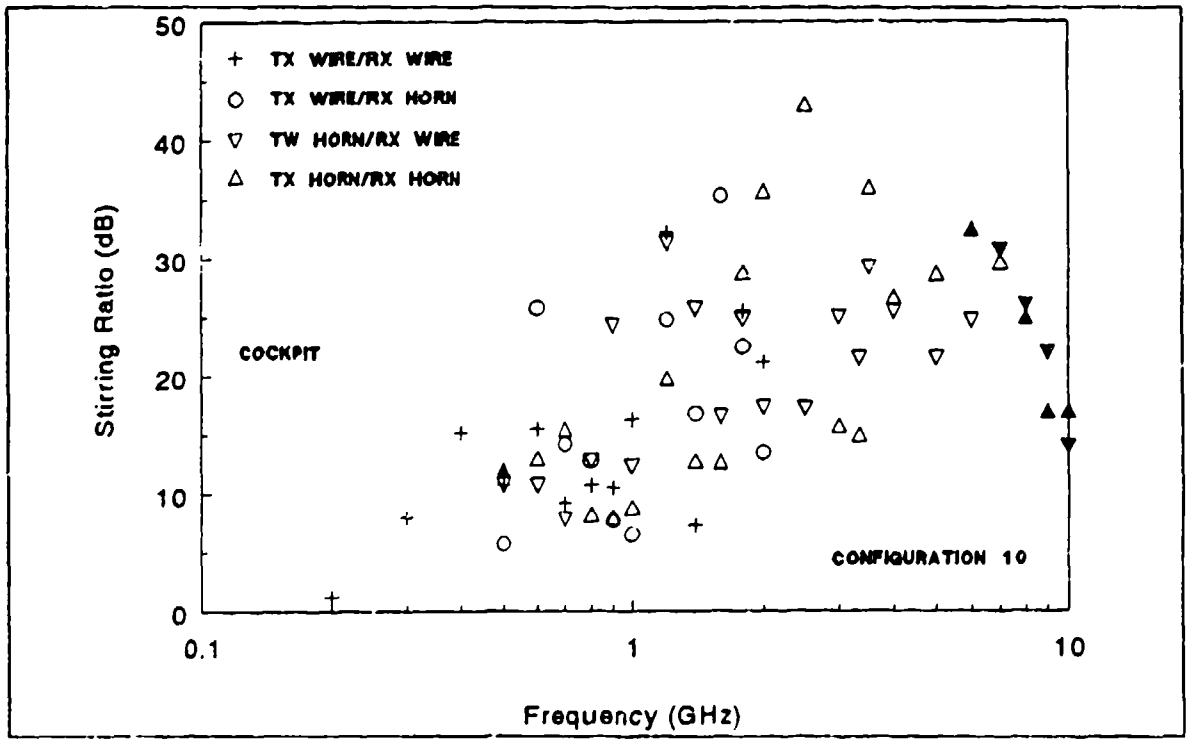

FIGURE 4-25. COMPOSITE OF ALL STIRRING RATIO DATA FOR COCKPIT CONFIGURATION 10

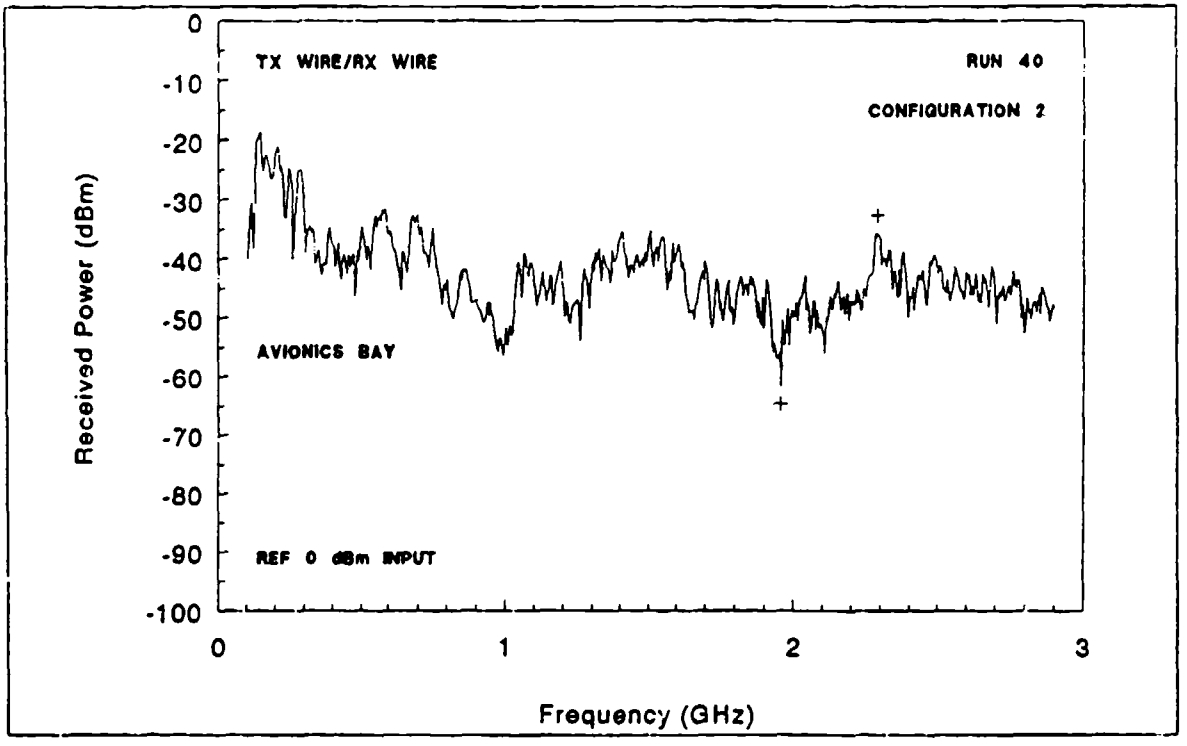

FIGURE 4-26. AVIONICS BAY SWEPT FREQUENCY DATA FOR CONFIGURATION 2

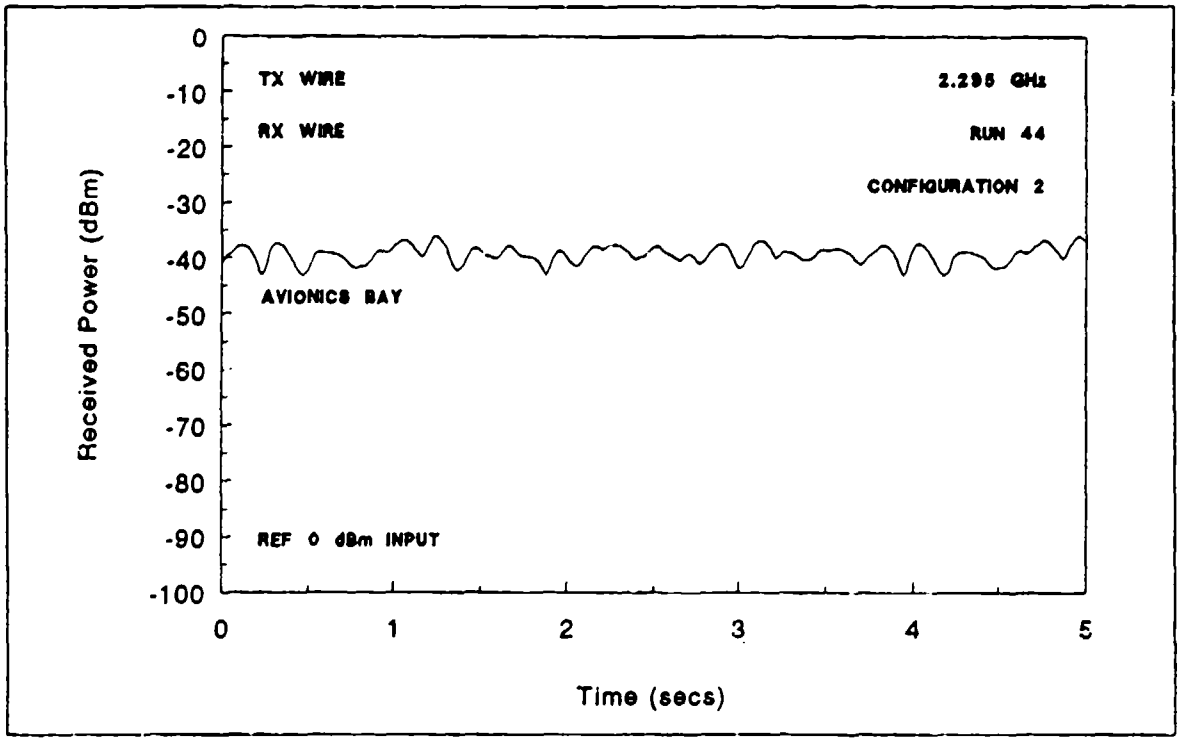

FIGURE 4-27. AVIONICS BAY DISCRETE FREQUENCY DATA (2.295 GHz) FOR CONFIGURATION 2

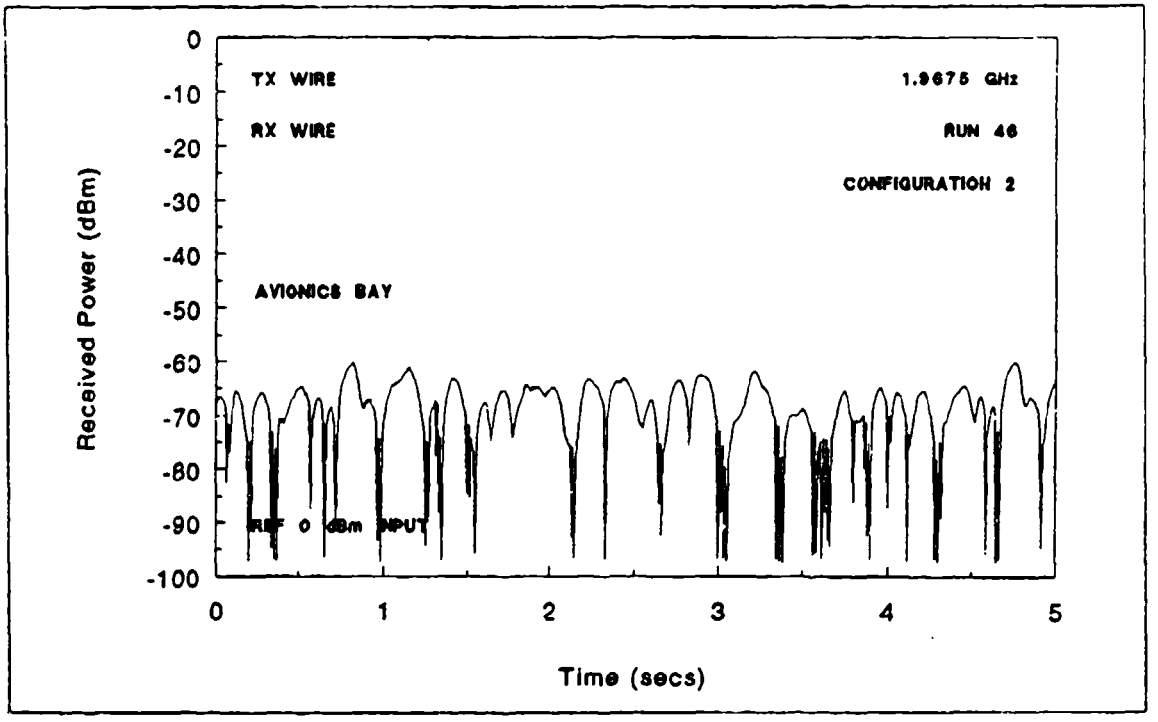

FIGURE 4-28. AVIONICS BAY DISCRETE FREQUENCY DATA (1.9675 GHz) FOR CONFIGURATION 2

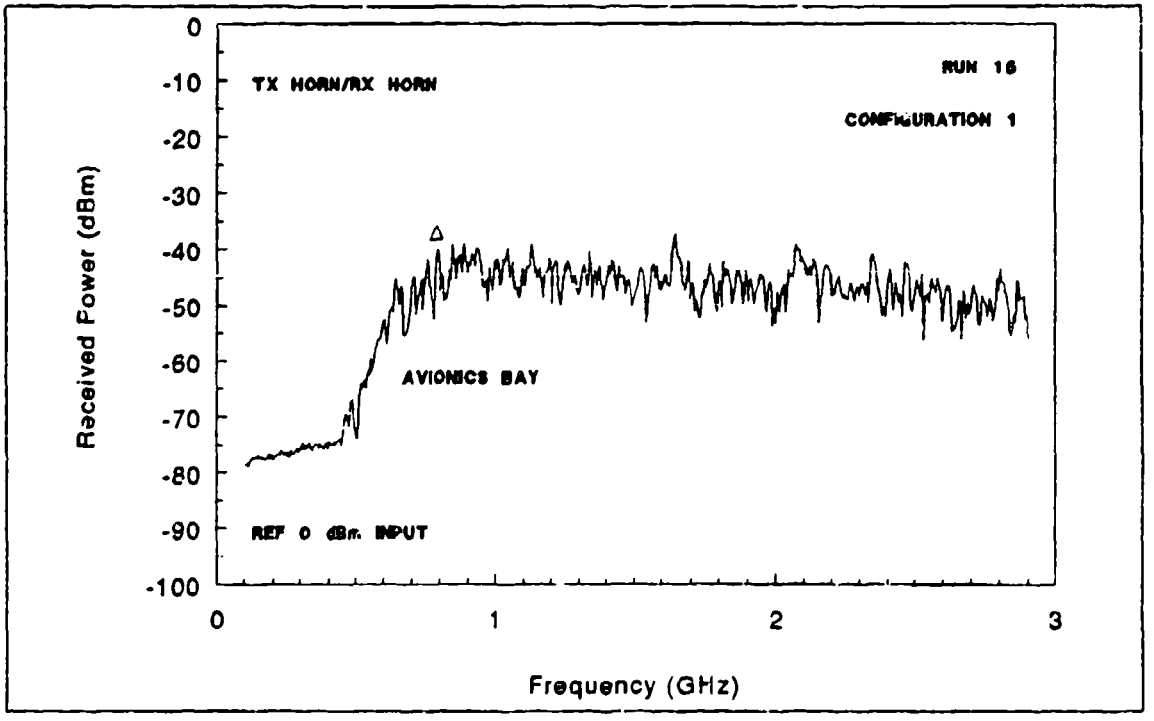

FIGURE 4-29. AVIONICS BAY SWEPT FREQUENCY DATA FOR CONFIGURATION 1

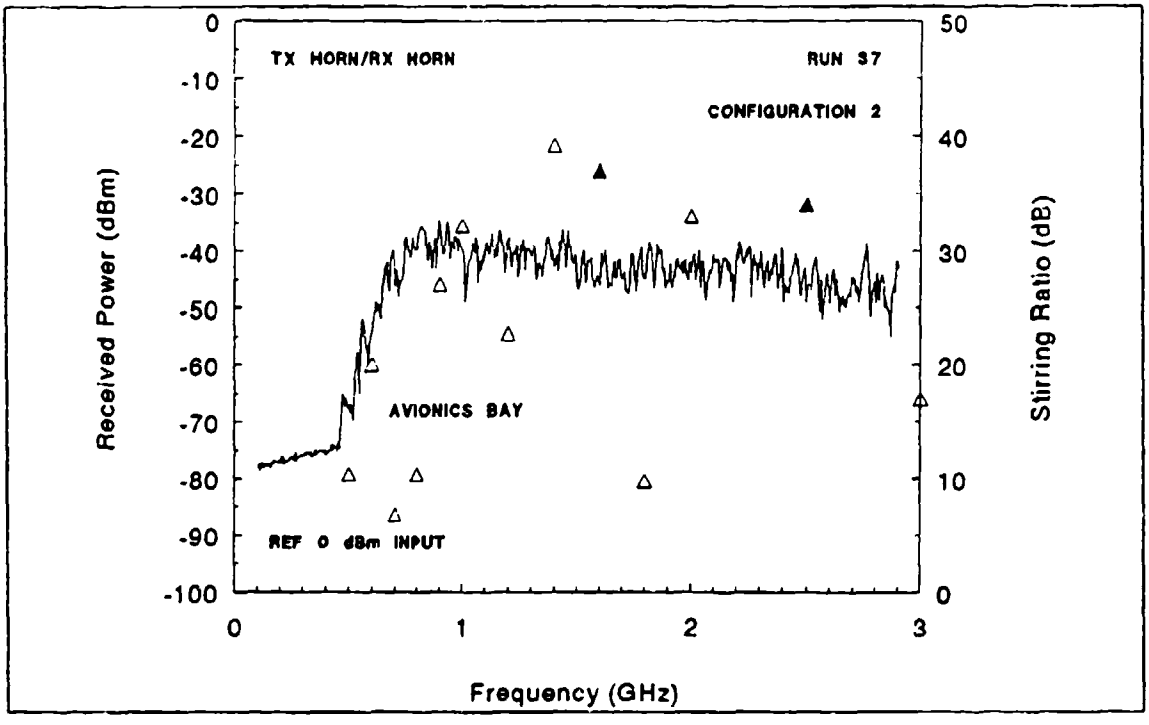

FIGURE 4-30. AVIONICS BAY SWEPT FREQUENCY AND STIRRING RATIO DATA FOR CONFIGURATION 2 (RUN 37)

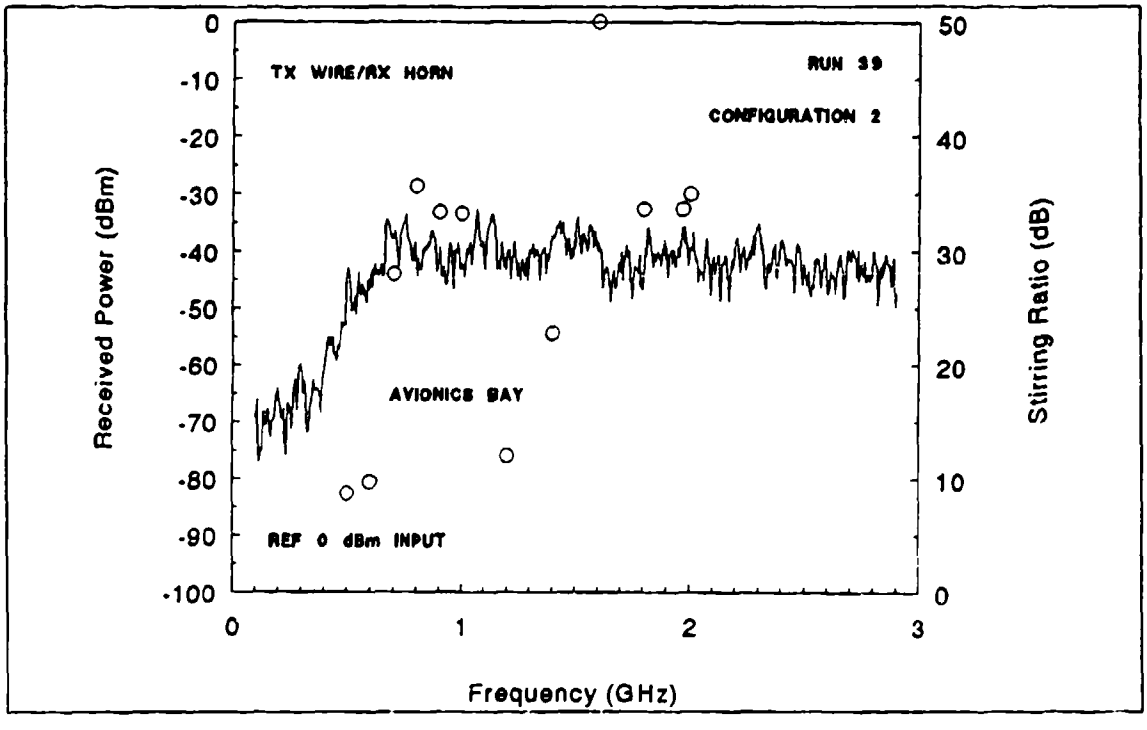

FIGURE 4-31. AVIONICS BAY SWEPT FREQUENCY AND STIRRING RATIO DATA FOR CONFIGURATION 2 (RUN 39)

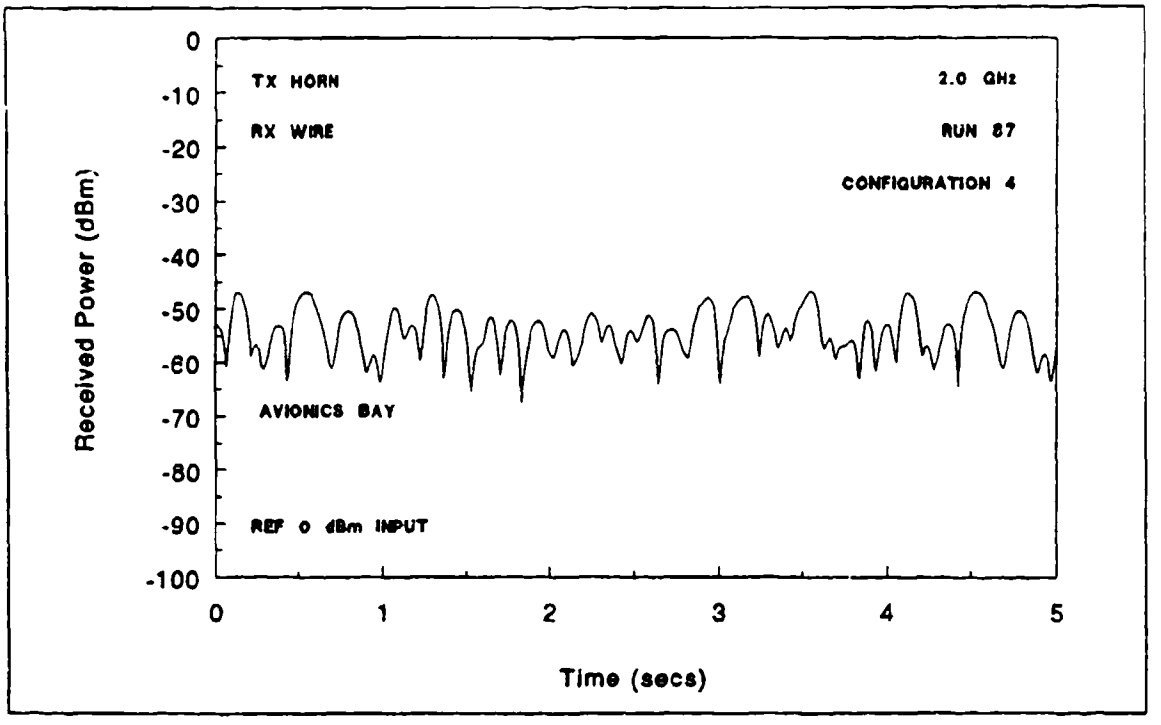

FIGURE 4-32. AVIONICS BAY DISCRETE FREQUENCY DATA (2.0 GHz) FOR CONFIGURATION 4

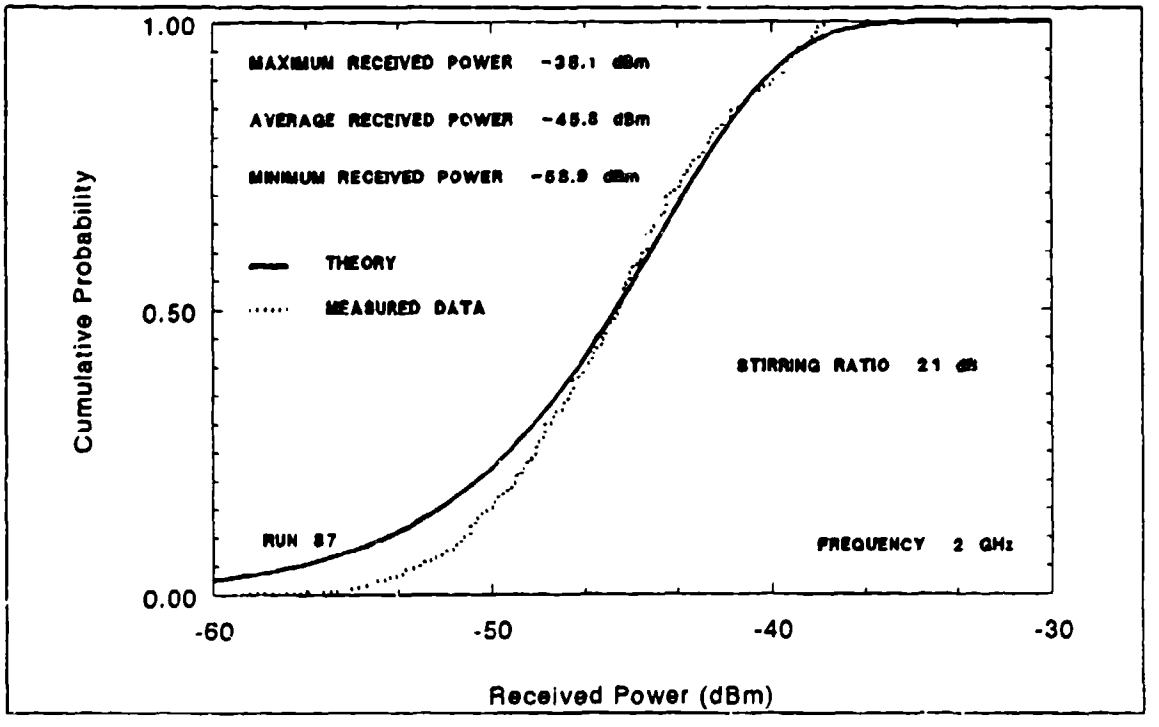

FIGURE 4-33. COMPARISON OF THEORETICAL AND EXPERIMENTAL CUMULATIVE DISTRIBUTIONS FOR DISCRETE FREQUENCY DATA (2.0 GHz)

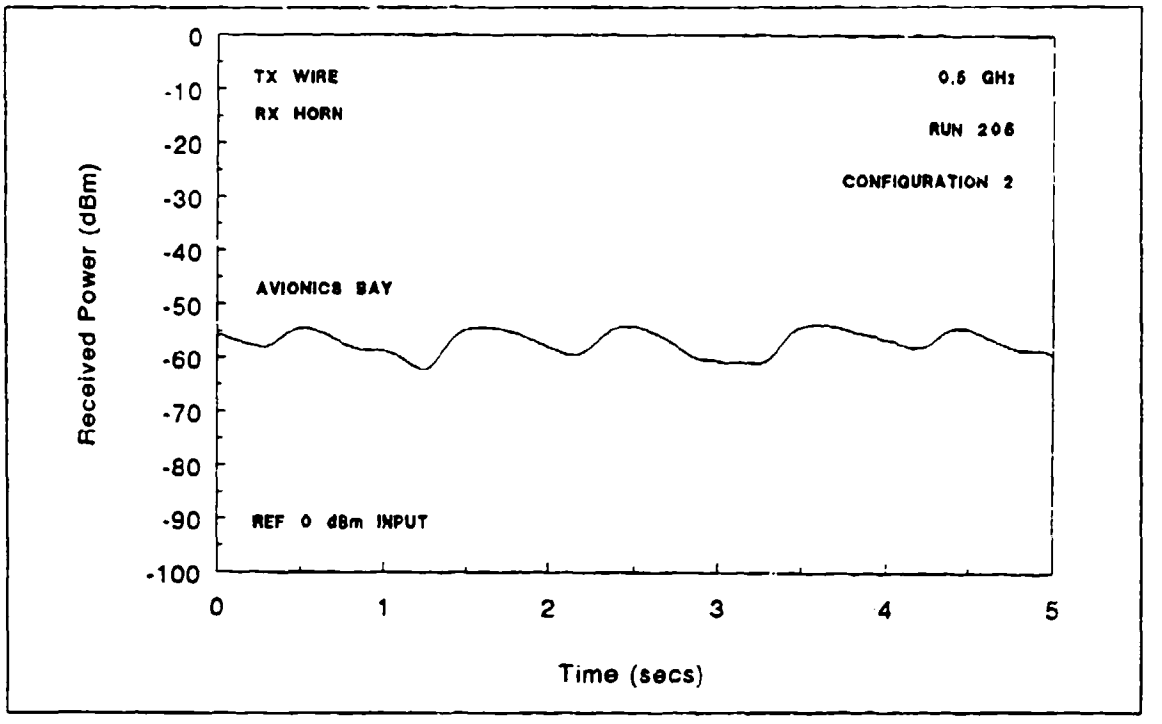

FIGURE 4-34. AVIONICS BAY DISCRETE FREQUENCY DATA (0.5 GHz) FOR CONFIGURATION 2

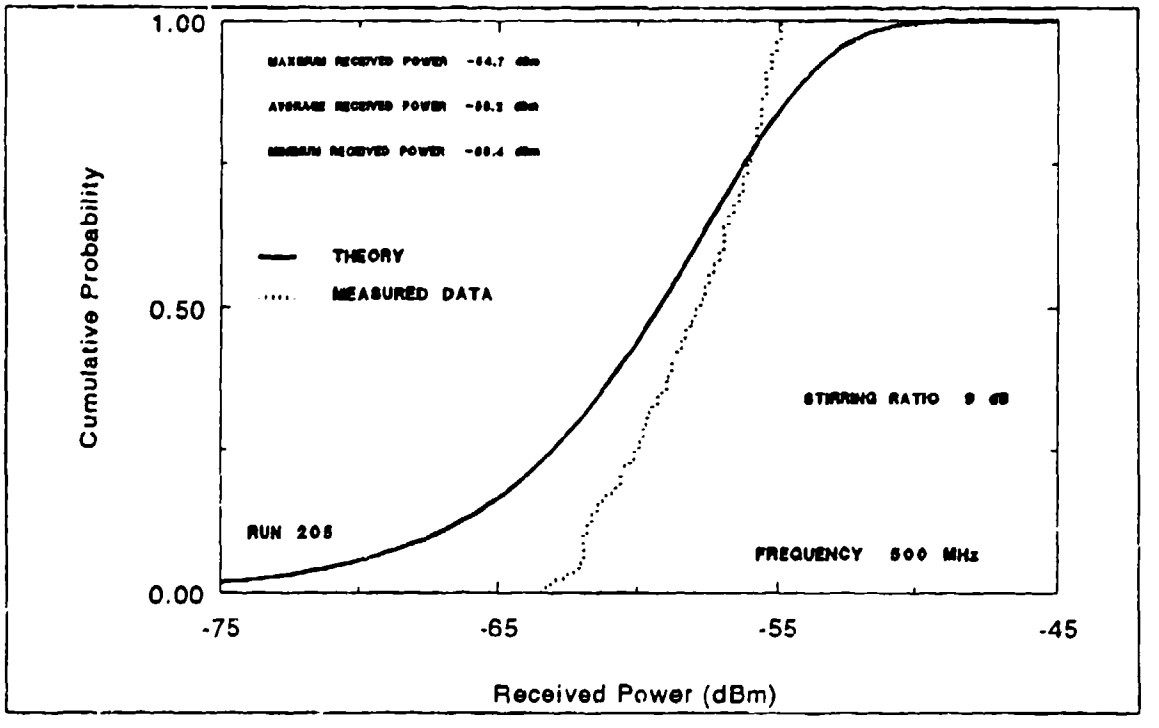

FIGURE 4-35. COMPARISON OF THEORETICAL AND EXPERIMENTAL CUMULATIVE DISTRIBUTIONS FOR DISCRETE FREQUENCY DATA (0.5 GHz)

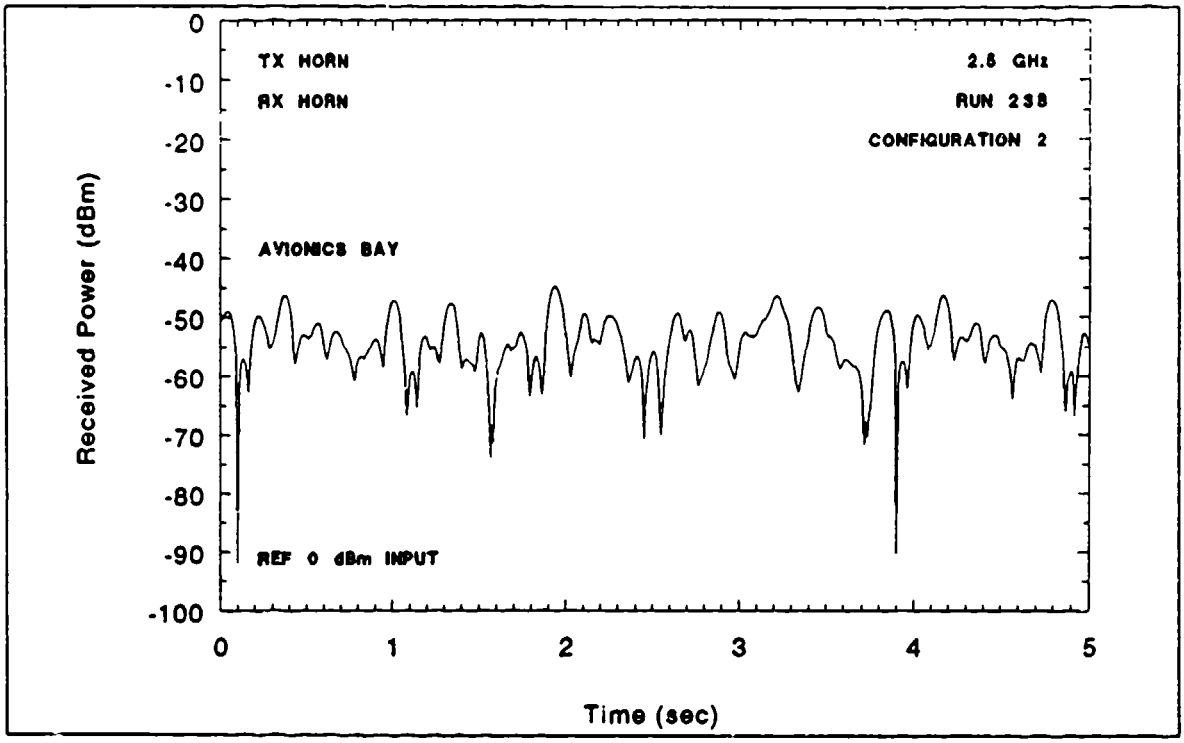

FIGURE 4-36. AVIONICS BAY DISCRETE FREQUENCY DATA (2.5 GHz) FOR CONFIGURATION 2

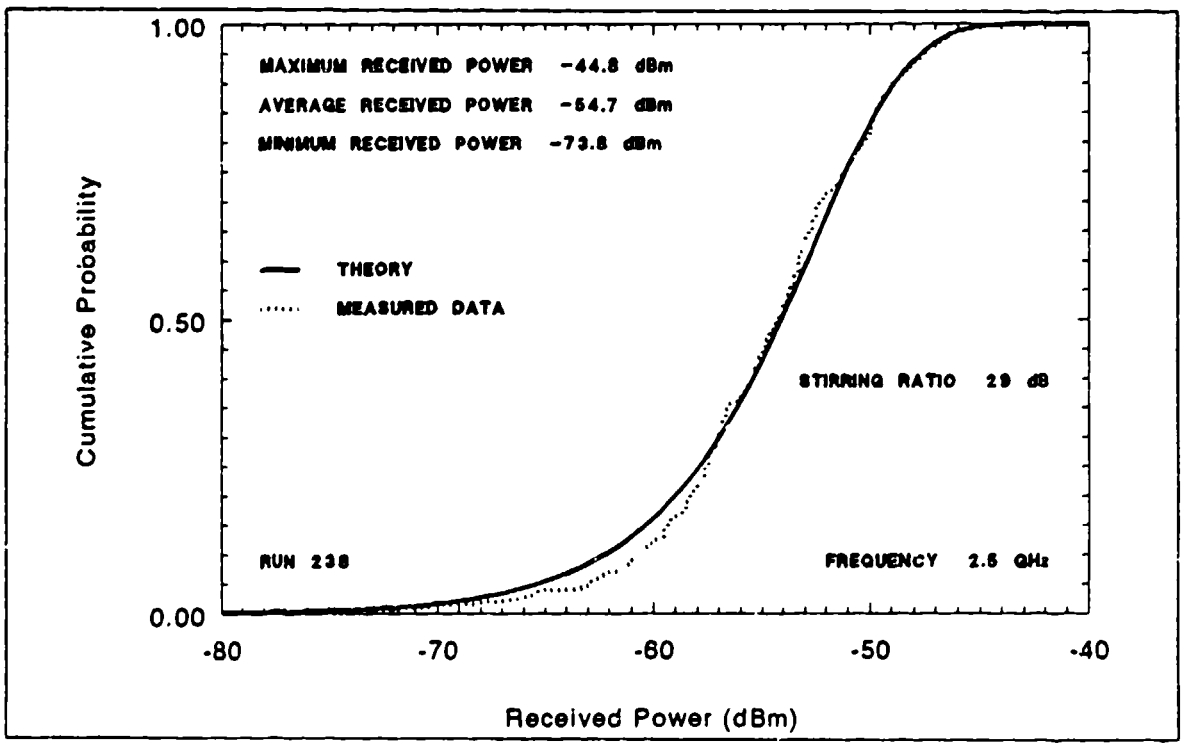

FIGURE 4-37. COMPARISON OF THEORETICAL AND EXPERIMENTAL CUMULATIVE DISTRIBUTIONS FOR DISCRETE FREQUENCY DATA (2.5 GHz)

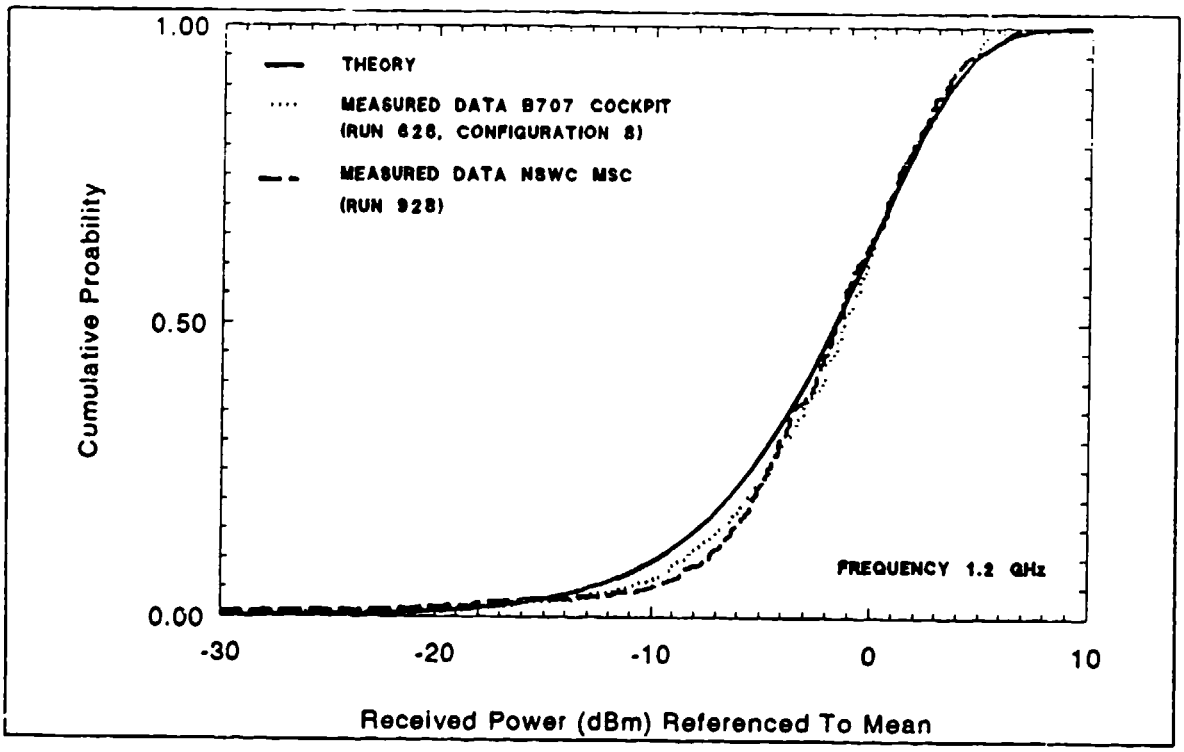

FIGURE 4-38. COMPARISON OF THEORETICAL AND EXPERIMENTAL CUMULATIVE DISTRIBUTIONS FOR DISCRETE FREQUENCY DATA (1.2 GHz) IN AIRCRAFT COCKPIT AND NSWCDD MODE STIRRED CHAMBER

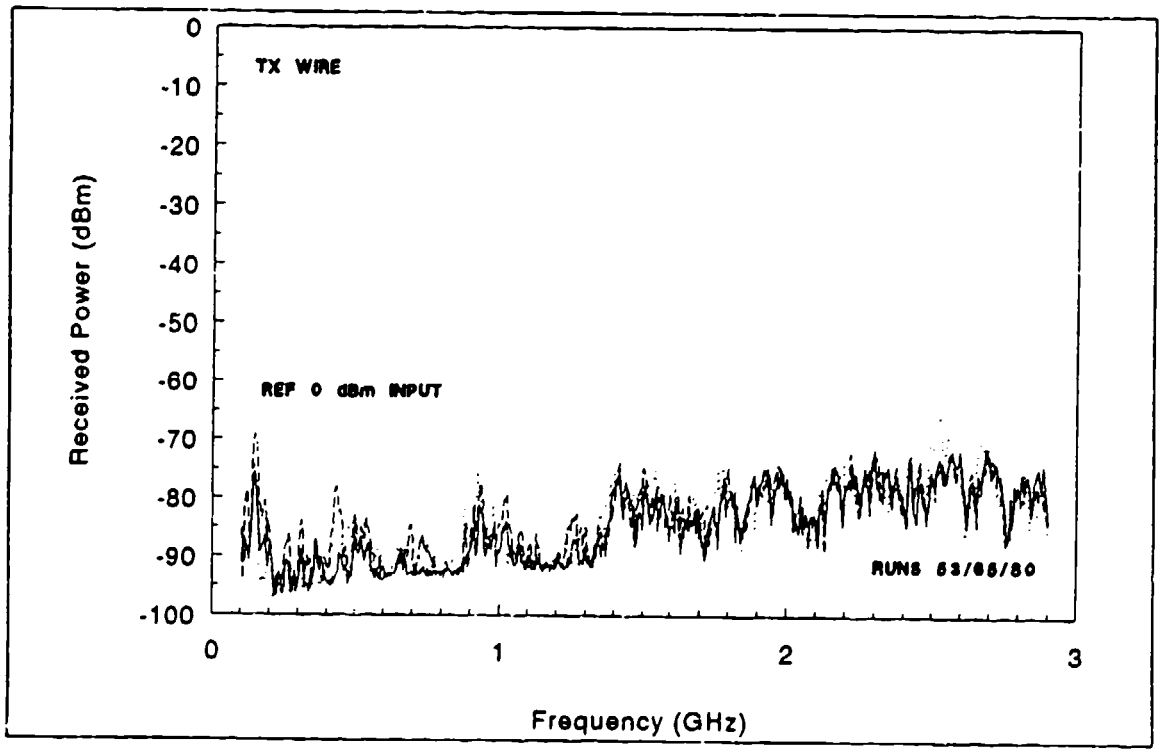

FIGURE 4-39. SIMULATED AVIONICS BOX RESPONSE WITH WIRE EXCITATION IN AVIONICS BAY

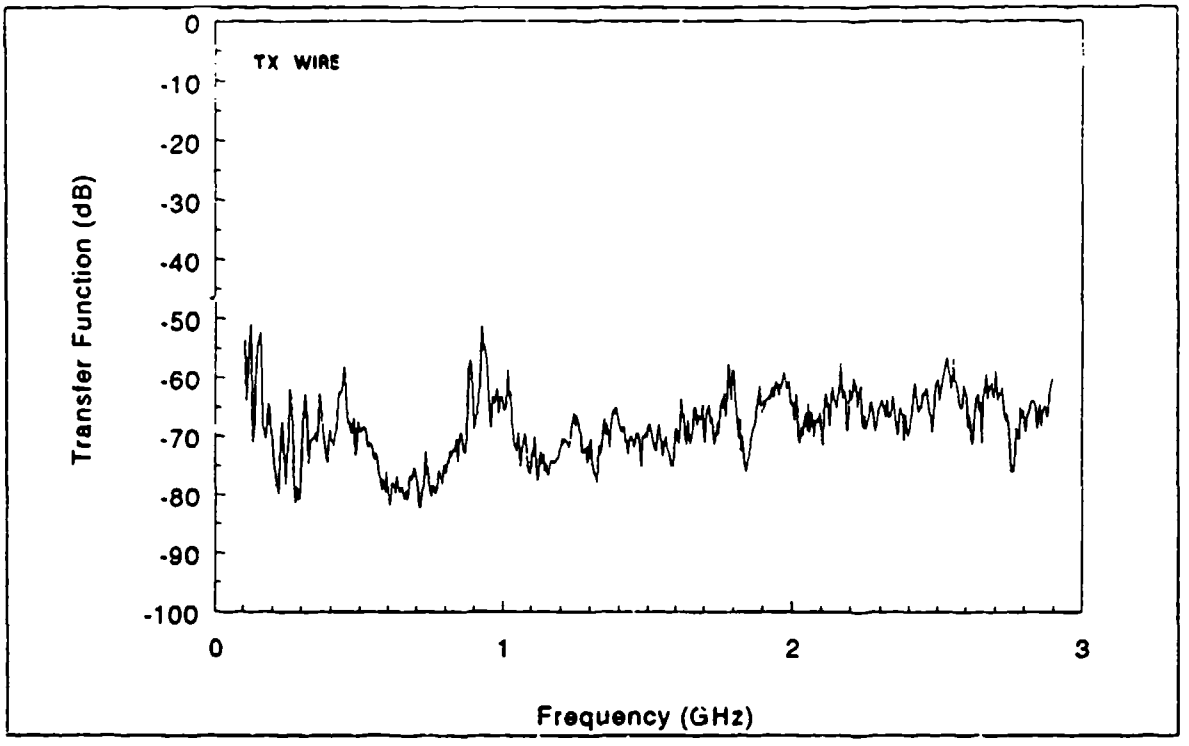

FIGURE 4-40. SIMULATED AVIONICS BOX TRANSFER FUNCTION WITH WIRE EXCITATION IN AVIONICS BAY

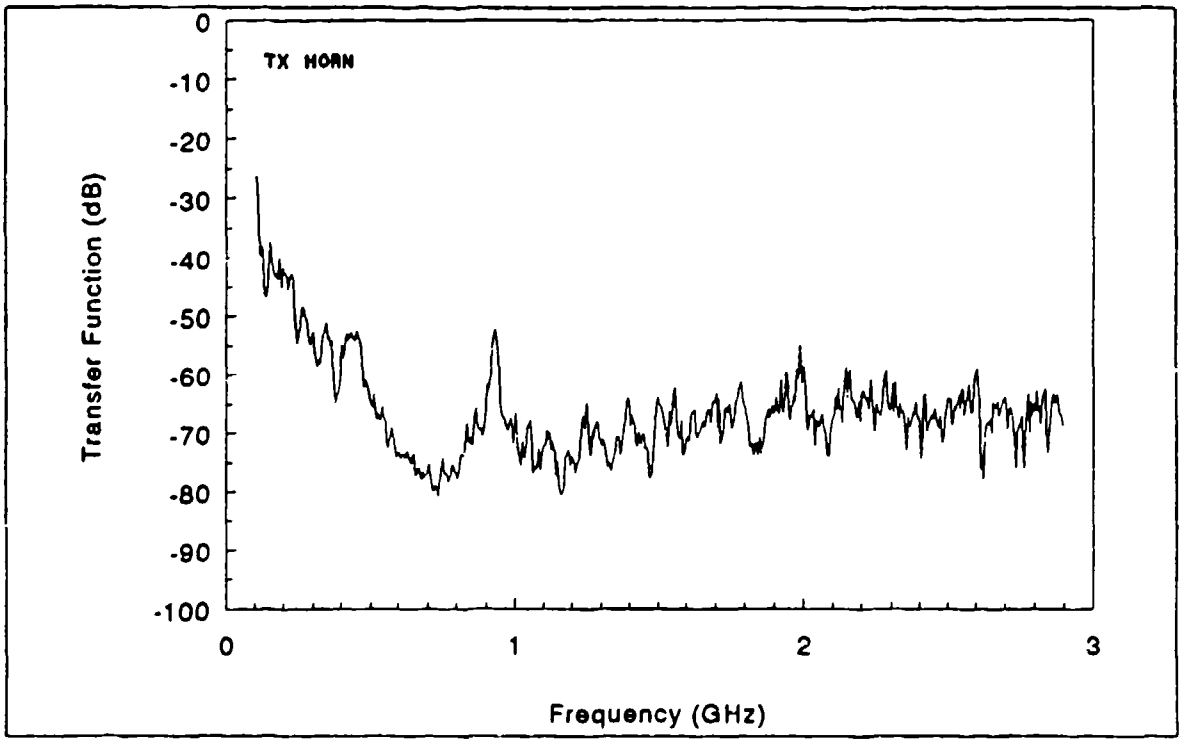

FIGURE 4-41. SIMULATED AVIONICS BOX TRANSFER FUNCTION WITH HORN EXCITATION IN AVIONICS BAY

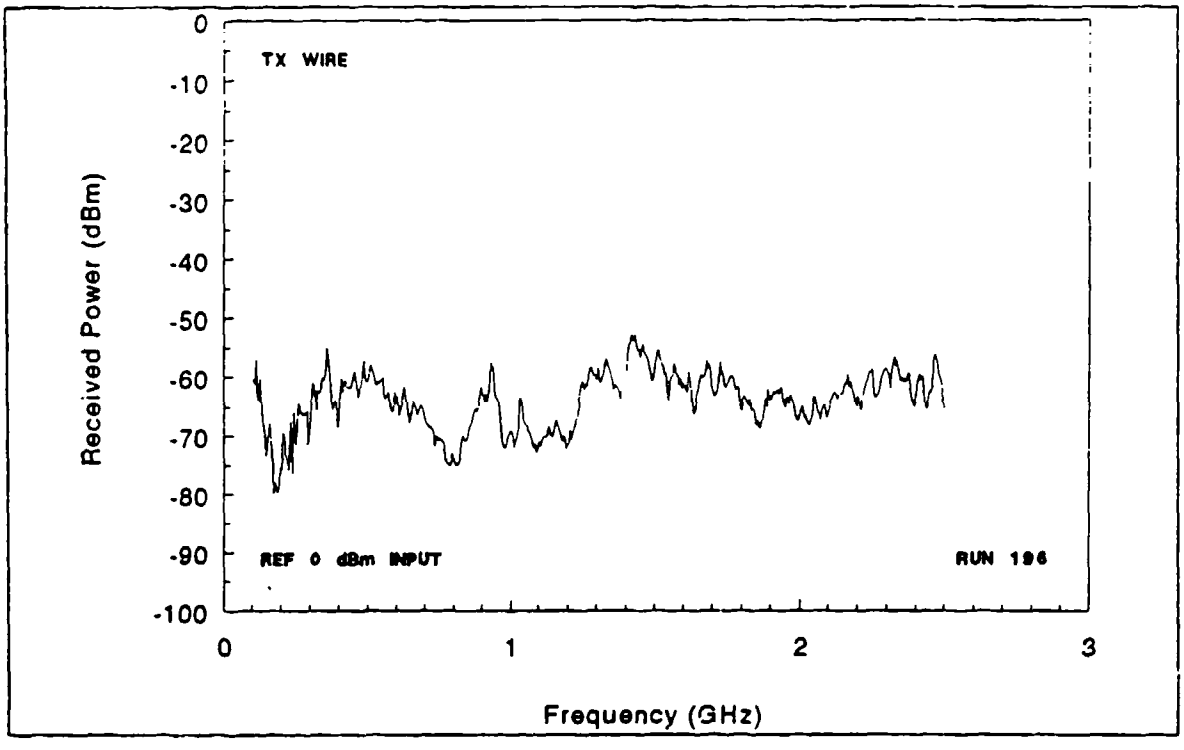

FIGURE 4-42. SIMULATED AVIONICS BOX RESPONSE WITH WIRE EXCITATION IN NSWCDD MODE STIRRED CHAMBER

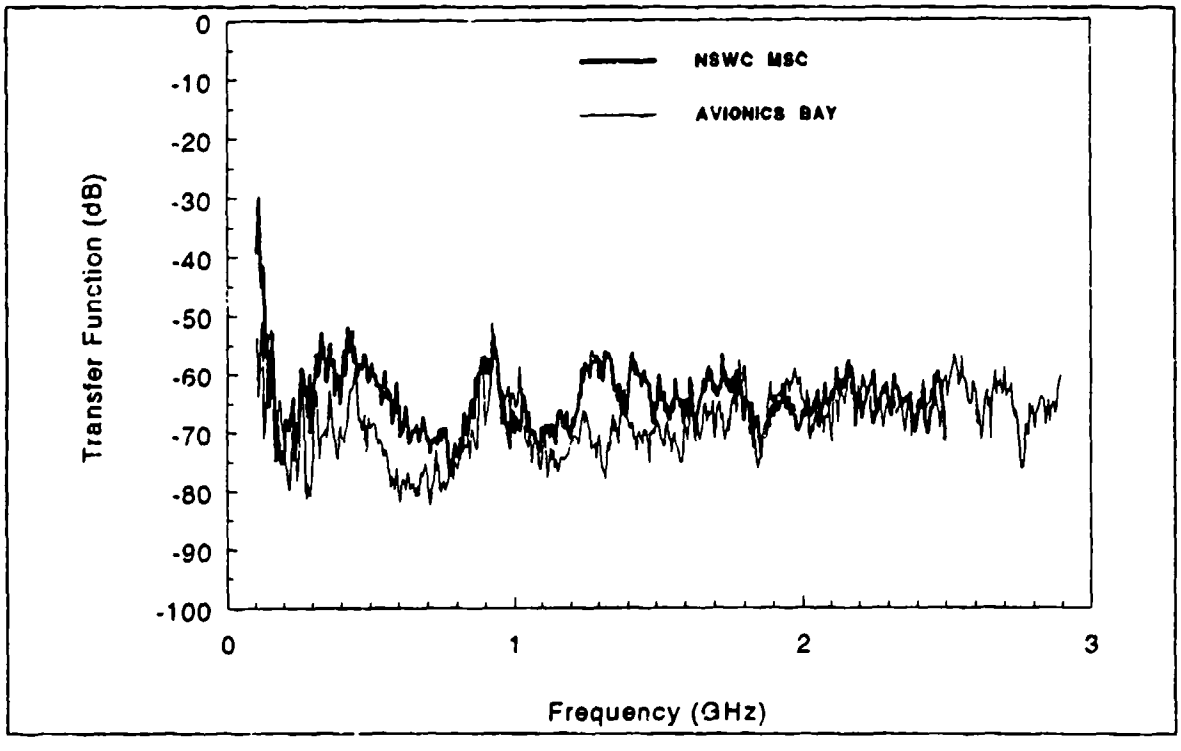

FIGURE 4-43. COMPARISON OF TRANSFER FUNCTIONS FOR SIMULATED AVIONICS BOX IN AIRCRAFT AVIONICS BAY AND IN NSWCDD MODE STIRRED CHAMBER

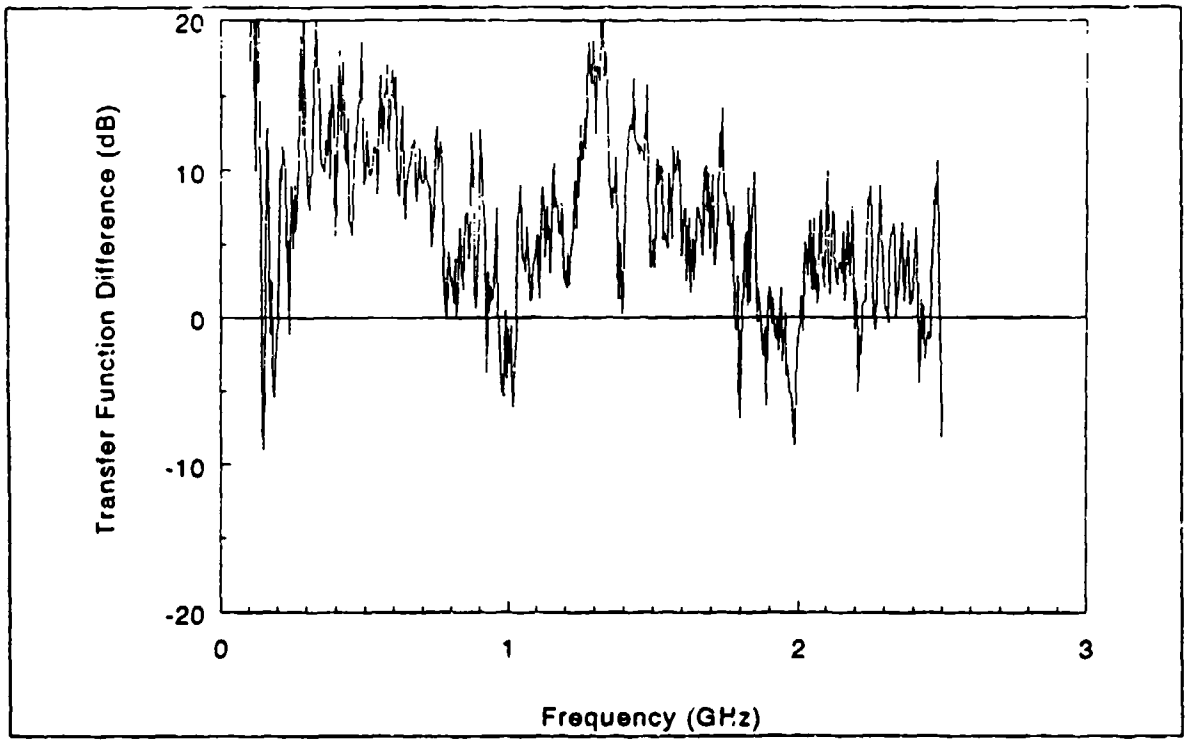

FIGURE 4-44. DIFFERENCE BETWEEN SIMULATED AVIONICS BOX TRANSFER FUNCTIONS FOR AVIONICS BAY AND MODE STIRRED CHAMBER

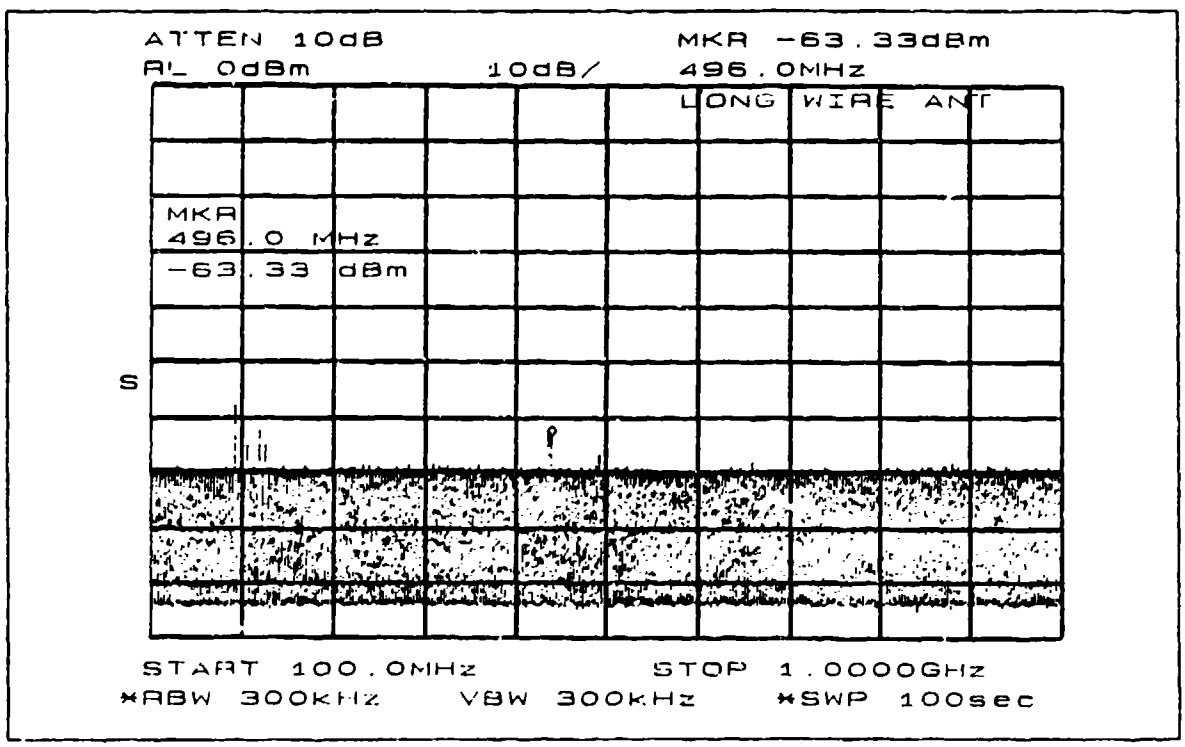

FIGURE 4-45. RECEIVED POWER IN AVIONICS BAY DUE TO EXTERNAL AMBIENT VHF/UHF BAND ENVIRONMENT

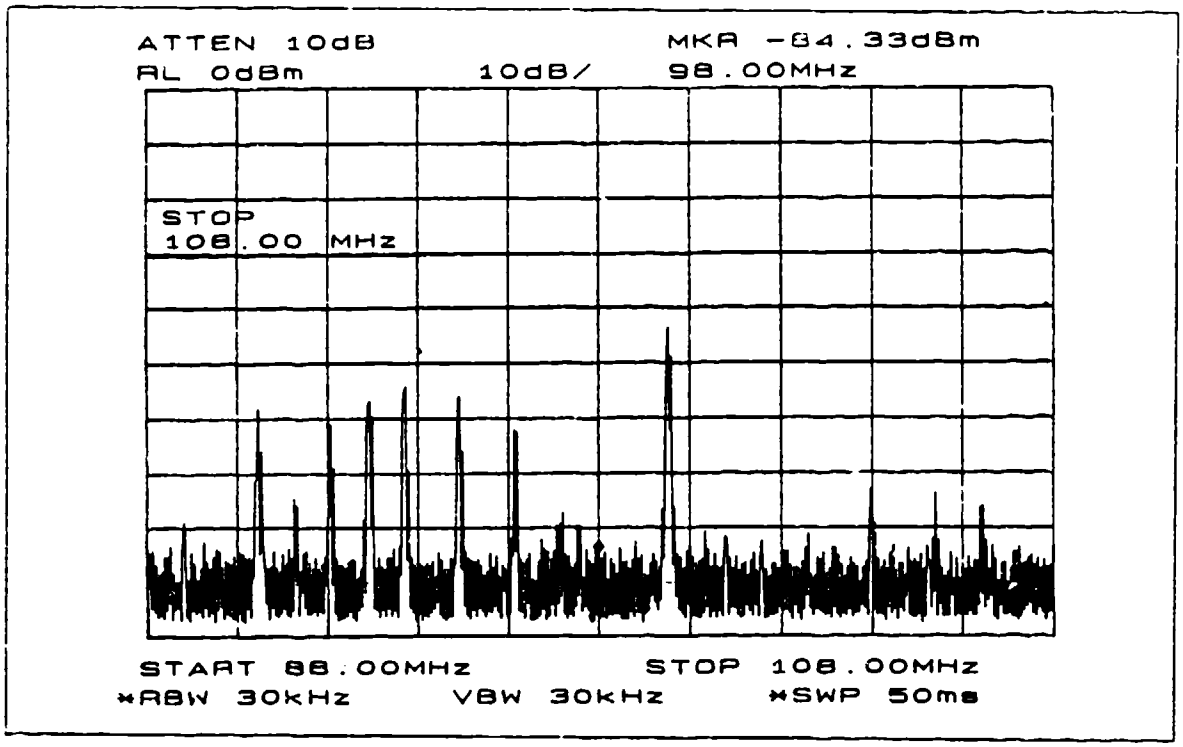

FIGURE 4-46. EXTERNAL AMBIENT FM BAND ENVIRONMENT

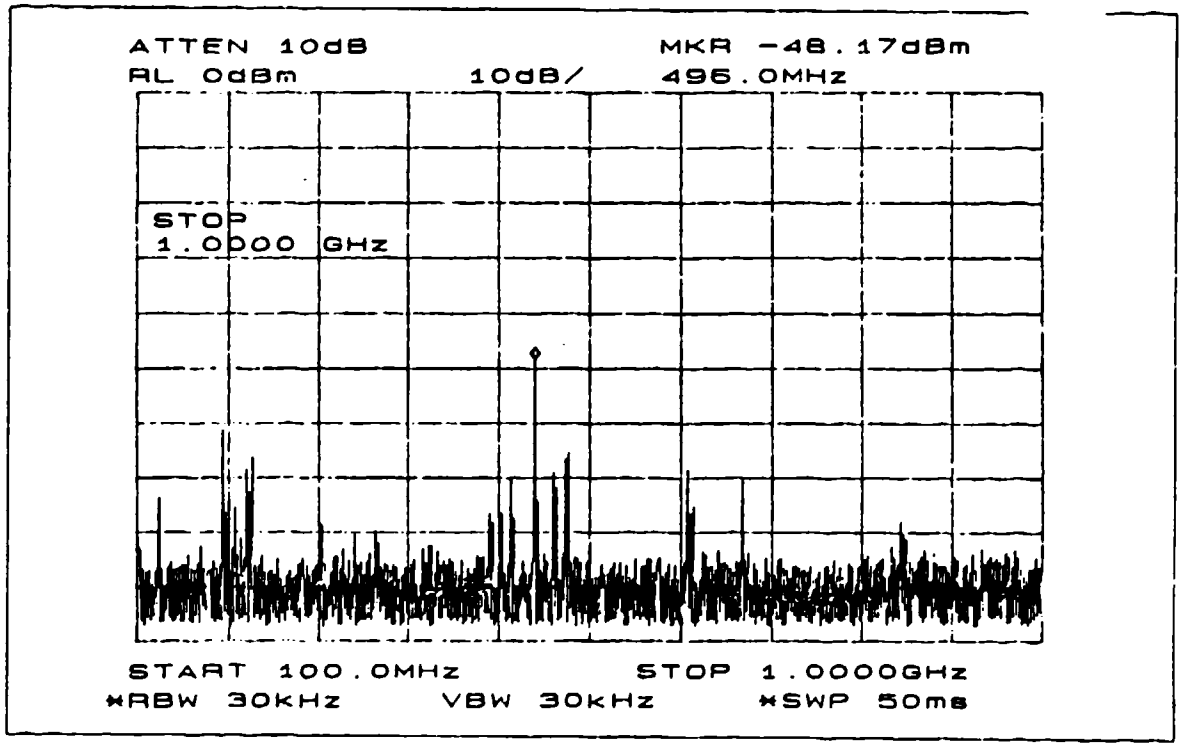

FIGURE 4-47. EXTERNAL AMBIENT VHF UHF BAND ENVIRONMENT MEASURED WITH WIRE ANTENNA

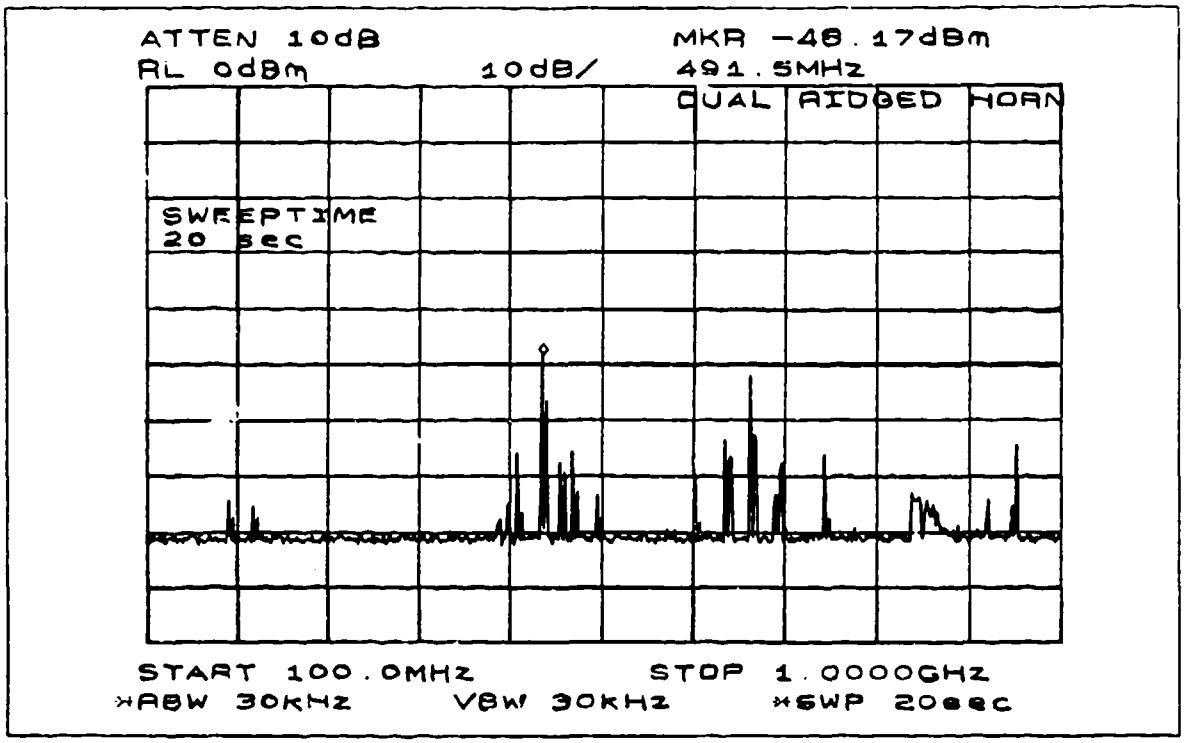

FIGURE 4-48. EXTERNAL AMBIENT VHF/UHF BAND ENVIRONMENT MEASURED WITH DUEL-RIDGED HORN

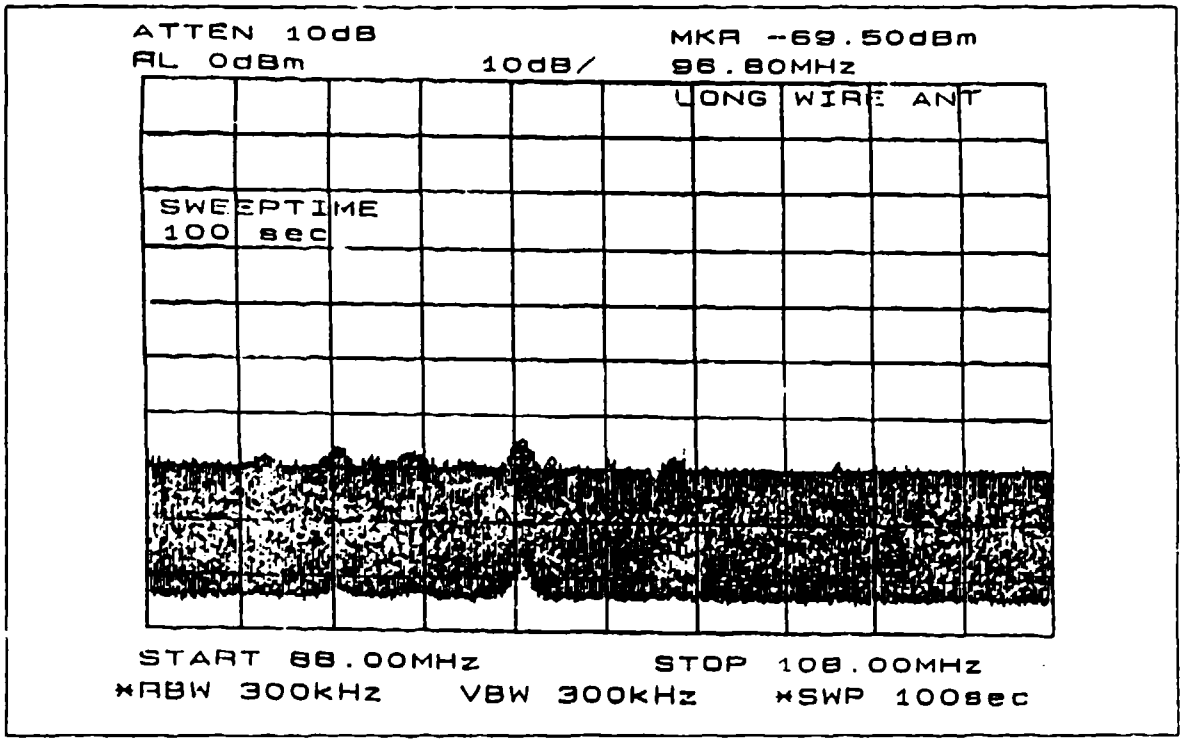

FIGURE 4-49. RECEIVED POWER IN AVIONICS BAY DUE TO EXTERNAL AMBIENT FM BAND ENVIRONMENT

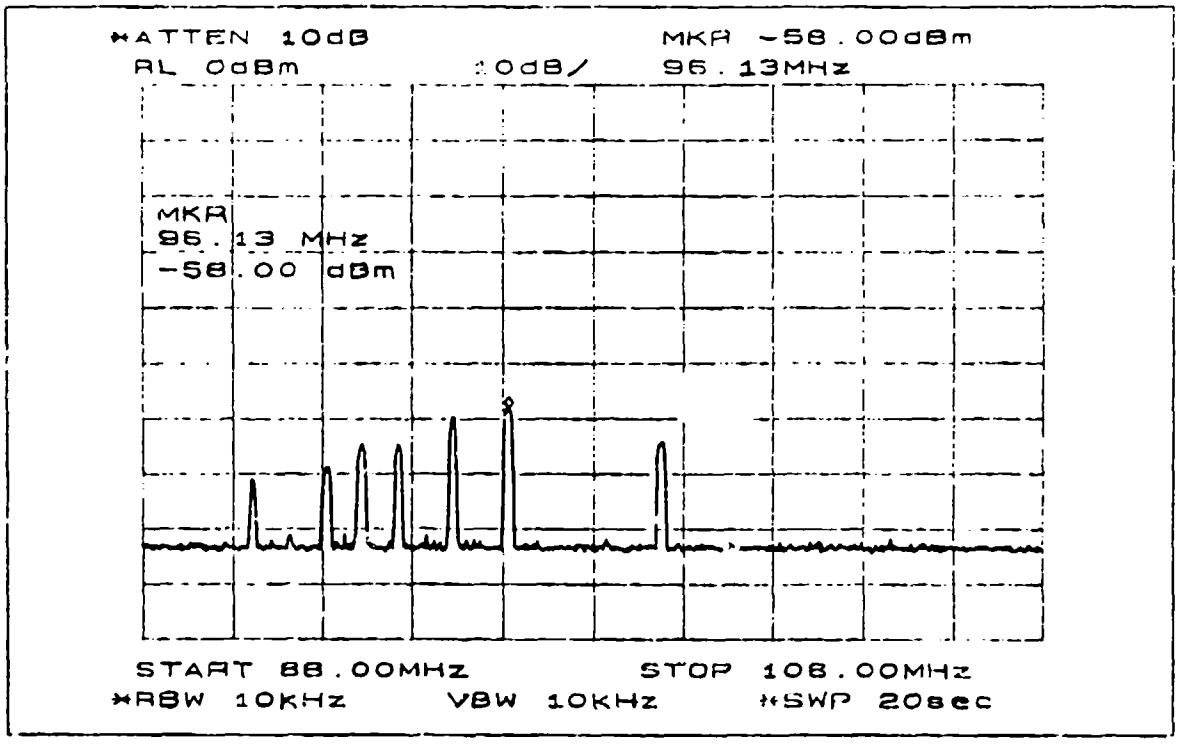

FIGURE 4-50. RECEIVED POWER IN COCKPIT DUE TO EXTERNAL AMBIENT FM BAND ENVIRONMENT

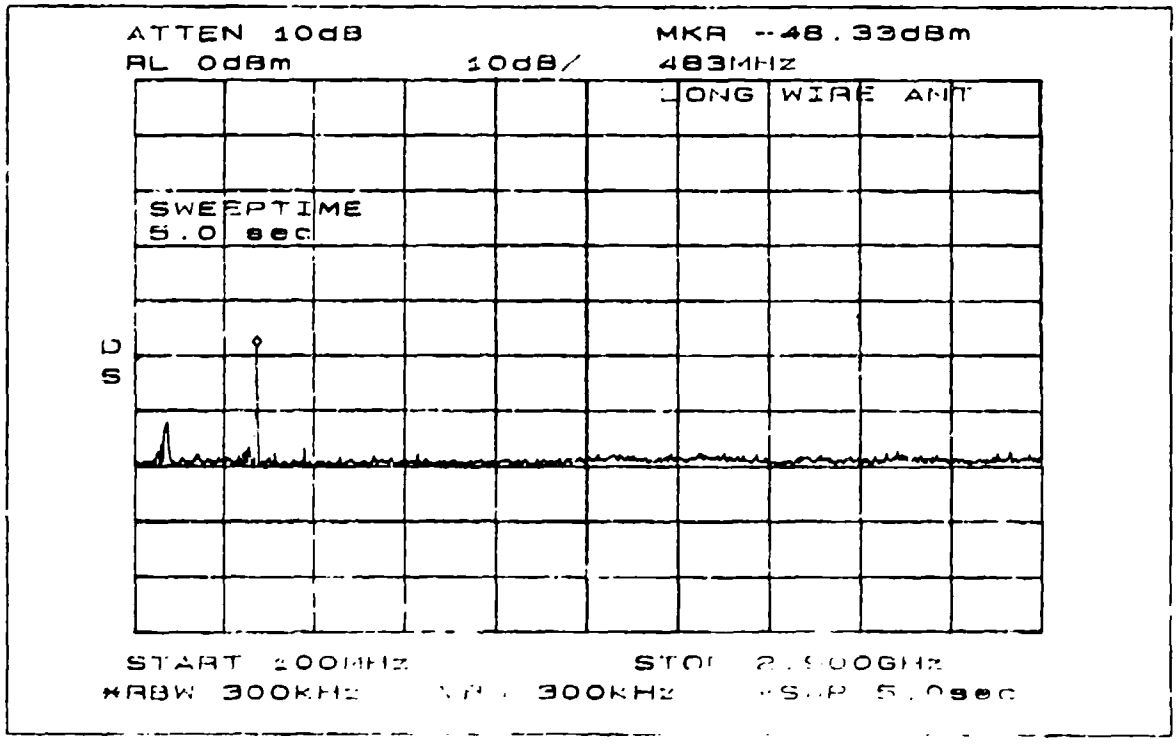

FIGURE 4-51. RECEIVED POWER IN COCKPIT DUE TO EXTERNAL AMBIENT VHF/UHF BAND ENVIRONMENT

5.0 SUMMARY OF ANALYSIS RESULTS

The Boeing 707-720B cavities tested had substantial suites of avionics equipment and many cable runs. The cables ran throughout the avionics bay and the cockpit as well as to other sections of the aircraft. The cavities contained insulating material, air conditioning ducts, etc., and the hatches and doors did not have EM seals. There was also a large, non-metallic compartment boundary between the avionics bay below and the passenger cabin above. This was a major violation of the shielding topology of the avionics bay and provided EME access from the passenger cabin to the avionics bay. The passenger cabin was essentially intact.

The test results should be reasonably applicable to more modern large aircraft since these aircraft do not (and probably will not) significantly improve on the integrity of the shield topology of the Boeing 707. Factors such as weight and initial cost penalties as well as maintenance considerations mitigate against tight control of a commercial aircraft's EM topology. For example, various aircraft cavities will generally not have a continuous metal shield topology and hatches and doors will not have EM seals. Except for critical systems, most cable bundles will not be shielded. Thus the EM characteristics of more modern aircraft should not depart appreciably from that of the test Boeing 707.

These test results should at least partially represent the response of cavities of smaller business/commuter-sized aircraft. The cockpit/passenger cabin of these aircraft typically is a single reasonably large cavity. The cavity will be complex and the mode density high enough at frequencies of interest to permit mode stirring. However the crew and passengers will load the cavity so the Q will be low. Although some data are available on low Q cavities, the impact of these loading conditions on cavity EME remains to be investigated. In addition, this aircraft type often has one or more small avionics bays. The equipment layout in these small bays may preclude the use of an adequately sized tuner and other techniques for mode mixing will be required. While this test provides no data on small cavities, other work suggests that with adequate mode mixing, small cavities will also have an isotropic, randomly polarized EME as the bounding condition. Under these conditions, MSC tests should provide a good simulation of the cavity EME.

Several factors that could impact the response of an avionics system in an aircraft were not investigated in this test. The most important factor up to approximately 1 GHz is energy coupling to an avionics system from long cable runs that penetrate the shields. As an example, consider a long cable run from the tail of the aircraft that could be exposed to a free field environment as it passes an aperture

in the aircraft shielding topology. Although the simulated avionics box in this test did have a cable bundle, it was too short to adequately simulate long cable excitation potentially significant at lower frequencies.

An important factor above 1 GHz is aperture coupling of the cavity EME into the avionics system. Aperture coupling of the bay EME to an avionics system was simulated in this test. While it is possible the location of a system might provide an unusual aperture exposure to the external EME, good aircraft design should minimize this problem.

The test did not evaluate the importance of simulating the physical structure of the immediate vicinity of the system-under-test. In the aircraft, the simulated avionics box was located in an avionics rack with other systems and cable runs present. In the MSC, the box was tested as a stand-alone system on a dielectric support. The agreement in the box responses, which was discussed in Section 4.6, implies that systems in the vicinity may have measurable but not overwhelming effects. The impact of remote cable excitation and the requirements for simulation of the physical structure around the system-under-test needs further investigation.

Another factor not investigated in this test is how the aircraft cavity will modify a pulsed threat environment. It is well known that a Q cavity will modify the rise time and perhaps the peak level of a pulsed signal. While aircraft cavities probably would not match a MSC for pulse modification, their loss rates may yield Q values sufficiently high to have a measurable effect. Therefore, the response of an aircraft cavity to a pulsed excitation should also be investigated.

5.1 CAVITY LOSS

Using the same TX and RX systems and the same reference input power, the received power in the avionics bay was approximately 15 dB less than the received power in the NSWCDD MSC. The difference was relatively constant over the frequency range 0.2 to 3 GHz. The received power in the cockpit was approximately 12 dB less than the MSC. Thus, the cockpit was a slightly less lossy cavity than the avionics bay.

5.2 COCKPIT TO AVIONICS BAY COUPLING

A bounding envelope for the energy coupled from the cockpit to the avionics bay varies from about 7 percent at 800 MHz to a peak of about 25 percent at 2.5 GHz.

5.3 STIRRING RATIO

Both the avionics bay and the cockpit were large enough and complex enough to provide sufficient number of modes and sufficient mode density to accommodate mode stirring over a substantial portion of the frequency range tested. The criterion used for evaluating the effectiveness of mode stirring in the aircraft was the empirically derived and widely accepted 20 dB or greater value for one rotation of the tuner at a discrete frequency.

Stirring was limited below about 800 MHz. From the data available, it cannot be determined if the cause was the lack of mode density in the bay itself, or because of the limited size of the tuner. While historical guidelines suggest that the tuner should have been effective at 250 MHz, other work suggests 500 MHz (or higher) would be a more realistic frequency. Based on engineering judgement, it would appear likely that the tuner size is the major factor.

Between 500 and 800 MHz, a typical value for the SR was 10 dB with occasional data in excess of 20 dB. Above 800 MHz, in all configurations in both the avionics bay and the cockpit, much of the SR data are above 20 dB or are noise limited to lower values. No correlation was found between the SR and peaks or nulls or with the absolute value of the received power.

While the discrete frequency stirring data often showed deep nulls in the minimum received power, no similar excursions in the maximum values were present in any of the more than 500 data runs obtained in the aircraft.

5.4 STIRRING STATISTICS

When mode stirring occurs in a complex cavity, the EME can be described in terms of statistical properties. The statistical parameters investigated for the aircraft cavities were the SR, the data mean and SD, the peak-to-average ratio, and the probability density and cumulative distributions for discrete frequencies. The SR summary was presented in Section 5.3. The aircraft cavity SD tended to be lower than theoretical predictions. With adequate stirring, the peak-to-average ratios were generally consistent with the higher empirically derived and theoretically supported value of 7 to 8 dB for isotropic and randomly polarized EME in a complex cavity. For sufficiently high SR (> 30 dB) the cumulative distributions for the received power in both the cockpit and the avionics bay show good agreement with the theoretical predictions.

5.5 SIMULATED AVIONICS BOX RESPONSE IN AIRCRAFT

Section 4.5 described a comparison of the frequency-dependent EME in the avionics bay with the received power from a trace on the circuit board in the simulated avionics box. The lack of correlation of the frequency-dependent box

response with the structure of the bay EME indicates that the energy coupled depends primarily on the intrinsic characteristics of the box and cables. This is confirmed by the transfer function that normalized the box response to the bay EME and shows significant, discrete resonant structures.

5.6 COMPARISON OF SIMULATED AVIONICS BOX RESPONSE IN AIRCRAFT AND MODE STIRRED CHAMBER

The simulated avionics box responses in the MSC and the aircraft avionics bay were similar. The absolute magnitude of the box responses in the two cavities was consistent with the additional 15 dB loss in the avionics bay. The calculated transfer functions for energy from the cavity to the monitored trace on the box circuit board generally agreed to within 10 dB for the frequency range 0.8 to 2.5 GHz. Finally, when differences in the transfer functions did occur, the MSC transfer function tended to be the larger. Thus, a MSC test of an avionics system should be a conservative test. The data imply that a MSC test would be an appropriate conservative simulation of the system response in an aircraft cavity.

5.7 SHIELDING EFFECTIVENESS

The external ambient EME in the FM and VHF/UHF bands was measured before and after the test. A substantial number of strong signals were observed. The ambient internal EME was measured in a few configurations in the avionics bay and cockpit. The same measurement system was used for both measurements so no calibration or correction factors were required. The database yielded estimates of the bounds of aircraft SE for the FM and VHF/lower UHF bands. The upper bound on SE for both the cockpit and avionics bay is 25 dB. The lower bound indicates the possibility of a few decibels of gain.

6.0 CONCLUSIONS

The Boeing 707-720B aircraft was a reasonable testbed for investigating the responses of avionics bays of older operational, medium-to-large, commercial airliners.

- The probable lack of a significant change in the electromagnetic topology control in next-generation, large commercial airliners should yield cavity characteristics similar to those of the test aircraft.

- The results may not be directly applicable to small cavities common to business class aircraft.

For frequencies over 800 MHz, the stirring ratios in the aircraft avionics bay and cockpit approached or exceeded the widely accepted guideline of 20 dB for adequate mode stirring in a cavity.

The aircraft cavity insertion loss was about 15 dB greater than the Naval Surface Warfare Center, Dahlgren Division Q mode stirred chamber.

For stirring ratios greater than approximately 30 dB, the Boeing 707-720B avionics bay and cockpit test results show good agreement with theoretical predictions for an isotropic, randomly polarized electromagnetic environment.

Mode stirred chambers provide an appropriate simulation of the limiting electromagnetic environments in the Boeing 707-720B cockpit and avionics bay.

Over the frequency range 800 MHz to 2.9 GHz, the bounding envelope for the energy coupled from the cockpit to the avionics bay varied from about 7 to 25 percent.

The simulated avionics box responses in the aircraft and the Naval Surface Warfare Center, Dahlgren Division mode stirred chamber were similar in

- Absolute magnitude (when corrected for the differences in cavity electromagnetic environment levels)
- Detailed resonance structure
- Derived transfer functions

A limited database using external ambient signals suggests the aircraft shielding effectiveness ranges from about 25 dB of attenuation to a few decibels of gain for the FM and VHF/lower UHF bands.

7.0 RECOMMENDATIONS

The following recommendations are offered.

- Perform detailed field characterization of an aircraft cavity using an array of three-axis probes. The purpose would be to demonstrate the spatial and field component uniformity characteristic of the randomized fields in a true mode stirred chamber.

- Perform field measurements with several different densities and configurations of metal boxes in the aircraft cavity. The purpose would be to characterize the impact of cavity complexity.

- Perform joint external excitation/internal cavity response characterization. The purpose would be to establish the final link in the proposed low-level, swept field excitation to full threat mode stirred chamber test procedure.

- Investigate aircraft cavity response to pulse excitation. The purpose would be to determine if an aircraft cavity has a sufficient Q to significantly affect the pulse rise time and peak value.

- Investigate the effects of varying tuner dimensions in an aircraft cavity. The purpose would be to determine if the limited stirring observed below 800 MHz is intrinsic to the aircraft cavity or is a tuner size problem.

- Perform similar test programs on both business class aircraft and medium-to-large aircraft currently under development. The purpose would be to show equivalence (or non-equivalence) to mode stirred chambers for cavities in these aircraft types.

- Investigate the effects of cable bundle lengths and the proximity to metal structures on the response of avionics systems in aircraft cavities and mode stirred chambers. The purpose would be to determine the fidelity required in simulating the cable bundles and nearby aircraft cavity configuration when testing an avionics system in a mode stirred chamber.

- Perform additional shielding effectiveness testing. The purpose would be to clarify the low shielding effectiveness values suggested by the limited test data.

- Repeat internal cavity excitation and perform external excitation/internal cavity response characterization using the newly developed Band Limited, White Gaussian Noise technique. The purpose would be to demonstrate the applicability and effectiveness of this mode excitation method.

DISTRIBUTION

Copies

DOD ACTIVITIES (CONUS)

DEFENSE TECHNICAL INFORMATION CENTER CAMERON STATION ALEXANDRIA VA 22304-6145	12

NON-DOD ACTIVITIES (CONUS)

ATTN GIFT AND EXCHANGE DIVISION LIBRARY OF CONGRESS WASHINGTON DC 20540	4
THE CNA CORPORATION PO BOX 16268 ALEXANDRIA VA 22302-0268	1
ATTN CODE 130 (CHARLES MEISSNER) NASA LANGLEY RESEARCH CENTER HAMPTON VA 23665-5225	30

INTERNAL

E231	3
E282 (SWANSBURG)	1
F50	1
F52	1
F52 (BEAN)	1
F52 (HATFIELD)	350
N74 (GIDEP)	1

REPORT DOCUMENTATION PAGE

Form Approved
OMB No 0704-0188

1. AGENCY USE ONLY *(Leave blank)*	2. REPORT DATE	3. REPORT TYPE AND DATES COVERED
	July 1994	Final

4. TITLE AND SUBTITLE

Electromagnetic Reverberation Characteristics of a Large Transport Aircraft

5. FUNDING NUMBERS

6. AUTHOR(S)

Michael O. Hatfield, Gustav J. Freyer, D. Mark Johnson, Charles L. Farthing

7. PERFORMING ORGANIZATION NAME(S) AND ADDRESS(ES)

Naval Surface Warfare Center, Dahlgren Division (Code F52)
17320 Dahlgren Road
Dahlgren, VA 22448-5100

8. PERFORMING ORGANIZATION REPORT NUMBER

NSWCDD/TR-93/339

9. SPONSORING/MONITORING AGENCY NAME(S) AND ADDRESS(ES)

10. SPONSORING/MONITORING AGENCY REPORT NUMBER

11. SUPPLEMENTARY NOTES

12a. DISTRIBUTION/AVAILABILITY

Approved for public release; distribution is unlimited.

12b. DISTRIBUTION CODE

13. ABSTRACT *(Maximum 200 words)*

A demonstration test to investigate the reverberation characteristics of the avionics bay and cockpit of a typical commercial aircraft was conducted on a decommissioned Boeing 707-720B aircraft. The aircraft, located at the Aerospace Maintenance and Regeneration Center, Davis Monthan Air Force Base, Arizona, had a significant fraction of its electronics equipment remaining in the avionics bay and cockpit and the passenger compartment was essentially intact. A simulated avionics box was placed in an equipment rack and a trace on an internal circuit board was monitored. The simulated avionics box was also tested in the Naval Surface Warfare Center, Dahlgren Division (NSWCDD) mode stirred chamber (MSC). The avionics bay and cockpit were internally excited from 100 MHz to 18 GHz using a pair of horn and wire antennas placed in several locations. Aluminum foil tuners, each 2 x 2 ft, were located in the avionics bay and the cockpit. The internal electromagnetic environment was measured by a horn and a wire antenna placed successively in several locations in the avionics bay and cockpit. Limited measurements of the local ambient environment, both external to the aircraft and within the aircraft, were obtained for the FM band (88 to 108 MHz) and the VHF/UHF bands (100 MHz to 1 GHz). Cavity losses were characterized by comparing the received power to the input power. The cavity loss for the avionics bay was about 15 dB greater than the loss in the NSWCDD MSC. The loss for the cockpit was about 12 dB greater than the NSWCDD MSC. The observed stirring ratios (ratio of maximum received signal to minimum received signal at a particular frequency as the tuner rotates) were generally less than 10 dB up to about 800 MHz. Above 800 MHz, a substantial number of data points exceeded 20 dB, the commonly accepted empirical criterion for adequate mode stirring in a MSC. The responses of the simulated avionics box in the avionics bay and in the MSC showed good agreement. The limited data obtained implies the possibility that the shielding effectiveness for the avionics bay and cockpit may be as low as 0 dB over a portion of the frequency range 88 MHz to 1 GHz.

14. SUBJECT TERMS

Reverberation, Avionics Bay, Cockpit, Electromagnetic Environment, Mode Stirred Chamber, Shielding Effectiveness

15. NUMBER OF PAGES

96

16. PRICE CODE

17. SECURITY CLASSIFICATION OF REPORT	18. SECURITY CLASSIFICATION OF THIS PAGE	19. SECURITY CLASSIFICATION OF ABSTRACT	20. LIMITATION OF ABSTRACT
UNCLASSIFIED	UNCLASSIFIED	UNCLASSIFIED	SAR

GENERAL INSTRUCTIONS FOR COMPLETING SF 298

The Report Documentation Page (RDP) is used in announcing and cataloging reports. It is important that this information be consistent with the rest of the report, particularly the cover and its title page. Instructions for filling in each block of the form follow. It is important to ***stay within the lines*** to meet ***optical scanning requirements***.

Block 1. Agency Use Only *(Leave blank)*.

Block 2. Report Date. Full publication date including day, month, and year, if available (e.g. 1 Jan 88). Must cite at least the year.

Block 3. Type of Report and Dates Covered. State whether report is interim, final, etc. If applicable, enter inclusive report dates (e.g. 10 Jun 87 - 30 Jun 88).

Block 4. Title and Subtitle. A title is taken from the part of the report that provides the most meaningful and complete information. When a report is prepared in more than one volume, repeat the primary title, add volume number, and include subtitle for the specific volume. On classified documents enter the title classification in parentheses.

Block 5. Funding Numbers. To include contract and grant numbers; may include program element number(s), project number(s), task number(s), and work unit number(s). Use the following labels:

C	- Contract	**PR**	- Project
G	- Grant	**TA**	- Task
PE	- Program Element	**WU**	- Work Unit Accession No.

BLOCK 6. Author(s). Name(s) of person(s) responsible for writing the report, performing the research, or credited with the content of the report. If editor or compiler, this should follow the name(s).

Block 7. Performing Organization Name(s) and address(es). Self-explanatory.

Block 8. Performing Organization Report Number. Enter the unique alphanumeric report number(s) assigned by the organization performing the report.

Block 9. Sponsoring/Monitoring Agency Name(s) and Address(es). Self-explanatory.

Block 10. Sponsoring/Monitoring Agency Report Number. *(If Known)*

Block 11. Supplementary Notes. Enter information not included elsewhere such as: Prepared in cooperation with...; Trans. of...; To be published in.... When a report is revised, include a statement whether the new report supersedes or supplements the older report.

Block 12a. Distribution/Availability Statement. Denotes public availability or limitations. Cite any availability to the public. Enter additional limitations or special markings in all capitals (e.g. NOFORN, REL, ITAR).

DOD	- See DoDD 5230.24, "Distribution Statements on Technical Documents."
DOE	- See authorities.
NASA	- See Handbook NHB 2200.2
NTIS	- Leave blank

Block 12b. Distribution Code.

DOD	- Leave blank.
DOE	- Enter DOE distribution categories from the Standard Distribution for Unclassified Scientific and Technical Reports.
NASA	- Leave blank.
NTIS	- Leave blank.

Block 13. Abstract. Include a brief ***(Maximum 200 words)*** factual summary of the most significant information contained in the report.

Block 14. Subject Terms. Keywords or phrases identifying major subjects in the report.

Block 15. Number of Pages. Enter the total number of pages.

Block 16. Price Code. Enter appropriate price code ***(NTIS only)***

Block 17.-19. Security Classifications. Self-explanatory. Enter U.S. Security Classification in accordance with U.S. Security Regulations (i.e., UNCLASSIFIED). If form contains classified information, stamp classification on the top and bottom of this page.

Block 20. Limitation of Abstract. This block must be completed to assign a limitation to the abstract. Enter either UL (unlimited or SAR (same as report). An entry in this block is necessary if the abstract is to be limited. If blank, the abstract is assumed to be unlimited.